UNIVERSITÀ DELLA CALABRIA

UNIVERSITA' DELLA CALABRIA

Dipartimento di Ingegneria Meccanica, Energetica e Gestionale

Dottorato di Ricerca in

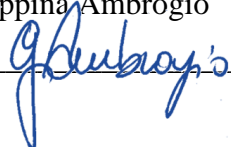**Ingegneria Civile e Industriale**

CICLO

XXXI

DESIGN AND EXPERIMENTAL VALIDATION OF DOWNSTREAM

MANUFACTURING PROCESSES ON POLYMERIC

AND COMPOSITE MATERIALS
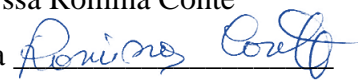
Settore Scientifico Disciplinare ING-IND 16

Coordinatore: Ch.mo Prof. Franco Furgiuele

Firma _____

Supervisore/Tutor: Ing. Giuseppina Ambrogio

Firma_____

Dottoranda: Dott. ssa Romina Conte

Firma _____

"Where shall I begin, please, your Majesty?" he asked.

"Begin at the beginning," the King said, gravely,
"and go on till you come to the end: then stop."

Charles L. Dodgson (Lewis Carroll)
Alice in Wonderland (1865)

TABLE OF CONTENTS

LIST OF FIGURES

LIST OF TABLES

ABSTRACT

Recently, the application of polymers and composites is growing in many industrial sectors. They are replacing traditional materials mainly because of their high-performances and excellent balance of properties. Furthermore, the industrial interest in innovative solutions for small-batches and prototypes and the necessity of reducing the relative costs are increasing as well.

According to that, two main categories of downstream processes have been investigated for the aim of this thesis. They are Incremental Forming (IS) and joining.

Single Point Incremental Forming belongs to the first category and is widely known as a flexible manufacturing technique. The scientific literature reports studies that performed the process on thermoplastic materials characterized by a rubbery state at room temperature. This thesis aims at proving the feasibility on polymeric and composite materials whose glass transition temperature is higher than the room one. The experimental tests have been performed using an apparatus designed and manufactured for this specific scope. An external control unit allowed to set the initial temperature of the material, which becomes a new process parameter to take into account and that has been never considered before. Macroscale and microscopic observations of the produced samples allowed to evaluate, qualitatively and quantitatively, the product soundness and accuracy, the surface integrity, and the influence of the process parameters and material composition (fibers content) on the produced outputs.

Concerning the second category, two joining process variants have been experimentally studied and proved.

The first one is a spot joining technique, known as *Friction Riveting*. Rivets of aluminium and titanium have been involved in the joint of thermoplastic polymeric and composite sheets.

The second alternative joining technique here proposed is based on the *Friction Stir Forming* process. This latter has been performed on aluminium sheets aiming at shaping metal pins to use like locking heads to connect dissimilar parts, in this specific case metal and composite.

The mechanical behaviour of the samples obtained by means of those technologies has been verified by tensile shear tests, while the material deformation and the integrity inside the connection volume were studied through Electronic Speckle Pattern Interferometry (ESPI) for Friction Riveting junctions and X-Ray micro-tomography analysis for ones obtained by the Friction Stir Welding based technique.

SOMMARIO

L'utilizzo di materiali polimerici e compositi negli ultimi decenni sta notevolmente aumentando investendo diversi settori industriali. In particolare, si sta assistendo ad una sostituzione dei materiali utilizzati tradizionalmente con materiali innovativi caratterizzati da notevoli proprietà chimiche, fisiche e meccaniche ed in grado di garantire alte prestazioni.

Le industrie hanno, altresì, evidenziato la necessità di introdurre nuove soluzioni per la produzione di prototipi e piccoli lotti che consentano la riduzione dei costi.

Al fine di contribuire al soddisfacimento di tali esigenze industriali, questo lavoro di tesi è stato finalizzato allo studio di due categorie di processi manifatturieri, rispettivamente di formatura e di giunzione, da inquadrare come processi secondari per la lavorazione di polimeri e compositi.

Alla prima categoria appartiene il processo noto come *Single Point Incremental Forming*, caratterizzato principalmente dall'essere una tecnologia molto flessibile. La letteratura scientifica riporta diversi esempi sull'utilizzo di tale processo per la formatura di materiali termoplastici in grado di essere deformati a temperatura ambiente. Obiettivo di questa tesi è stato quello di dimostrare la fattibilità di formare in maniera incrementale materiali caratterizzati da una temperatura di transizione vetrosa superiore a quella ambiente. A tal fine è stata progettata e realizzata una apposita attrezzatura il cui elemento principale è rappresentato da una centralina per il controllo della temperatura del materiale. Quest'ultima, infatti, non è mai stata considerata tra i parametri di processo. I provini realizzati sono stati sottoposti ad analisi macroscopiche e microscopiche al fine di poterne valutare, qualitativamente e quantitativamente, l'accuratezza della forma, l'integrità superficiale e l'influenza dei parametri di processo.

Per quanto concerne la categoria dei processi di giunzione, sono state analizzate due varianti, entrambe testate sperimentalmente. La prima è nota come *Friction Riveting*, usata per connettere due lamine di materiale polimerico prima, e di composito poi, attraverso un rivetto metallico (di titanio e di alluminio). La seconda variante, invece, si basa sul principio di funzionamento del *Friction Stir Forming.* Tale processo è stato testato impiegando una lamiera di alluminio per la realizzazione dei pin da utilizzare in una seconda fase per creare una giunzione con una lamina di composito.

I provini realizzati con entrambe le tecnologie sono stati sottoposti a test di trazione per verificarne il comportamento meccanico. Inoltre, la deformazione e l'integrità del materiale sono state analizzate tramite osservazioni SEM.

INTRODUCTION

"I am among those who think that science has great beauty"

Marie Curie

In recent years, in many engineering applications, traditional materials have been replaced by high-performance polymers and composites characterised by an outstanding balance of properties, such as high thermal stability, excellent chemical resistance and good weatherability. In addition, the need of innovative solutions for small-batches and prototypes is growing, together with the necessity of reducing capital costs. In this context, two main processes, belonging to the downstream category, have been discussed and investigated for the aim of this thesis.

Single Point Incremental Forming (SPIF) is the first one and it may be considered a cost-effective innovative technology for the development of polymeric components. Traditionally, this process has been used for the manufacturing of metal parts and the flexibility is its main advantage, if compared with conventional processes (Filice et al., 2002; Micari et al., 2007). Recently its application has been extended to thermoplastic polymers (Fiorotto et al., 2010; Martins et al., 2009). A deep study of the scientific literature allowed to identify a gap of knowledge related to the application of SPIF to polymeric materials that are difficult to work at room temperature and therefore the gap is also related to influence of the local temperature increasing of the material due to an external heating source. Forming at elevated temperature is certainly a more expensive solution, but it allows to increase the formability, lowering at the same time the required forming forces. According to that, one of the objectives of this thesis is to propose the Single Point Incremental Forming as a downstream process for polymers. To this aim, experimental investigations have been carried out for proving the *SPIFability* of thermoplastic polymeric sheets. Two materials have been selected: the first one characterized by a glass transition temperature lower than the room one, while the second was higher. As regards this latter, the local increase of the temperature has been necessary to perform the process; therefore, a specific equipment has been designed.

The SPIF analysis has been then extended to composite materials and more in detail, the workability of thermoplastic sheets reinforced with short glass fibers has been tested. In this regard,

it is worth pointing out that the use of composite structures is increasing constantly in the last years in several sectors, such as aircraft, automotive, naval ship, medical, pushed mainly by the advantages related to the reduced weight and high strength. Furthermore, the recent scenario denotes a great attention on thermoplastic matrix composites, due to their not negligible advantage associated to the intrinsic recyclability as well as for the possibility of re-using and re-manufacturing (Boria et al., 2017; Moreno and Saron, 2017). This peculiarity of the thermoplastic materials, that allows them to be subjected to subsequent manufacturing steps, changes completely the way of designing both upstream and downstream processes. This aspect and the increasing industrial demand of thermoplastic composite parts determine therefore the request of investigating new manufacturing processes and the possibility of considering their secondary workability. To this aim, experimental researches have been carried out to demonstrate the possibility of re-manufacturing thermoplastic composites without using expensive dies and avoiding long set-up times. Despite this latter consideration, the proposed SPIF process can be slower than other processes, but it is a good option for producing prototypes and small batches.

The polymeric and composite outcomes produced by SPIF, have been evaluated qualitatively and quantitatively through 1) macroscale observations for highlighting the influence of the process variables, included the process temperature, on the soundness and accuracy of the part and 2) microscopic analyses for examining the integrity grade of the sample surface at different combinations of process parameters.

The successive analysed downstream processes belong to the joining technologies category and they have been tested to prove the connection of polymers/composites and metals. The combination of dissimilar parts has become a key technology for developing lightweight structures. One of the first examples of hybrid structure designed for weigh saving was introduced by Horvat and Surface (1989) who assembled and experimentally tested a first attempt of hybrid structure of camshaft. Hayashi and Nakagawa (1994) introduced the concept of car body made of aluminium combined with mild steel or high strength steel as countermeasures for environmental pollution and driving safety. Nowadays, the adoption of dissimilar parts has become a standard in various application fields not only because of the influence of green policies but also for improving the performance of the manufactured parts. In the transportation field, for instance, the combination of multi-materials has become a necessity for optimizing the fuel consumption and CO_2 emissions.

The joining technologies allow to assemble single parts for achieving specific mechanical, physical and chemical performances, but the process may become difficult if the materials to combine are characterized by different properties (Amancio-Filho and dos Santos, 2009). Some joining techniques have been developed combining various technologies pushed by the need of improving the quality of the connection.

To the aim of this thesis, two innovative joining techniques have been tested. The first one is based on Friction Riveting while the second one on Friction Stir Forming. Connections between polymers/composites and metals have been performed. The quality of the joints has been measured by tensile tests and microscopic observations allowed to analyse the deformation of the materials involved in the joint.

According to the above mentioned objectives of this thesis, the following text has been divided in four chapters:

- *Chapter 1* provides an overview of polymeric and composite materials that are widely used nowadays in different fields. Advantages, drawbacks and properties are discussed. The description of the main manufacturing techniques, that allow to transform the raw materials in ready to use or semi-finished products, is provided as well.
- *Chapter 2* aims at discussing the secondary manufacturing processes that are employed i) to produce polymeric and composite finished products starting from primary shaped parts and/or ii) to re-manufacture dismissed parts. The state-of-the-art of traditional and non-traditional downstream processes is provided.
- *Chapter 3* focuses on the Single Point Incremental Forming process that can be considered an innovative downstream technique for shaping polymers and composites. To demonstrate that, experimental investigations have been performed on polypropylene, poly(methyl methacrylate) and glass fiber reinforced polyamide 6. The obtained results have been extensively commented.
- *Chapter 4* introduces the arising need of using hybrid structures in several industrial applications, highlighting the difficulties of connecting materials that are physically, chemically and mechanically different. Two innovative joining techniques are here proposed: 1) Friction Riveting has been performed to combine metal rivets and polymeric/composite sheets and 2) Friction Stir Forming has been tested to prove the feasibility of producing metal pins to connect with fiber-reinforced plastics.

Finally the *Conclusions* summarize the carried out experimental investigations and the all obtained results.

CHAPTER 1

MATERIALS AND PRIMARY PROCESSES

"The triumph of engineering rests on a chemical foundation"

H.G. Deming

1.1. POLYMERS

The development of the plastics industry began at the end of the XIX century when the manufacturers of billiard balls sponsored a competition for finding out other materials, which could replace ivory.

Experimental activities carried out in the 1930s and 1940s led to the production of long chains of molecules: polymers. A better understanding of their chemical composition and structure allowed the manufacturing of several goods by the packaging and housewares industry.

The World War II period was characterized by a continuous research on materials, which could both guarantee specific insulating properties and be applied for various military uses. Safety helmets, for instance, were made of polymers.

After the War, the research did not stop. Indeed, in 1950s the first engineering thermoplastics were developed, placing them in a competition with metals, widely used in the engineering industry. The aerospace industry started to require materials, which could withstand high temperature, and after 1960s, new thermoplastics were introduced for this aim.

Since that time the relationship between the polymers structure and their properties has been widely investigated, indeed nowadays the combination of new and low cost monomers is possible, allowing the creation of specific polymers, according to the quality and structural properties required

for the final product. Some polymers are comparable, because of their characteristics, to some materials traditionally used by industries, like metals, but their economic value makes them actually incomparable.

Furthermore, another interesting aspect is related both to the wide variety of polymers that may be produced (e.g. solid and foams, porous and no porous) modifying their chemical and physical structure and to the broad range of sectors where they may find application. It's worth to pointing out that polymers are present in daily life's people, going from their houses to their cars and in their free time activities (e.g. sport accessories). These materials have become essential and imaging the world without them seems impossible.

Further investigations are currently in progress for dealing with the recycling process of polymers, which represents a big challenge. A big amount of plastics is used and wasted every day; therefore, developments are necessary for reusing somehow those materials, so that the environmental impact related to their use might be reduced.

FIGURE 1.1 EXAMPLES OF POLYMERIC OBJECTS

In the next sections of this chapter, details on the classification of polymers and on the processes involved in their manufacturing are provided.

An infinite number of polymers exists and several classifications could be discussed. To report a brief example, according to the molecular structure, polymers may be *elastomers* characterized by elasticity, *fibers* characterized by strength and toughness and *plastic films* characterized by flexibility. This work focused on specific polymers, which have been selected according to their chemical and mechanical properties and for carrying out the experimental investigations, which this research is based on.

Before introducing the main polymers and their characteristics, it is interesting highlighting how industries deal with these materials. It is possible to distinguish three main typologies of industry that may, in some cases, overlap: the first one produces the raw materials which polymers are made

of, the second one processes the raw materials for getting semi-finished products and the third one produces end-use products.

The first step involves the transformation of monomers into polymers using polymerization techniques, which are chosen according to the properties that the industry needs for its polymers. The macromolecules may be oriented during the process and this represents one of the main advantages of these materials, since the same polymer can become softer or stronger as a function of the macromolecules orientation (Fakirov, 2008). Therefore, versatility may be considered the principal characteristic of polymers and the main reason of their growth and wide use during the years. Furthermore, manufactures may process polymers using additives or other chemical substances to enhance the basic properties or to confer specific characteristics (e.g. coloured, heat resistant, fiber-reinforced). Finally, they may be provided to the processing industries in several forms, such as liquid, granules, pellets and powder too.

The plastic industry for converting polymeric raw materials into useful semi-finished or finished products of a specific shape may employ several processing operations and companies are usually categorized according to the processes they perform. The main processes are:

- Injection molding
- Blow molding
- Extrusion blow molding
- Injection blow molding
- Rotational molding
- Compression molding
- Transfer molding
- Casting

1.1.1. POLYMERS CLASSIFICATION

Polymers are made of monomers repeated along a chemical chain. Depending on the monomers repetition, on their variety, on their links, on their composition, polymers are classified in many ways.

The first one is related to the origin and chemical composition. Polymers can be *inorganic* (glass) or *organic* (epoxy resin). Organic may be further divided in *natural* (proteins) and *purely synthetic*. Many polymers families belong to the synthetic category, such as fibers, elastomers, plastics, adhesives.

The second classification is based on the material structure, which is defined in terms of crystallinity. Indeed, after the cooling from the molten state, the molecules are attracted to each other and reach a solid state which may be defined as *crystalline* or *amorphous* (Figure 1.2). In crystalline polymers, the molecular chains are orderly locked to each other and, if a load is applied, the material breaks rather than bends.

In amorphous polymers, molecules are randomly positioned and this makes the material flexible and elastic. Actually, there are not polymers that are completely crystalline, there is always a percentage of material that has an amorphous structure. In detail, there are crystals that do not have a regular shape, are smaller and are connected in a disordered manner. For this reason they are

called *semi-crystalline* and the degree of crystallinity helps to characterize the material and therefore to define its properties. The amorphous phase defines the nature of crystalline polymers since that phase can exist in a rubbery and glassy state. A crystallization of that phase may modify the global properties of the polymer and the effects of this process on an amorphous phase in a rubbery state are more evident than on an amorphous phase in a glassy state, obviously, because in this latter case the modulus is already high.

Polyethylene is an example of semi-crystalline polymer, while Poly(methyl methacrylate) and polycarbonate are examples of amorphous polymers.
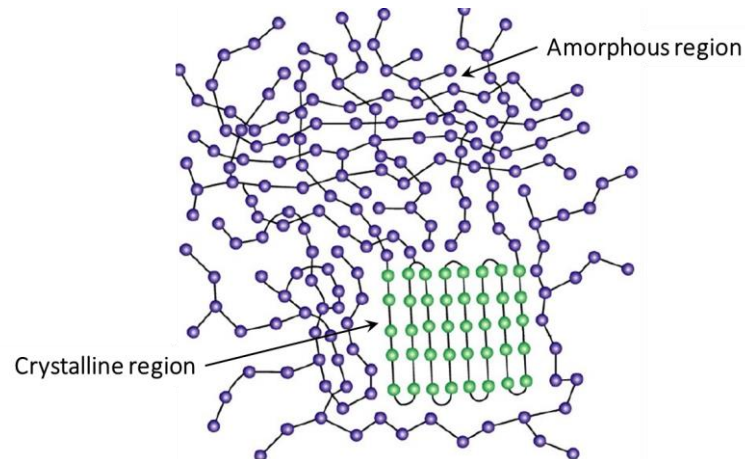
FIGURE 1.2 AMORPHOUS AND CRYSTALLINE REGIONS IN POLYMERS

The graph in Figure 1.3 shows the relation between the thermal behaviour and the polymer structure. The molecules of a polymer are able to move according to the cohesive forces that characterise the material structure and that depend on the thermal energy. This latter is responsible of the transition of a polymer from a solid state to a viscous one. In this regard, two temperatures have to be defined: the glass transition temperature T_g and the crystalline melting point T_m.

When a polymer reaches its T_g, the amorphous region gets from a glassy state to a rubbery one (or from rubber to glass during cooling). This means that, in case of a semi-crystalline polymer, just the amorphous part undergoes this first transformation. If the temperature continues increasing, the crystallites start melting and when the last crystallite melts means that the T_m temperature is reached. Therefore, the T_m value is a function of the crystallinity degree and of the crystallites size.

In detail, when an amorphous polymer is heated, at first its volume starts expanding at a constant rate until the T_g is reached. After that the hard and glass material becomes rubber until the temperature reaches the T_m value. A further increase of the temperature leads the material to a viscous liquid state until decomposition. For a crystalline polymer, on the other hand, the change of state after the T_g is less evident because, as mentioned before, the crystalline part is not affected by the temperature increase, so in the region between T_g and T_m the crystallites are dispersed in an amorphous matrix, which has become rubber, and therefore the material appears still rigid. After reaching T_m, the crystalline material becomes a viscous liquid.
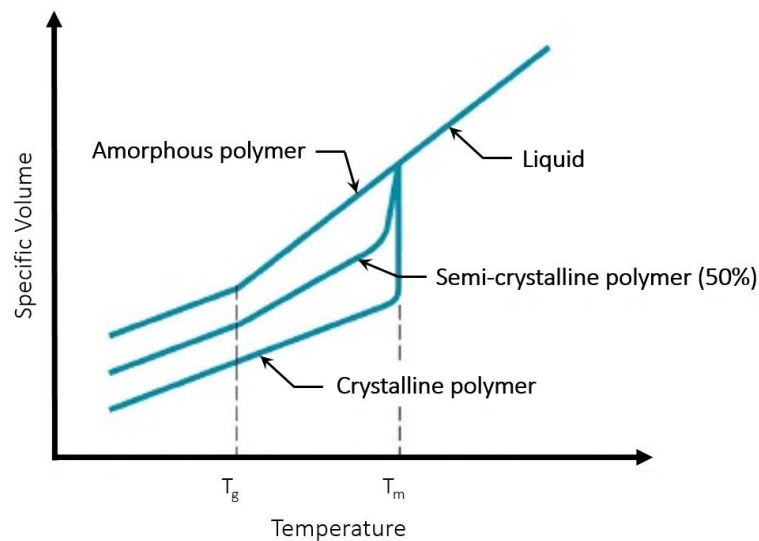
It is worth noticing that for industries the knowledge of the T_g and T_m values is a fundamental requirement because, according to them, the processing technologies may be selected and the end use of products designed. Furthermore, a material operational limit (MOL) value has been introduced, in order to provide a safety margin of the material temperature.

A further classification is based on the molecules bonds due to the polymerization techniques, which define the atoms configuration. Polymers may be classified as *fibers*, *elastomers* and *plastics*. Fibers are linear polymers with high symmetry and high intermolecular forces, so that they are characterized by high modulus, high tensile strength and moderate extensibilities (nylon is an example). In elastomers, the molecular structure is irregular and the intermolecular attractive forces are weak. This allows their flexibility and high extensibility, which is reversible when the stress is removed. High modulus and strength characterize the elastomers when are stretched. Plastics are a compromise of structural properties of fibers and elastomers (polypropylene and polyvinyl chloride are examples).

Depending on their thermomechanical response, polymers can be classified as *thermosets* and *thermoplastics*. Their different thermal behaviour is due to the different chemical bonds and intermolecular forces. Indeed, when a thermoset polymer is heated and pressure is applied to confer a desired shape, its chemical structure undergoes an irreversible transformation, because the cross-links are strong, so chemically linked, and the heating cannot break the attractive forces and chains are not free to flow. This means that just one cycle of softening and curing is tolerated. Phenol–formaldehyde, epoxies, bakelite are examples of thermoset polymers.

On the contrary, thermoplastics can be heated and cooled many times without compromising the structural properties of the material. This happens because thermoplastics are characterized by linear molecules and weak forces between the molecular chains. Therefore, by warming, molecules can move and deform easily. Polyethylene and polyamide are examples of thermoplastic polymers.

The graph below (Figure 1.4) shows how the modulus of thermoplastics and thermosets changes as a function of the temperature. Thermoplastics get from a glassy state to a rubbery state when the temperature starts increasing and reaches a flow state when the temperature is high. On the other

hand, thermosets are characterized by a high modulus even in the rubbery region and the flow region for these materials does not exist absolutely.
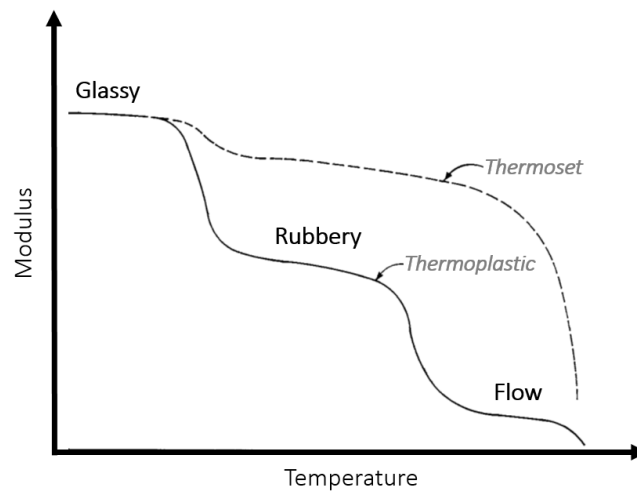
FIGURE 1.4 MODULUS–TEMPERATURE FOR THERMOPLASTICS AND THERMOSETS

Finally, considering the end of use, polymers may be classified as *engineering plastics* (polyimide, PEEK, polyamide, polycarbonate) and *general purpose plastics* (polypropylene, PVC). In detail, engineering polymers are defined as high-performance materials because of their excellent properties. They are mostly strong, stiff, tough with high thermal stability and have excellent chemical resistance, good weatherability, high tensile, flexural, and impact strengths and can withstand a wide range of temperatures. They are replacing conventional materials in many sectors, like metals in automotive applications and for further engineering purposes where high strength-to-weight ratio is a priority requirement (Ebewele, 2000; U.S. Department of Defense, 2002a).

A complete description of the materials used for the experimental investigations, presented in the next chapters, is provided as follows.

POLYAMIDES

Polyamide (PA) is a polymer whose chemical chain is characterized by amide linkages. This is a synthetic material commercially known as *nylon* and two products belong to this category: nylon 6 and nylon 6.6 that differ for the molecules, which react to each other during the condensation mechanism (Ebewele, 2000).
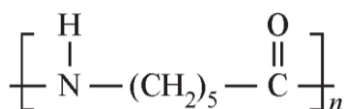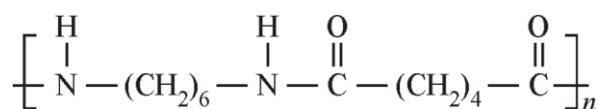
FIGURE 1.5 NYLON 6   FIGURE 1.6 NYLON 6.6

They are widely used for several applications because of a good balance of properties (good impact, tensile and flexural strengths, low-friction properties and good electrical resistivity) and cost.

The manufacturing processes affect the dimensions of polyamide products. After moulding, for example, the moisture absorption causes an increase of the part and for this reason, when they have to be used in such applications where the performance of the part is strictly related to the dimensions, a subsequent phase of annealing is required to fix the accurate shape. Furthermore, their tendency of absorbing water make them not good insulators and not suitable for those applications where humidity could be a condition. Their high melting point allows the use of polyamide parts in such circumstances where 150 °C could be reached, but not for a long exposure because in that case the material is easy of oxidizing its surface in air (Salamone, 1996).

Further polyamide exist but they are much more expensive (Ashter, 2013). Their properties can be improved incorporating into the basic material some additive, such as heat stabilizers and fiber reinforcements (Ebewele, 2000; Fakirov, 2008).

The mechanical properties of the main polyamides are listed in Table 1.1.

TABLE 1.1 MECHANICAL PROPERTIES OF POLYAMIDES (SALAMONE, 1996)

Polyamide	Tensile Strenght [MPa]	Tensile Modulus [GPa]	Flexural Modulus [GPa]	Elongation at break [%]
PA6	70	2.8	2.2	15
PA6.6	85	3.0	2.8	5
PA6.10	55	2.1	1.1	70
PA11	38	1.4	1.2	250

The polyamide industry serves several markets according to specific applications of the parts and to the required properties. The main sectors and examples of the manufactured elements are (Ebewele, 2000):

- *Automotive* (speedometer gears, door lock wedges, distributor point blocks, wire insulation, fuel vapor canisters, mirrors and grilles; pneumatic tubing and lubrication lines, fuel and fuel-vent lines).
- *Electrical and electronics* (connector, tie straps, wire coil, bobbins, tuner gears).
- *Industrial/machinery* (window and furniture guides, pump parts, power tools, fans, housings, gears, bearings, bushings, screws, nuts, bolts).
- *Monofilament/film coatings* (fish nets, brush bristles, food and medical packaging, coatings for wire and cable)
- *Appliances* (refrigerators, dishwashers, ranges, hair dryers and curlers, corn poppers, smoke detectors)
- *Consumer items* (combs, brushes, housewares, buttons, rollers, slides and racquets).

TABLE 1.2 PA PROPERTIES FOR SPECIFIC APPLICATIONS (EBEWELE, 2000)

Applications	Responsible Nylon Properties
Gears, bearings, bushings, cams	High tensile and impact strength, toughness, lubricity, low coefficient of friction

Screws, nuts, bolts	High strength, corrosion resistance
Food packaging	Low permeability to water and air to preserve freshness, high strength, puncture resistance
Coatings for wire and cable	Resistance to stress cracking, abrasion, and corrosion, low moisture absorption

Polypropylene

Polypropylene (PP) belongs to the thermoplastic polyolefin polymers, which means that is obtained by polymerizing the olefin propylene (British Plastics Federation, 2018).
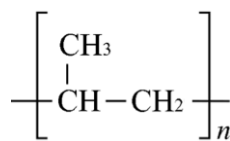
FIGURE 1.7 POLYPROPYLENE

Polypropylene resin was produced for the first time in 1954 by the Italian Professor Giulio Natta. The first commercialization dates back to 1957 and after that this polymer has become a popular and successful raw material for producing a wide range of products.

Polypropylene is considered very versatile because of its wide applications both as plastic and as fiber. As plastic, it is used, for instance, for producing food containers, because of its thermal property of melting over 160 °C; as fiber, it is suitable for outdoor applications, mainly because it is easy to colour and because it is moisture resistant.

Furthermore, excellent electrical and insulating properties, good chemical and heat resistance, low density, high softening point, high tensile strength, stiffness, and hardness characterize PP. These latter three properties are due specifically to the high degree of crystallinity of the material.

Polypropylene is considered the second most widely produced polymer in the world and it may processed by several manufacturing technologies, mostly by extrusion and injection moulding.

The processing technologies are chosen according to the end-use of the product. Examples are:

- *Packaging*. Food, tobacco and clothing sectors make use of PP in the film form. Blow moulding allows the production of rigid PP containers, like bottles or cups.
- *Automotive*. PP is mainly used for interiors, but also bumpers are made of this material as well.
- *Medical devices and instruments*. Syringes, diagnostic cuvettes, urine and sample cups as well as contact lenses are examples of products for medical applications.
- *Consumer products*. PP is utilised for producing furniture, luggage, toys and other sustainable goods for gardens and houses.

It is important to highlight that, due to the PP versatility, the properties of the material vary in a quite wide range of values (Table 1.3). This depends on the specific molecules weight that industry have to consider during the product design according to the specific final requirements.

TABLE 1.3 PHYSICAL, MECHANICAL, THERMAL AND PROCESSING PROPERTIES OF PP

Property	Metric
Density	0.880 - 2.40 g/cc
Tensile Strength, Ultimate	9.00 - 80.0 MPa
Tensile Strength, Yield	4.00 - 369 MPa
Elongation at Break	3.00 - 900 %
Modulus of Elasticity	0.00800 - 8.25 GPa
Flexural Modulus	0.0260 - 6.89 GPa
Melting Point	61.0 - 220 °C
Crystallization Temperature	110 - 115 °C
Processing Temperature	87.8 - 274 °C
Melt Temperature	160 - 320 °C

ACRYLICS

A wide number of plastics belong to the acrylics, of which crylates and methacrylates are the main components. The broad variety is due to the large combinations of monomers and this provides products with different properties ranging, for instance, from soft to hard.

Acrylic resins are generally characterised by excellent chemical resistance, weather resistance, discoloration resistance, good electrical properties and furthermore they show low water absorption and slow burning rate.

The glass transition temperature of acrylics is around 105 °C and they have a wide rubbery range. Indeed, before decomposition, a temperature of around 170 °C has to be reached.

Injection molding, extrusion, thermoforming and machining are the main processing technologies involved in the production of acrylics components (Brydson, 1999; Pielichowski and Njuguna, 2005).

POLY(METHYLMETHACRYLATE)

Poly(methyl methacrylate) (PMMA) is an amorphous polymer and may be considered the most important acrylic (Ashter, 2013).
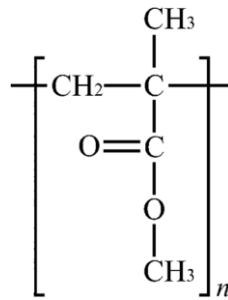
FIGURE 1.8 PMMA

It is a transparent and hard plastic, characterized by an excellent weatherability and by good chemical, electrical and thermal (Table 1.4) properties.

TABLE 1.4 PMMA THERMAL PROPERTIES (ASHTER, 2013; EBEWELE, 2000)

Tg	Heat deflection temperature	Service Temperature
85 -165°C	74 - 100 °C	93 °C

The temperature ranges are due to the broad compositions commercially available.

These properties combined with its intrinsic stiffness, density and moderate toughness make the PMMA a material to use for outdoor applications or for those that require light transmission. Typical PMMA applications involve the following sectors (Ebewele, 2000):

- *Construction.* Enclosures for swimming pools, shopping malls and restaurants, tinted sunscreens to reduce air conditioning and glare, domed skylights.
- *Lighting.* Lighted signs, luminous ceilings, diffusers, contact lenses, instrument panels, signals and nameplates.
- *Aviation* Windows. Instrument panels, lighting fixture covers, radar plotting boards, canopies.
- *Household.* Housings, room dividers, decorating of appliances, furniture, vanities, tubs, counters.
- *Others.* Display cabinets and transparent demonstration models in museums, exhibits, and departments stores.

PMMA is generally processed by extrusion and molding.

1.1.2. Forming processes for polymers

The production of a polymeric component with a specific shape involves first the material selection and then the adoption of a processing technique. The material choice is not an easy phase because a wide number of polymers exist. Their specific properties and their unit cost are the driving factors that usually bring to the material selection, according to the end-user requirements.

Several technologies are available for processing polymers. Furthermore, the increasing use of plastics led to the introduction of new materials as well as of new manufacturing techniques, whose success is linked to the cost-quality ratio.

In Figure 1.9 a schematic of a generic production cycle for obtaining a polymeric object is shown.
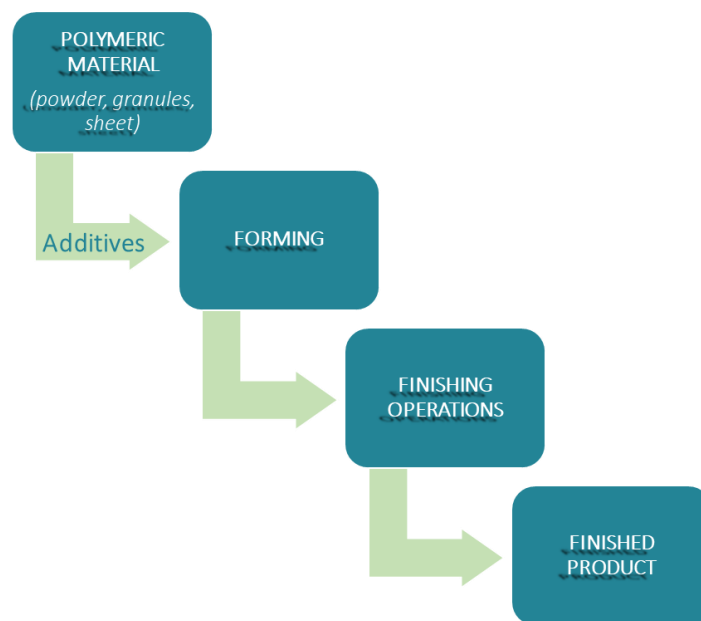
FIGURE 1.9 PRODUCTION CYCLE OF POLYMERIC PRODUCTS

The main and most common polymer processing methods are discussed below. The processing operations, the characteristics and the typical applications of each specific method are described and reported.

It is worth pointing out that the same product, such as a bottle, may be fabricated using different manufacturing technologies and the choice is related to the selected material and to the production requirements, in terms of costs, quality and performance.

Injection Molding

Injection molding is one of the main techniques for manufacturing plastic components both from thermoplastic and from thermosetting pellets or powders.

The injection-molding machine consists basically of an injection unit and of a clamping unit (Figure 1.10). In the first part, the polymer granules are inserted into a hopper and heated until they melt. A rotating screw allows the mixing of the material and the injection by pressure into a mold cavity, where the material is then cooled. The mold, made of steel plates which define the shape to confer

to the final product, and the water cooling channels belong already to the clamping unit where the temperature is controlled and the material remains until solidifies. After that, the formed part is ejected by opening the mold (Ebewele, 2000; Thompson, 2007).
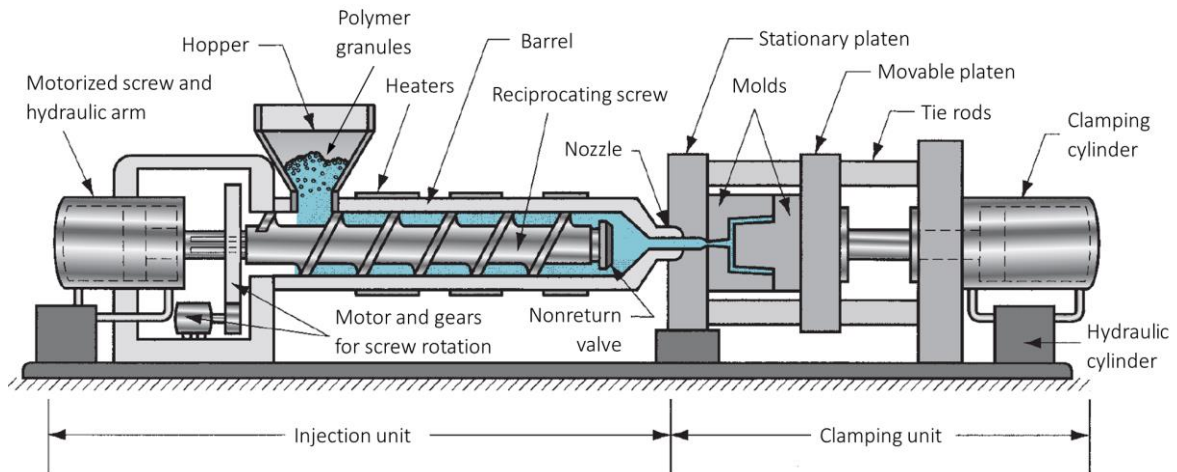
FIGURE 1.10 INJECTION MOLDING PROCESS (MIKELL P. GROOVER, 2010)

Excellent repeatability, speed and good surface finish characterize the process. The cost of the process is mostly related to the mold size and shape: the more complex the shape is, the more expensive the process becomes.

Injection molded components find application in several sectors, such as automotive and household. Typical examples are car seats and bumpers, cutlery, buttons, shopping baskets, garden furniture (Thompson, 2007).

BLOW MOLDING

Blow molding is a process usually employed for manufacturing large volumes of bottles, packaging containers and other thin wall items.

The basic principle of the process is: the polymeric raw material is melted and hallow tube or parison are shaped. Air is then blown into the soft material, which is expanded into the cold mold.

The plasticizing of the resin and the formation of the parison may be carried out in two main ways, appropriate for different industries. The techniques are *extrusion blow molding* and *injection blow molding*.

EXTRUSION BLOW MOLDING

When the extrusion blow molding process is performed, an extruder is utilized for plasticizing the resin and forming the parison.
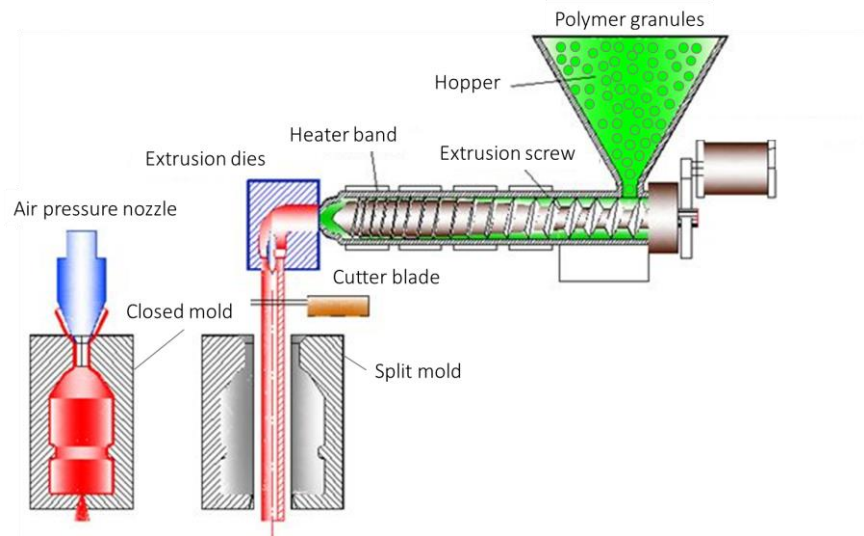
FIGURE 1.11 EXTRUSION BLOW MOLDING PROCESS (KALPAKJIAN AND SCHMID, 2014)

The polymer granules are inserted into a hopper, coloured if necessary, mixed, pushed by a screw and extruded by an extruder in a downward direction. The parison is positioned between the two halves of the mold and cut at the top as soon as reaches a specific length. For the blowing phase, a rod is inserted into the parison for blowing air and conferring the mold shape to the material. After cooling, the part is removed from the molds. A sketch of the process is shown in Figure 1.11.

In a continuous extrusion blow molding process, the synchronization between the parison forming rate and the blowing-cooling-removal rates is ensured. On the other hand, when the intermittent extrusion blow molding process is perfomed, the parison formation is not continuous. Indeed, after the extrusion of the parison, the other melted material is accumulated at the end of the screw and is extruded just when the previous molded part is extracted from the machine.

Medical, chemical and consumers industries perform the extrusion blow molding process of several materials (e.g. polypropylene (PP), polyethylene terephthalate (PET), polyvinyl chloride (PVC)) for the production of a wide variety of shapes and products, such as medicine bottles and consumer packaging (Ebewele, 2000; Thompson, 2007).

INJECTION BLOW MOLDING

The injection blow molding process consists of three main steps. First, a preformed part is injection molded with some finished details (see the neck of the bottle in Figure 1.12) and secondly it is transferred into the blow mold where the process is completed by the air blowing and the material takes the mold shape. The last step involves the cooling of the part and its removing from the mold.
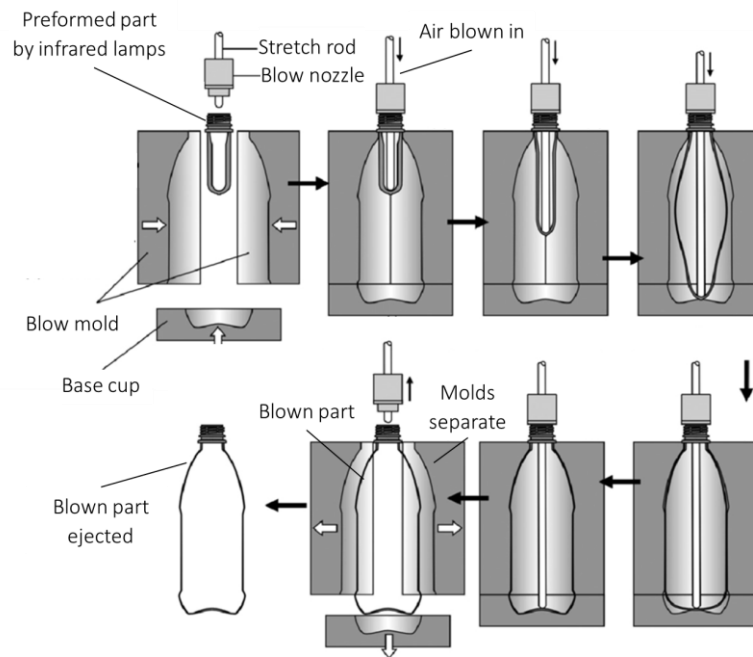
FIGURE 1.12 INJECTION BLOW MOLDING PROCESS (LIM ET AL., 2008)

This process is mainly suggested when the part to manufacture has limited size and does not have handles. The injection blow molded parts do not show variations in weight, volume and wall thickness and furthermore do not require additional finishing operations (Ebewele, 2000; Thompson, 2007).

ROTATIONAL MOLDING

Rotational molding is the process that allows the manufacturing of hallow and complex forms. The polymer material, in powder or liquid state, is positioned inside half mold that is then locked with a second half mold. The tool is heated at a controlled rate to avoid the degradation of the material that starts to melt. At the same time, the molds are put in rotation on vertical and horizontal axes. The rotation allows a uniform distribution of the material on the mold surfaces building up a coating with a constant thickness. The tool is then moved into a cooling chamber where both tool and material are cooled by air or water. After cooling, the output is ejected and the mold is ready for a new production cycle (Figure 1.13) (Ebewele, 2000; Thompson, 2007).

Rotational molding can be considered a cost-effective process since tooling is not expensive, furthermore since the material matches perfectly with the mold, the process is often preferred when finishing operations have to be reduced (Thompson, 2007).
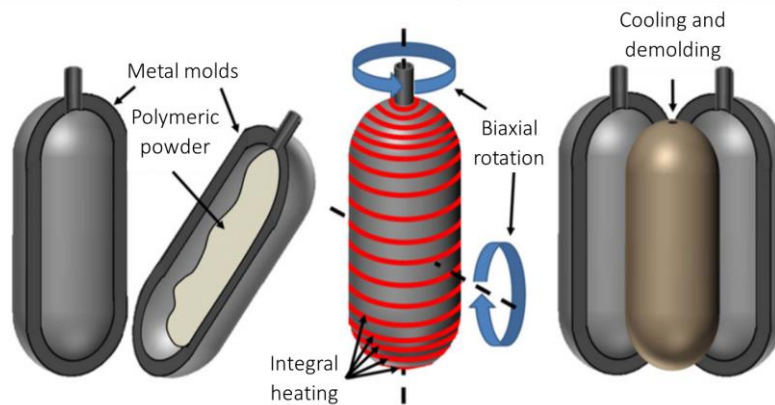
FIGURE 1.13 ROTATIONAL MOLDING PROCESS (MURRAY ET AL., 2017)

COMPRESSION MOLDING

Compression molding, together with transfer molding, are the main techniques used for forming thermoset materials (Ebewele, 2000), but the process is suitable also for thermoplastics.

Figure 1.14 shows the three main phases of the process. First, a measured quantity of polymeric compound is located into the mold cavity. A punch then acts on the material, which flows into the mold and due to the action of gradual pressure, generated by the contact of the mold halves, and of the heat, generated by steam, electrical or hot oil systems, the material starts melting. Finally, the tool is opened and the molded part is removed from it for cooling.
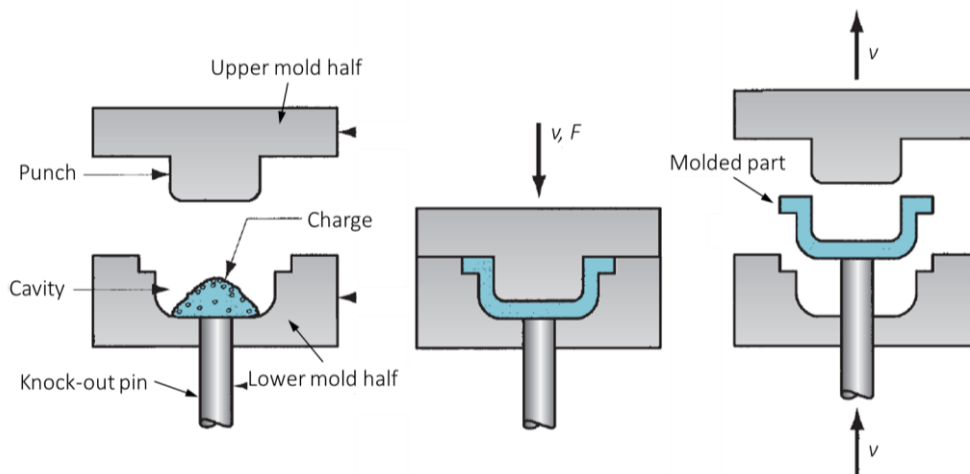
FIGURE 1.14 COMPRESSION MOLDING PROCESS (MIKELL P. GROOVER, 2010)

An advantage of compression molding is its cost, because a simple tool is required, the cycle time is rapid and no other finishing operations are needed. Nevertheless, an adequate control system for the material flow, temperature and cure time is strictly necessary, because these processing parameters influence the properties of the final product (Ashter, 2013; Ebewele, 2000; Thompson, 2007).

TRANSFER MOLDING

In transfer molding, before the process takes place, a specific amount of material is positioned into a portion of the mold called *pot*, where it is heated. The polymer is then forced, through the action of a plunger, into the closed cavity of the mold and at the same time, the air can escape from it through designed channels. Once the mold is filled, it is cooled at a controlled rate for ensuring the optimal curing of the material. When the cure cycle is completed, the part is ejected.
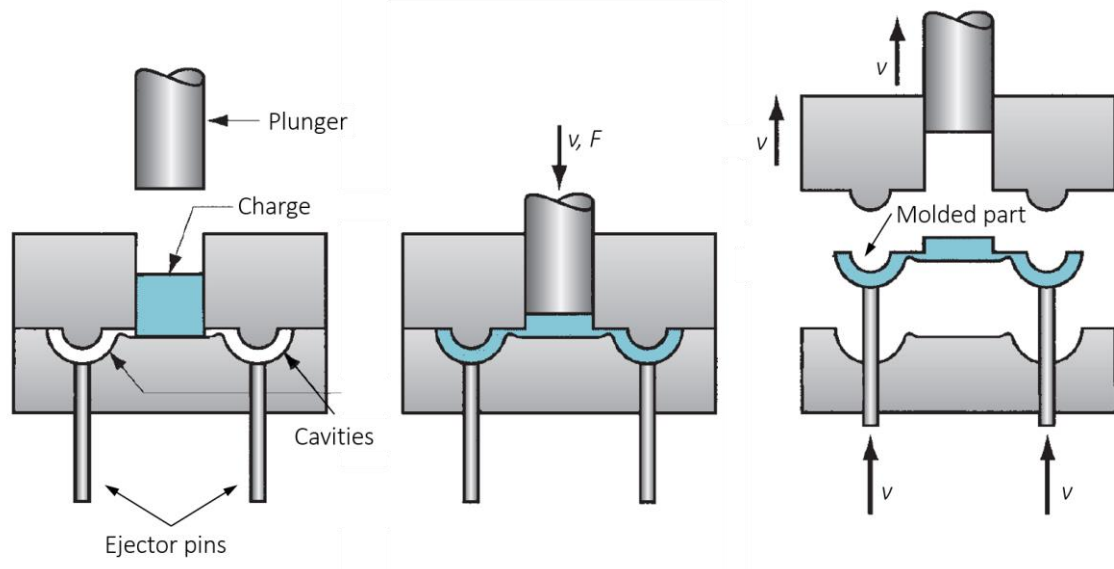
FIGURE 1.15 TRANSFER MOLDING PROCESS (MIKELL P. GROOVER, 2010)

Compared to compression molding, the processing time is shorter, but the cost of the mold is usually higher, because it tends to be complex and also the cleaning of the tool is very time and cost consuming. Furthermore, more scrap is produced, due to the presence of channels, besides it is not reusable when thermosets are processed (Ebewele, 2000).

CASTING

Casting is a process mainly used for prototypes and low volumes of products in automotive, sport and medical fields.

This process allows to replicate almost all the capabilities of injection molding. Compared to this latter, casting requires less pressure, a simpler equipment and more flexible tools, which make the process versatile.

The equipment consists of two molds, male and female and, if necessary, other parts may be added to form more complex shapes, for instance. Tools and material are heated at different temperatures and under appropriately controlled conditions. When the material is melted, it is drawn into the mold through a gate and flows up the risers, which ensure that the mold is completely filled. The molds remains closed until the material solidifies physically, by cooling, or chemically, by polymerization. When the curing time passes, the part is ejected and risers and excess material are removed (Ebewele, 2000; Thompson, 2007).
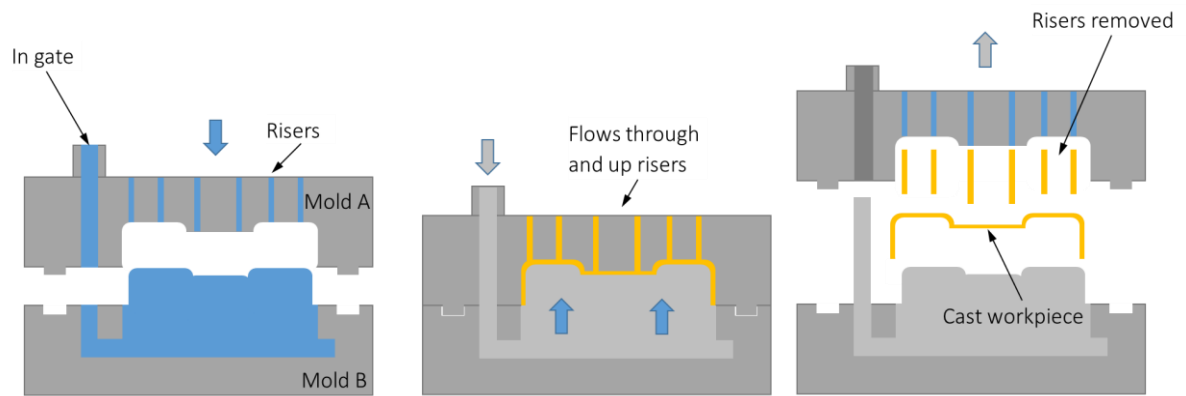
FIGURE 1.16 CASTING PROCESS

1.2. Composites

Composites, which definition and details are provided below, exist since ancient times when people started to combine different materials for their daily needs and applications.

The first composite dates back 3400 B.C. when Mesopotamians glued wood strips at different angles for creating plywood. Egyptians for instance, a millennium later, used plaster and papyrus for preparing death masks, as well as other populations used a combination of clay and hay for getting stronger buildings bricks.

From those times, infinite substances have been combined for getting new materials, such as synthetic plastics (like bakelite in 1907), glass fibers (1935), carbon fibers (1961), widely used today in many industrial sectors for improving the structural performance of parts, going from automotive to aerospace and marine and from medical devices to sport goods. Innovation in materials and the development of new manufacturing techniques has led to expand the application of composite, replacing traditional materials, like metals.

Universities, manufacturers, industries aim at investing in composite research for developing new manufacturing processes, new applications and for meeting the demand of more lightweight and more environmental friendly products.

FIGURE 1.17 EXAMPLES OF COMPOSITE PRODUCTS

A composite material consists of two main constituents (or phases), *matrix* and *reinforcement*, combined at a macroscopic level for producing new typologies of structural materials. Other substances, such as additives, may be added if necessary to enhance properties.

The combination of the two phases, characterized by different physical, chemical and mechanical properties, provides as output a material with unique properties, for instance in terms of strength,

stiffness and chemical resistance. These can be considered the main advantages, mainly when the strength/stiffness-to-weight ratio is considered and a comparison with conventional material, like metals, is carried out.

In Figure 1.18 is schematically represented the mechanical behaviour of a generic composite and of its single constituents. In the *1° stage,* the matrix and the fibers deform elastically and the curve is linear. In the *2° stage,* the matrix starts deforming plastically and the fibers continue stretching elastically, because of its higher tensile strength. As regards the composite behaviour, its failure begins when the fibers start to break, but since they are still embedded within the matrix that continues deforming plastically, the composite is still able to sustain the load.
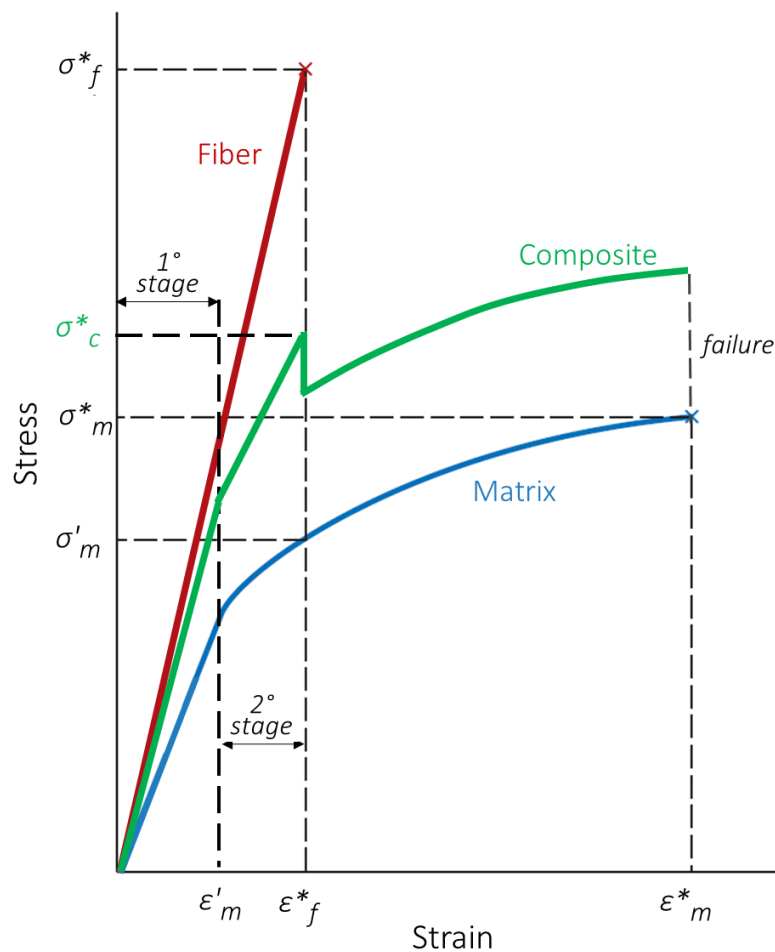
FIGURE 1.18 STRESS-STRAIN CURVE OF COMPOSITE

Limitations related to the composites are mainly due to the high processing costs and to the lacking of knowledge on some aspects, like the mechanical behaviour, which is not so easy to simulate also with available design tools. The composite characterization plays an important role to understand how the molecular weight distribution, the crystallinity of the matrix, the fiber type and orientation, and the strength of the interface may affect the properties and therefore the long-term performance of the part.

1.2.1. COMPOSITE CLASSIFICATION

Generally, composites are classified considering two levels: the constituent matrix, in terms of nature and typology, and the reinforcement form.

Figure 1.19 shows a schematic of the composite classification.
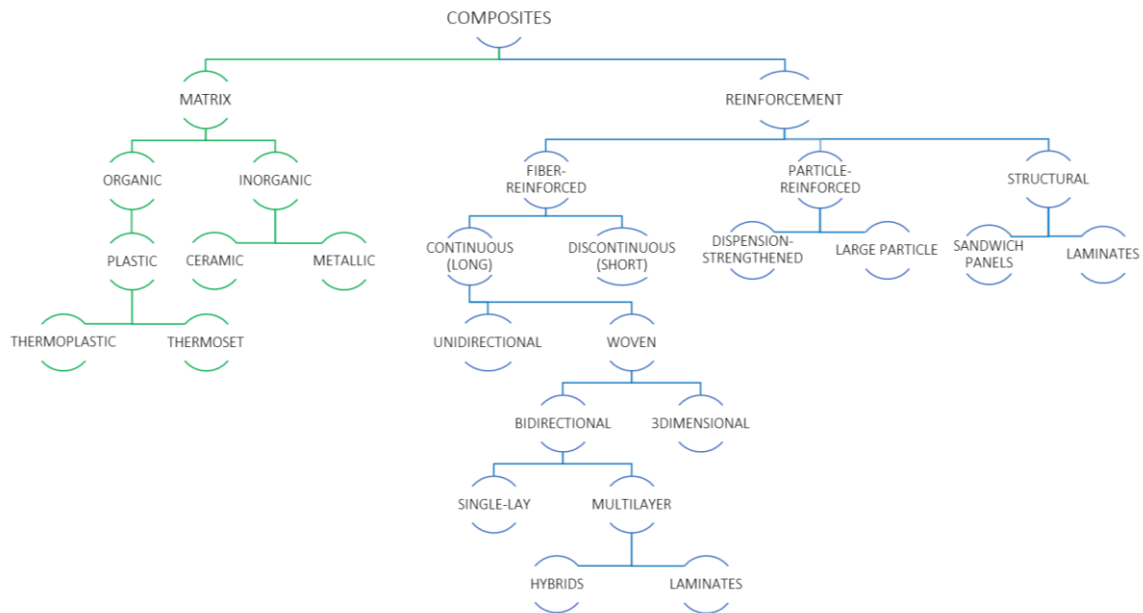
FIGURE 1.19 COMPOSITES CLASSIFICATION

The matrix can be made of plastic (PMC's), ceramic (CMC's) or metallic (MMC's) material. The first one is the most common and fiber such as glass, carbon and aramid are used as reinforcement. The second one is used when high temperatures characterize the application and short fibers or whiskers are used as reinforcement. The last typology is widely used in the automotive sector and silicon carbide fiber are, for instance, applied for reinforcing the aluminium matrix.

The matrix allows to i) hold the fibers in a specific position, ii) transfer the external loads to the reinforcement, iii) support the reinforcement when compression occurs and iv) protect the reinforcement from external factors and operating conditions. Even if the performance of the composite is mainly dependent on the reinforcement, the matrix plays an important role in terms of temperature, chemical, impact damage, moisture resistance (Ahmad, 2009; U.S. Department of Defense, 2002a).

As already explained in 1.1.1, according to the molecular chains, polymers can be classified as *thermoplastics,* where macromolecules are held together by secondary bonds (van der Walls) and *thermosets,* where the macromolecular chains are held together by covalent bonds, which are stronger than the previous ones. Therefore, if a matrix is made of a thermoplastic polymer, it means that it can be heated (325-450°C) and gets from a solid to a liquid state many times without compromising the material properties and after cooling (it can take few seconds) the material solidifies getting a specific shape. On the other hand, a thermoset matrix cannot be melted by heating, because it is not able to break the covalent bonds. Therefore, during the processing,

molecules react in an irreversible manner and the solidification of the material can take hours or even days to complete (Ahmad, 2009).

For the specific aim of this study, thermoplastic matrices have been investigated. The interest in thermoplastics increased in the last decades especially because of their intrinsic recyclability, the short processing time and their property to withstand high temperatures (Boria et al., 2017; Moreno and Saron, 2017).

In the following Table 1.5, a comparison between thermoplastic and thermoset is presented:

TABLE 1.5 THERMOPLASTIC VS THERMOSET MATRICES (AHMAD, 2009)

Characteristic	Thermoplastic	Thermoset
Cost	High	Low
Damage tolerance	Good	Average
Environmental durability	Exceptional	Good
Fiber impregnation	Difficult	Easy
Know-how	Limited	Extensive
Processing cycle	Short	Long
Processing temperature	High	Low
Processing pressure	High	Low
Reformability	Good	None

Furthermore, composite may have a *semi-crystalline* or *amorphous* matrix. In semi-crystalline polymers, molecules form ordered arrays, whereas in amorphous polymers molecules are randomly oriented. Semi-crystalline thermoplastics can be combined and reinforced with short/long fibers and, due to their excellent thermal/chemical stability, corrosion resistance and low moisture absorption, they are widely used in automotive, electronics and chemical industries.

Amorphous thermoplastics are also used in combination with short fibers in medical, communication, transportation, chemical industries. Reinforcing amorphous thermoplastics with long fibers is a recent development in the aerospace sector mainly because of their low cost processing at high production rates, good mechanical properties before and after impact, chemical stability. They are furthermore characterized by higher temperature capabilities, lower solvent and creep resistances and less property retention above the glass transition temperature than semi-crystalline thermoplastics (U.S. Department of Defense, 2002b).

The main techniques available to process semi-crystalline and amorphous thermoplastic composites are stamp molding, thermoforming, autoclave molding, diaphragm forming, roll forming, filament winding, pultrusion (U.S. Department of Defense, 2002b), which are widely discussed in the next paragraphs.

Based on the reinforcement typology, composites can be fiber reinforced, particle reinforced or structural. In fiber reinforced composites, long/continuous or short/discontinuous fibers are embedded in a matrix; particle composite are made of particles, in powder forms for instance, which are distributed in a matrix; structural composites, or also known as laminar composites, are made

layer by layer of different materials which are kept together by the matrix (sandwich structures for instance) (Figure 1.20).

A)   B)   C)
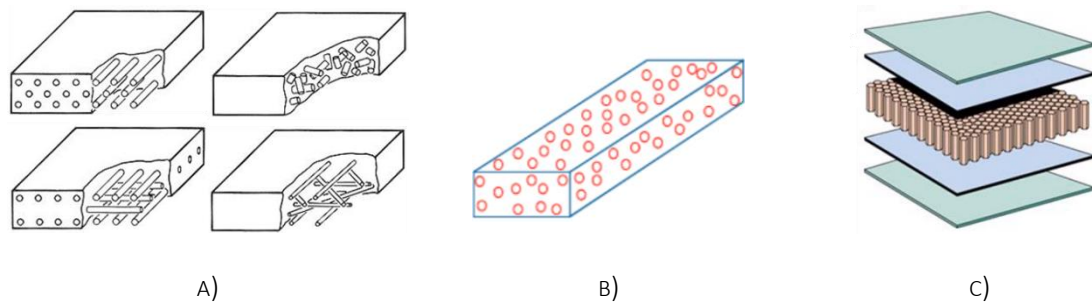
FIGURE 1.20 REINFORCEMENT TYPOLOGIES (ALHASHMY, 2012): A) LONG AND SHORT FIBERS, B) PARTICLE AND C) STRUCTURAL

According to the volume fraction of the reinforcement and its direction inside the composite, this latter can be isotropic or anisotropic (properties dependent or independent on direction).

Yarn   Plain weave   Twill weave   Satin weave

Woven fabrics

Knitted fabrics   Braids
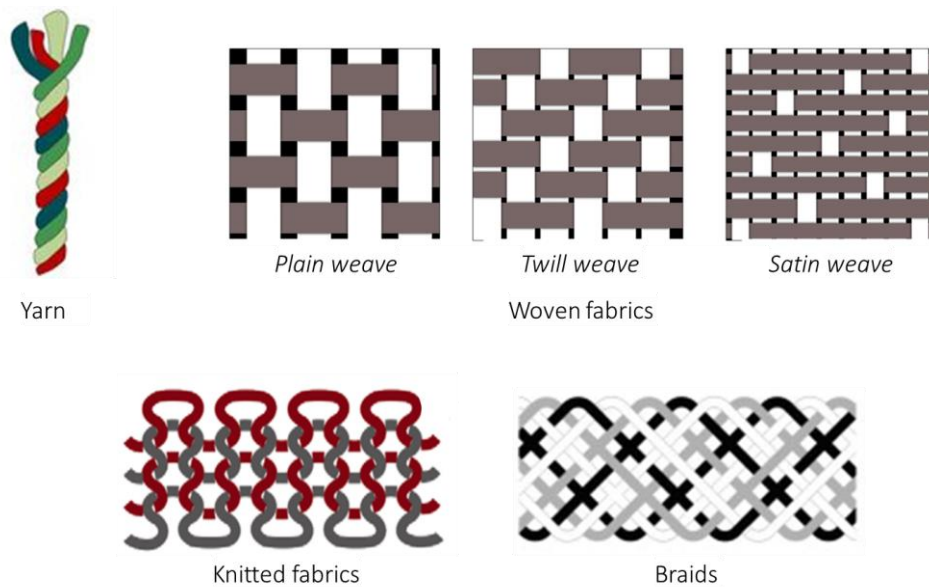
FIGURE 1.21 APPLICATION FORM OF FIBERS

A further classification regards the application form of fibers (Figure 1.21); their position inside the matrix influences the properties of the final part. Examples are: *yarns* when twisted fibers are collected (Tuttle, 2012), *woven fabrics* when continuous fibers are woven to form a fabric (Nurul Fazita et al., 2016), *knitted fabrics* when yarns are inter-looped (Abounaim et al., 2010), *braids* when more yarns are intertwined and two yarns are never twisted around one another (Gessler, 2011). As regards fabrics, it is worth pointing out that generally, the lighter or thinner the fabric is, the greater the fabric cost is (U.S. Department of Defense, 2002b).

This study focuses on fiber-reinforced plastics (FRP), which have gained a key role in the engineering materials development. A description of this typology of composite is provided below.

FRPs are composite made of a polymeric matrix and reinforced with carbon/glass/aramid fibers (Figure 1.22).

| A) | B) | C) |
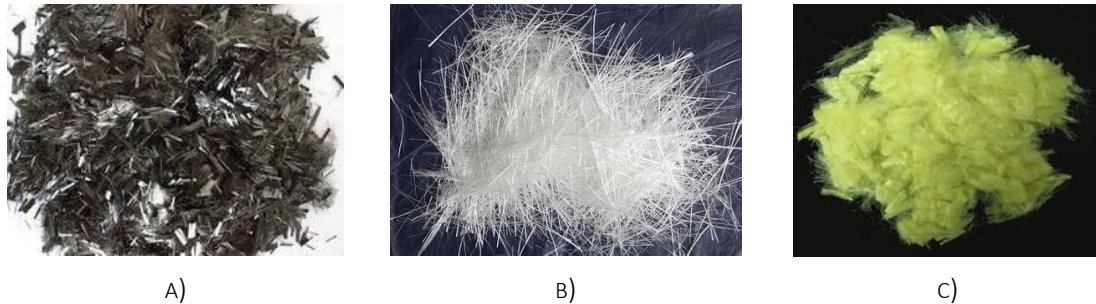
FIGURE 1.22 CARBON A), GLASS B) AND ARAMID C) FIBERS

They are characterized by high strength and stiffness and are corrosion and fatigue loading resistant. The special properties of these materials guarantee their application in several sectors, including aerospace, aircraft, automotive, marine, sporting, chemical, construction and commodity (Table 1.6).

TABLE 1.6 FRPS APPLICATIONS (AHMAD, 2009)

Sector	Examples
Aerospace	Satellite antenna, space structure, high pressure fuel tanks, rocket motor cases
Aircraft	Access doors, floor beams, entire wings, helicopter blades, seats, interior panels
Automotive	Body panels, dashboards, spoilers, bumpers, drive shafts, frames
Marine	Hulls, decks, masts, engine shrouds, interior panels, boat structure
Sporting	Tennis racquets, ski poles, protective helmets, bicycle frames, fishing poles
Chemical	Pipes, tanks, pressure vessels, hoppers, valves, pumps, impellers
Construction	Bridges and walkways, handrails, cables, frames, grating
Commodity	Chair, tables, ladders

A description of the main fibers used in combination with polymers is provided below.

Glass fibers

Glass fibers are by far the most predominant fibers used in the reinforced polymer industry for high-performance applications. In the XVI century glass started to be used as structural material, and two centuries later it started replacing metals and applied as reinforcement for military and aerospace structural purposes.
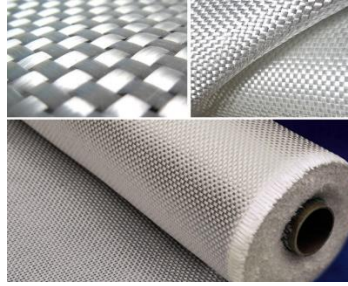
FIGURE 1.23 GLASS FIBER WOVEN ROVING

They are characterized by low cost and good mechanical and thermal properties. More in detail, they show low stiffness, low fatigue endurance, rapid degradation when exposed to moisture, high mechanical strength, high resistance to chemical and galvanic corrosion and excellent insulating capacity.

Many varieties of glass fibers are manufactured according to their specific use. They usually contain at least 50% of silica and the composition with different mineral oxides gives the resulting products distinct characteristics. The main typologies of glass fibers are briefly presented below:

- E-glass. It is an alkali free fiber used for general purposes made with alumina-calcium borosilicates. Its highly electrical resistance (E=electric), strength and low cost make the E-glass fiber the most commonly used for reinforcing polymers.
- S-glass. It is made with magnesium aluminosilicates and is known because of its high strength (S=strength), high stiffness, extreme temperature resistance, and corrosive resistance. It is considered the most expensive glass fiber.
- C-glass. It is a corrosive (C=Corrosion) resistant glass fiber made with calcium borosilicates used in acid corrosive environments.
- D-glass. It is a fiber made with borosilicates, characterized by a low dielectric constant (D=Dielectric), used therefore in electrical applications.

TABLE 1.7 GLASS FIBERS PROPERTIES (MATWEB)

	E-glass	S-glass	C-glass	D-glass
Density [g/cm^3]	2.54-2.6	2.48-2.49	2.52-2.56	2.11
Tensile Strength [MPa]	3450-3790	4585	3310	2415
Modulus of Elasticity [GPa]	72.4	85.5-86.9	68.9	51.7
Elongation at Break [%]	4.8	5.4	4.8	4.6
Dielectric Constant [GHz]	6.3-6.6	5.2-5.34	6.9	3.8

Carbon fibers: their mechanical properties are much better than glass fibers, in terms of high stiffness and high strength-to-weight ratios and, due to that, they are also more expensive. This explains their special application in aerospace and defence industries for manufacturing structural parts. Their first use dates back to 1950s for high temperature missiles (U.S. Department of Defense, 2002b).
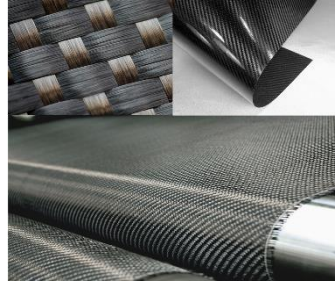
FIGURE 1.24 CARBON FIBER WOVEN ROVING

Carbon fibers are anisotropic, therefore the properties of the composite depend on the orientation degree of fibers. Indeed it is demonstrated that a carbon fiber reinforced composite is much more resistant when fiber are longitudinally rather than transversally oriented (Ahmad, 2009).

Another special property of carbon fibers is the high electrical conductivity, but in some cases, like in processing or in use, this represents a disadvantage and some problems may arise.

Aramid fibers: these fibers have been created industrially from a chemical liquid blend and are characterized by high strength, low density, good impact and heat resistance and good vibration damping. Because of those properties, they are widely used for ballistic applications (Lee et al., 2003) and sport equipment.

FIGURE 1.25 ARAMID FIBER WOVEN ROVING

The main synthetic aramid fiber is commonly known with its trade name Kevlar®, patented by DuPont™ in more than fifty years ago, thanks to the young researcher Stephanie Kwolek. It is a lightweight, durable and incredibly strong material, used at the beginning for replacing steel in racing tires. Its application increased during the years, going from sport and personal accessories (protective jackets, breeches, gloves, shoes) to construction, transport and electronics (DuPont).

1.2.2. FORMING PROCESSES

The manufacturing of composite parts involves the combination of matrix and reinforcement. This operation requires manual or automated methods for fibers distribution and can take place in a closed mold or on a mold surface. The final shape of the product is therefore dependent on the mold typology used during the forming.

Several processes may be involved in the manufacturing of a composite component. The choice is strictly related to the reinforcement (material, short/long, oriented/random), to the matrix

(thermoset/thermoplastic), to the final shape and size of the part and to the accuracy that has to be guaranteed.

In order to provide a general overview of the processes involved in the manufacturing of final composite products, they have been classified in Table 1.8 according to the nature of the matrix (thermoset or thermoplastic) and to the fiber typology (short or long). The most important ones are described in the next paragraphs.

TABLE 1.8 MANUFACTURING PROCESSES FOR COMPOSITES

Manufacturing Process	Thermoset		Thermoplastic	
	Short fibers	Long fibers	Short fibers	Long fibers
Composite Laminating				
Wet/Hand Lay-Up		✓		
Spray-up	✓			
Prepreg Lay-Up	✓	✓		
Resin Transfer Molding (RTM)		✓		
Compression molding				
Sheet Mould Compound (SMC)	✓			
Bulk Moulding Compound (BMC)	✓			
Filament winding		✓		
Roll wrapping		✓		
Autoclave process		✓		✓
Pultrusion		✓		✓
Injection molding	✓		✓	
Bladder molding		✓		
Blow molding			✓	
Additive Manufacturing (AM)	✓	✓	✓	✓

COMPOSITE LAMINATING

In *wet/hand lay-up* woven/bonded fabrics are placed in a mold and the resin is then impregnated by a roller in order to force it into the raw material, to ensure a uniform distribution and to remove porosity (Figure 1.26 A)). Actually, the process starts spraying on the mold surface a gel coat, which cure when there is no oxygen. Fiber and resin are laid on this gel and the curing takes place under room temperature conditions. It is a simple and low-cost process, but due to the manual forming, the quality of the part is dependent on the worker skills. The resin amount is not easy to control and this can cause voids inside the composite; to solve this problem the fabric may be pre-impregnated with resin, laid in a mold and kept at a low temperature (to prevent premature curing) and then cured by heating in an autoclave (*prepreg lay-up*) (Mazumdar, 2001; Thompson, 2007).

In *spray lay-up* long fibers are fed to a gun and chopped into suitable length before being sprayed on a mold, together with the resin (Figure 1.26 B)). The process stops when the desired thickness is obtained and after that, the materials are cured under standard atmospheric conditions. It is a low-cost process (tooling and materials), suitable for small/medium components that do not have high structural requirements and do not require high dimensional accuracy and repeatability (Mazumdar, 2001; Thompson, 2007).

Resin Transfer Molding (RTM) is a vacuum based process suitable for large and complex items with high strength-to-weight, structural and high quality finish requirements. The long fiber-reinforced material is placed on a preheated die, which is then clamped to a second mold, and pressure is applied. After removing the air by a vacuum pump, an injector allows the transfer of the resin into the mold until it is filled. After the resin curing, the molds are separated and the part removed (Figure 1.26 C)). Some variations of RTM exist and they can be classified according to the method used for combining the dry reinforcement and the resin during the forming (Ahmad, 2009; Mazumdar, 2001; Thompson, 2007).
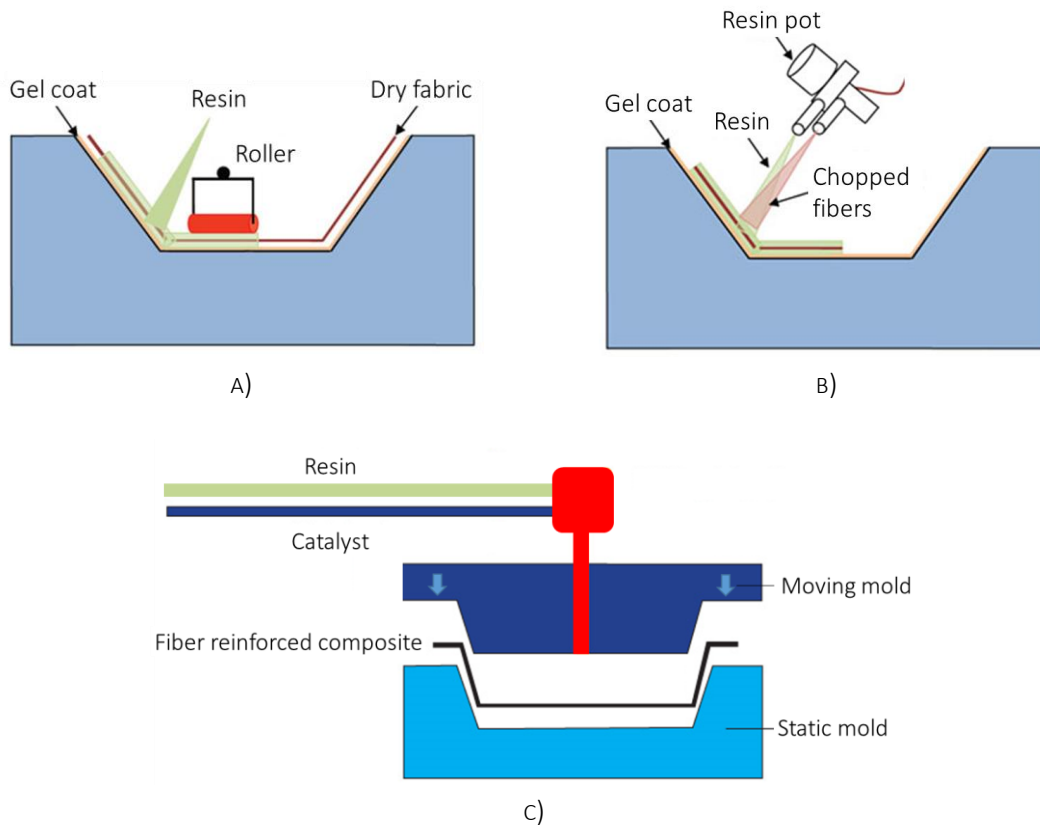
FIGURE 1.26 A) WET/HAND LAY-UP, B) SPRAY LAY-UP AND C) RESIN TRANSFER MOLDING (RTM)

COMPRESSION MOLDING

Sheet Molding Compound (SMC) and Bulk Molding Compound (BMC), or also known as Dough Molding Compound (DMC), are the main raw materials to perform the *compression molding* process for forming structural and lightweight composite parts.

For manufacturing the *Sheet Molding Compound*, long fibers are chopped, placed between two layers of a paste and rolled for abtaining a single sheet of a required thickness (Figure 1.27 A)). A *Bulk Molding Compound*, instead, is produced mixing chopped fibers and resin and a billet is extruded (Figure 1.27 B)).
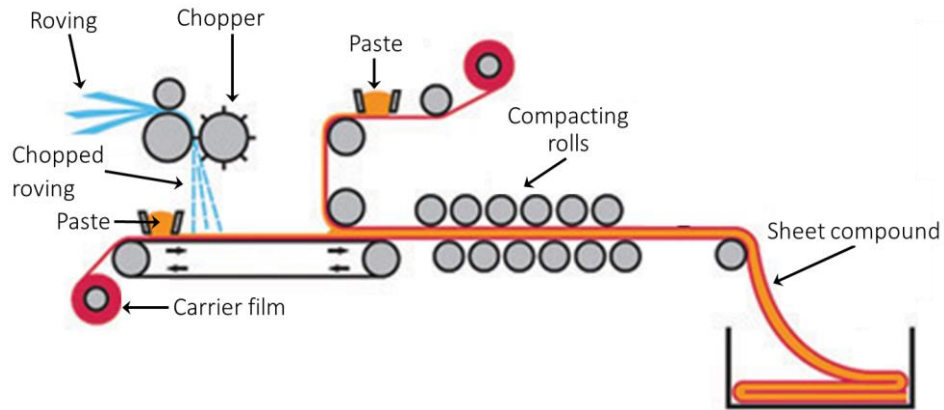
A)
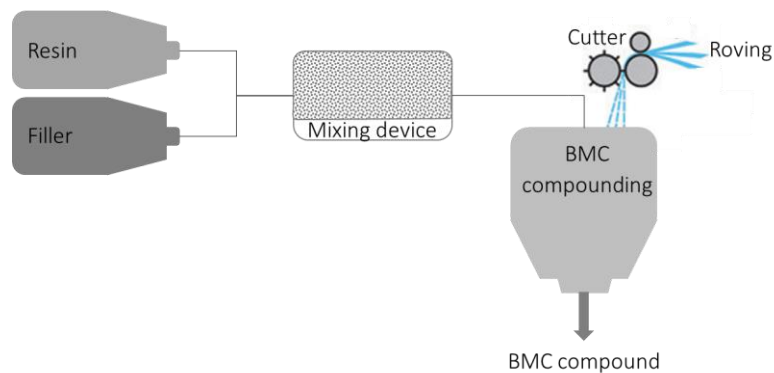
B)

FIGURE 1.27 A) SHEET MOLDING COMPOUND (SMC) AND B) BULK MOLDING COMPOUND (BMC)

The *compression molding* operations are the same for the two raw materials (SMC and BMC): i) loading of the sheet/bulk compound between two steel molds, ii) forcing the compound by moving the upper mold, ensuring an uniform distribution of the material into the cavity, iii) heating and curing for obtaining the desidered shape, iv) extraction of the part from the molds by means of ejector pins (Figure 1.28). The manufactured part is characterized by high quality surface finish. It is a very expensive process, therefore it is recommended for big shapes and high volume production.
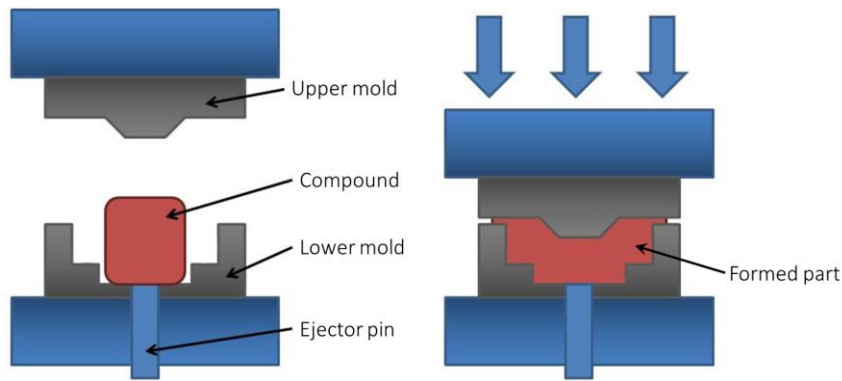
FIGURE 1.28 COMPRESSION MOLDING

FILAMENT WINDING

In *filament winding* a continuous yarn is impregnated in a resin bath and wound around a rotating mandrel for producing high strength and lightweight cylindrical parts (Figure 1.29). It is an automated process and this allows to obtain high-quality and high-volume components in a cost-effective manner (U.S. Department of Defense, 2002b).
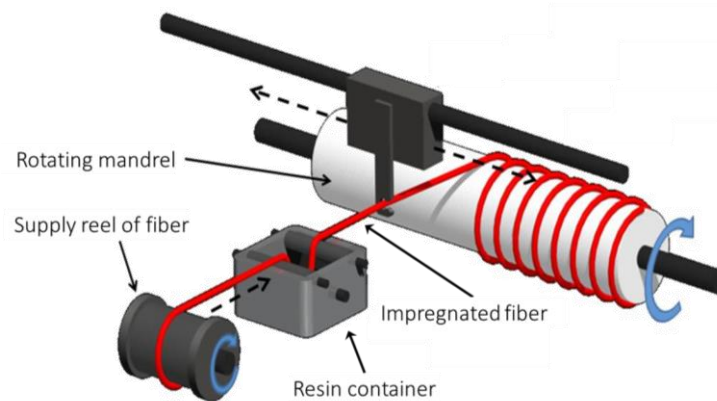
FIGURE 1.29 FILAMENT WINDING

Roll wrapping is a similar process with the exception that the mandrel has always a cylindrical/tubing shape. Pre-impregnated long fibers are rolled onto a mandrel and then wrapped with a consolidation tape, which applies pressure holding the part in place during the curing phase. After curing, the part is extracted from the mandrel and the tape removed, therefore the part is ready for further finishing operations.

AUTOCLAVE

Autoclave is a forming technology that may be performed both on thermoset and on thermoplastic composites. It is widely used in the aerospace industry for manufacturing complex shapes, characterised by high quality and high resistance. During the process pre-pregs are:
-    laid onto the surface of an open mold and spot welded;

- vacuum bagged;
- inserted into an autoclave for being processed.

In the autoclave, pressure and heat are applied for the consolidation phase. More in detail:

- vacuum is created inside the vacuum bag by means of a pump for removing air from interfaces;
- temperature and pressure are set according to the processed material respectively for melting the resin and helping the flow, filling up the empty spaces, and for creating contact and good consolidation.

After forming, the part is cooled at a specific rate, according to the degree of crystallinity that has to be reached. Finally, the autoclave is opened and the part is removed from the vacuum bag first and from the mold then (specific tools may be necessary during this phase). The mold is cleaned and prepared for the next processing cycle.

PULTRUSION

Pultrusion is an automated, economical and high-volume forming process which allows the manufacturing of open or closed profiles characterized by a uniform cross-section (circular or rectangular).

The technology consists of a wet resin system that allows the impregnation of yarns, placed on a creel, that are then pulled through a heated steel die, with the aim of shaping and curing continuous profiles. Finally, the material is pulled by means of hydraulic clamp pullers for cooling down and being cut to the desired length before packing (Figure 1.30) (Ahmad, 2009; U.S. Department of Defense, 2002b).
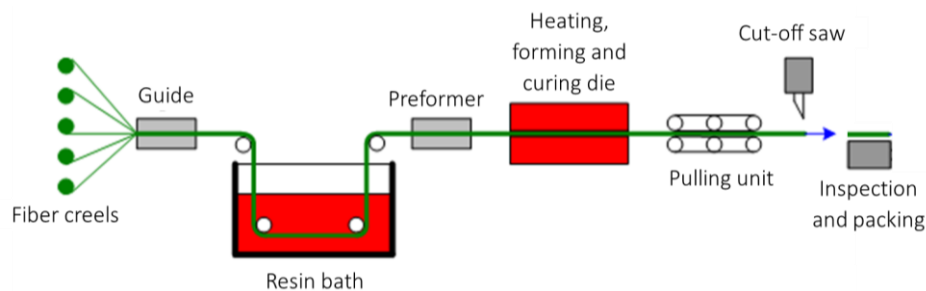
FIGURE 1.30 PULTRUSION

INJECTION MOLDING

Injection molding is a high-volume manufacturing process, widely used both in the thermoplastic industry and in the thermoset one. The process involves the loading of the composite into a hopper that address the material to barrel with screws where heating elements are placed for softening and melting the polymeric matrix. The material flow is then driven by injection to a steel mold cavity that is equipped with a cooling system. After curing, the mold is opened and the manufactured part ejected (Figure 1.31).
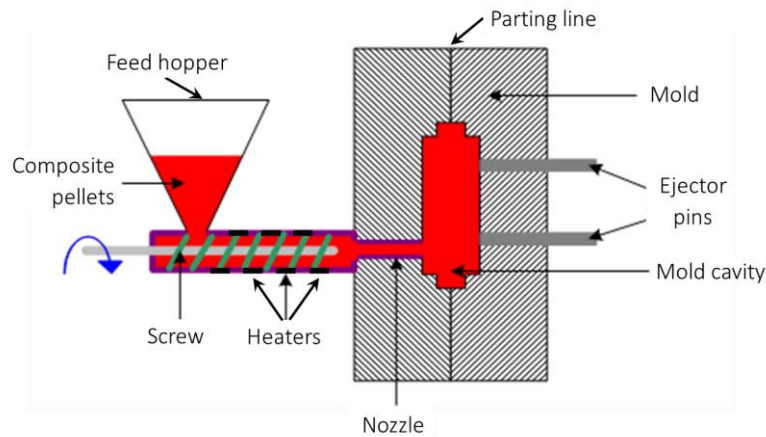
FIGURE 1.31 INJECTION MOLDING

ADDITIVE MANUFACTURING (AM)

Additive Manufacturing is a recent technology which working principle is relatively simple. As opposed to machining, where material is removed from a solid block, or molding, where material is melted and forced into a cavity, additive processes work by 'building-up' the required geometry particle-by-particle, from the bottom-up without the need for tools or molds. The material is locally merged thanks to a local energy source (usually a laser or an electron beam) which follows a programmed trajectory. When thermoplastic composites are involved in the process, a feed spool provides the composite filament, which is then heated and deposited layer-by-layer for forming the object (Figure 1.32).

According to the composite composition, a specific AM method has to be chosen for producing the part. In fact, many process variants exist. Tekinalp et al. (2014) proved that composites with highly dispersed and highly oriented carbon fibers can be printed by Fused Deposition Modeling (FDM) process. Furthermore, the authors analysed the void formation, the fiber length distribution and orientation. Another example is reported in (Shen et al., 2017) where the authors demonstrated the feasibility of selective laser melting (SLM) of glass fiber reinforced composites. Microstructural examinations showed that, by properly setting and controlling the laser process parameters, the fibers do not damage during the process.
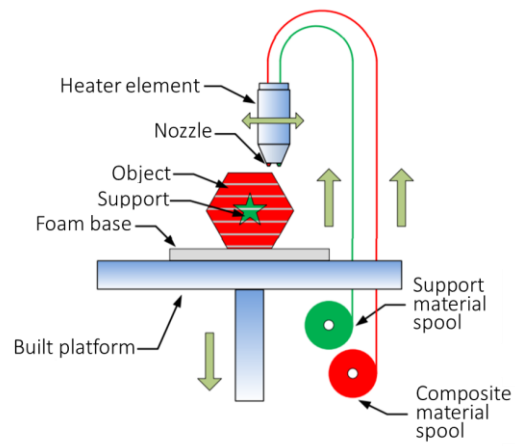
FIGURE 1.32 ADDITIVE MANUFACTURING TECHNOLOGY (NING ET AL., 2015)

CHAPTER 2

SECONDARY FORMING PROCESSES

"Scientists have become the bearers of the torch of discovery in our quest for knowledge"

Stephen Hawking

As widely known, manufacturing refers to combined processes that allow to add value to raw materials, transforming them into useful products and therefore satisfying the final users demand. According to the aim of the manufacturing processes, each one can be categorized in:

- primary forming processes, discussed in Chapter 1, which convert raw materials into primary shapes;
- secondary manufacturing processes, which allow to turn primary shaped parts into finished products, to add details, to re-manufacture some components or to finish and improve the material properties, dimensional tolerance, surface quality and integrity.

In the following paragraphs, the main downstream processing technologies, used for polymeric and composite semi-finished parts, are presented.

2.1. MACHINING

TRADITIONAL PROCESSES

Machining is one of the most important manufacturing processes. It is a material removal process, traditionally used for cutting metals by means of various cutting tools. It generally requires

minimum tool wear rate and provides good surface finish with low energy requirement. For these reasons, its use has been expanded to other typology of materials, such as glass and carbon fiber reinforced polymer based composites (Uhlmann et al., 2014; Xavior and Kumar, 2017), for meeting dimensional and functional requirements of the parts (Qiu et al., 2017). Cutting speed, feed rate and spindle speed are the main parameters to set (Altin Karataş and Gökkaya, 2018). All of them affect the surface and machining accuracy, while the spindle speed is the main factor that may cause delamination (Shetty et al., 2017).

MILLING

Milling belongs to the machining operations and it is the most required and established when excess of material has to be removed from polymeric/composite parts for controlling tolerances, therefore it tends to be a finishing process. A rotating tool acts on the workpiece and more than one cutting tool may be engaged at the same time (Figure 2.1 A)).

The available knowledge on metal machining cannot be completely extended to fiber-reinforced polymers due to their inhomogeneous composition and anisotropic properties. The fiber orientation is one of the main factor to take into account for setting the cutting conditions. Indeed, it affects the cut quality, the cutting force and the tool wear. Furthermore cutting forces, strictly influencing the cutting temperature, and chip formation are used to assess the machinability of fiber reinforced material (Ahmad, 2009; Jahanmir et al., 1999).
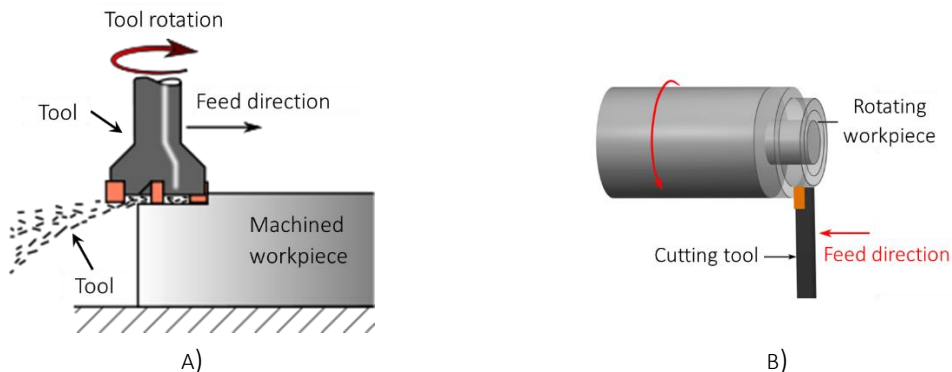
FIGURE 2.1 A) MILLING AND B) TURNING

Hocheng et al. (1993) carried out a study on unidirectional carbon fibre-reinforced plastics for investigating how the cutting mechanism influences the chip formation, observing that the produced chips could be hazardous to humans. The same authors examined the rake angle: for positive values, the debonding between fibers and matrix occurred, while for zero or negative values the chips tended to buckle rather than delaminate (Puw and Hocheng, 1993).

Delamination represents a further issue that may occur (Hintze et al., 2015) and many authors investigated on it (Davim, 2015; Geis et al., 2014) and it still represents a challenge. Recently, Hintze and Brügmann (2017) developed an analytical model for estimating the maximum fiber protrusion lengths for circular feed paths of various radii and this contributed to the optimization of the strategy for reducing delamination. Prashantha et al. (2018) investigated a method based on the Taguchi

technique for obtaining a desirable milling force and surface roughness, stating that the main significant factors are respectively the feed rate and the spindle speed. Furthermore, the authors observed that the main surface damages were obtained setting higher feed rates and lower spindle speeds.

TURNING

Turning is a further machining technique used for finishing composite parts with high accuracy. As opposed to milling, the cutting tool do not rotate during the process (Figure 2.1 B)).

It has been studied and demonstrated that, in turning, the fiber orientation influences mostly the chip formation, the cutting forces and the quality surface. The machinability of composite has been studied in terms of these factors (Ahmad, 2009).

The cutting forces increase when the cutting speed increases, but since the cutting temperature is related to the cutting speed, at high values of this latter the polymeric material soften or melt, reducing the cutting forces. The surface quality and integrity depend on the chemical and physical changes that occur on the material during the process, such as fiber damage, delamination, matrix melting. All of them are function of the process parameters and workpiece characteristics, and may furthermore affect the final performance of the machined part (Spur and Wunsch, 1988). Davim and Mata (2005) carried out a study for optimizing the cutting parameters in order to obtain a specific surface roughness and calculate the material removal rate. Rajasekaran et al. (2011) and Hussain et al. (2011) used a fuzzy based model for predicting the surface roughness of a composite machined part. Both concluded that the feed rate is the main parameter that affects the investigated process output, followed by the cutting speed and by the fiber orientation angle.

DRILLING

Drilling is that machining operation performed on composite components mainly for fastening purposes of structural parts (Gaugel et al., 2016). More in detail, using a specific rotating cutting tool, made of a drill point design, the material is removed for forming a designed number of holes (Figure 2.2 A)). Temperature increase, tool wear and delamination, fiber breakage are the main problems that may arise and that is necessary to manage for avoiding the damages of the processed part (Xu et al., 2016). The temperature, for instance, may be controlled using a proper coolant, and, different than metal, on composite the heat is dissipated by the workpiece and tool, rather than the produced chips. Matsumura and Tamura (2016) carried out a study for analysing the cutting temperature involved in the drilling of carbon fiber reinforced plastics (CFRP). The cutting forces were predicted and the heat generation estimated, stating that the maximum temperature is near the tool tip because of the low thermal conductivity of the material. Sorrentino et al. (2015) developed a numerical model and a sensory system for measuring the heat distribution on the drilling tool and on the workpiece, aiming at optimizing the process for various thickness composite parts. Tool wear is mostly due to the presence of the fiber reinforcement, because of their abrasive nature; if the cutting tool is damaged, the manufactured holes may compromise the next assembly operations (Abrate and Walton, 1992; Piquet et al., 2000). Delamination creates a crack between the plies, the

composite is made of, and this causes a degradation of the mechanical performance and of the structural integrity of the machined part. Recently, El Bouami et al. (2016) carried out a study for investigating the influence of the tool geometry and of the process parameters on delamination, demonstrating that the feed rate is the most influencing. The straight flute carbide drill (Figure 2.2 B)) seems to be the design that causes the lowest delamination. It has been found that this undesirable feature is due to the thrust force that increases with the wear of the cutting edge (Ahmad, 2009). The thrust force is also affected by the cutting speed and feed rate. More in detail, Singh et al. (2008) proposed in their study a statistical investigation on these parameters, demonstrating that the thrust force increases with the increase in the feed rate. As regards the influence of the tool geometry, Bhatnagar et al. (1993) and Kumar et al. (2016) experimented different drill point geometries, stating that the eight faced one allows to get the best holes and lower delamination factor and surface roughness values.
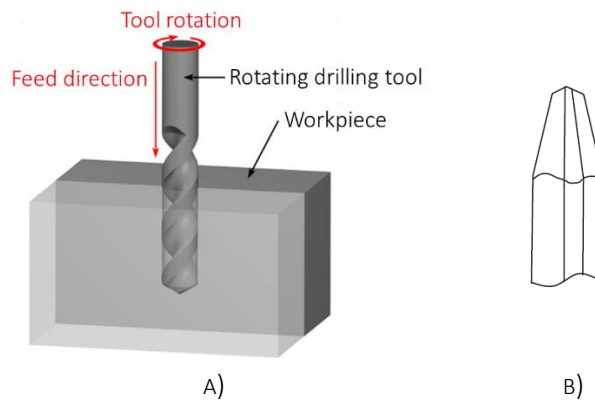
FIGURE 2.2 A) DRILLING AND B) STRAIGHT FLUTE DRILL DESIGN

ABRASIVE MACHINING AND GRINDING

Both processes are used to remove material from the workpiece surface using a tool made of small hard particles. The two processes are quite similar and three parameters make the main difference. In general, abrasive machining has higher cutting depth, smaller cutting diameter and lower workpiece feed rate than grinding.

In abrasive machining, the hard particles are made of diamond grit and the surface roughness depends on the size of these particles, rather than on the feed rate (Ahmad, 2009).

In grinding, the chip thickness plays an important role, in fact it is even smaller than the fiber diameter. This causes higher heat generation, exceeding the T_g of the matrix, than abrasive machining, therefore a proper flood coolant has to be applied for not burning the machined surface. In addition, the production of tiny chips involves a better quality surface in terms of roughness (Ahmad, 2009). Liu et al. (2017) investigated the grinding forces, demonstrating that they decrease with the increase in the spindle speed, but increase with the increase in the feed rate.

NON-TRADITIONAL PROCESSES

New machining variants have been investigated for polymer based composites and suggested when traditional machining operations are difficult to be performed, offering important advantages, such as high flexibility and high production rate, but obviously they have also their own limitations (Ahmad, 2009).

Abrasive water jet (AWJ), laser machining and electrical discharge machining (EDM) are the non-traditional machining processes discussed below.

ABRASIVE WATER JET (AWJ)

The process was introduced in the Seventies for cutting several typologies of materials and seems to be the only technique that reached a certain industrial application level (Davim, 2015). It is based on the combination of the high-speed water jet and of abrasive particles, which accelerating remove material from the workpiece without further cutting tools (Figure 2.3 A)). The main advantages of this process are related to i) the possibility of cutting plastics, metals or composites without damaging the part because there is not heat generation, ii) the no need of specific cutting fluids and therefore no dangerous wastes for the environment are produced, iii) the possibility of recycling and reusing water and abrasive particles. Disadvantages are instead due to the high initial investment, as well as to the high operational costs, and to the higher noise if compared with the previous described machining technologies. Furthermore, one of the main issues that may arise, because of the high-velocity waterjets, is delamination, as discussed by (Shaw and Tseng, 1992). An optimization of the process for reducing this cited effect was carried out by Dhanawade and Kumar (2017), who suggested to increase the fluid pressure and the abrasive flow rate.

LASER CUTTING MACHINING

Laser machining is a highly flexible thermal process that allows to cut different kinds of materials, regardless of hardness, without a contact between the cutting tool and the part. An infrared beam is focused on the workpiece for removing the material from a predefined position (Figure 2.3 B)). Two process variants may be defined: in the first case, the laser is still and the workpiece moves, in the second case, the workpiece is instead fixed. Despite the advantages related to the absence of cutting forces or of the tool deterioration, some drawbacks, which may be reduced with a proper setting of the process parameters may arise: the physical/chemical modification and degradation of the material, which also may lead to a reduction of the part strength, and the development of hazardous chemical substances, which size depends on the thermal conductivity of the part, on the laser beam power and on the cutting speed (Ahmad, 2009; Lau and Lee, 1991). Walter et al. (2014) evaluated qualitatively and quantitatively the emission of particulates and gases according to the set process parameters. The emission rate was measured at different processing conditions and the multipass cutting resulted to be the most suitable when CFRP are involved in the process. El-Taweel et al. (2009) studied the laser cutting performance on Kevlar, revealing that the laser power is the

main parameter that affects the cut quality and defining the optimal combination of process parameters. A further investigated material was nylon 6 (Antończak et al., 2013).

ELECTRICAL DISCHARGE MACHINING (EDM)

Electrical Discharge Machining is a further thermal process that erodes electrically the material by using spark discharges, which shape defines the resulting cavity. Just materials that have the characteristic of being high electrical conductors may be processed by EDM (carbon/polymer for instance). Two main variants of the process exist: plunge and wire type. In the first one, the electrode is a mirror image of the part that has to be removed, while in the second type (Figure 2.3 C)), a wire electrode, provided by using a guide, moves continuously for cutting the defined part. EDM, which does not require a direct contact between the cutting tool and the workpiece and therefore there are not contact forces, guarantees high cutting accuracy and high quality of the finished surface. On the other hand, the high heat generated modifies the microstructure and the properties of the material close to the cut and it is the main cause of delamination. Guu et al. (2001) tested experimentally the process on a carbon fiber reinforced composite, stating that the best quality surface and holes are obtained under low discharge energy conditions. Lauwers et al. (2004) in their work aimed at understanding the influence of the process on the material, observing that the main phenomena that may occur are melting, evaporation, spalling, oxidation and decomposition.

A)   B)

c)
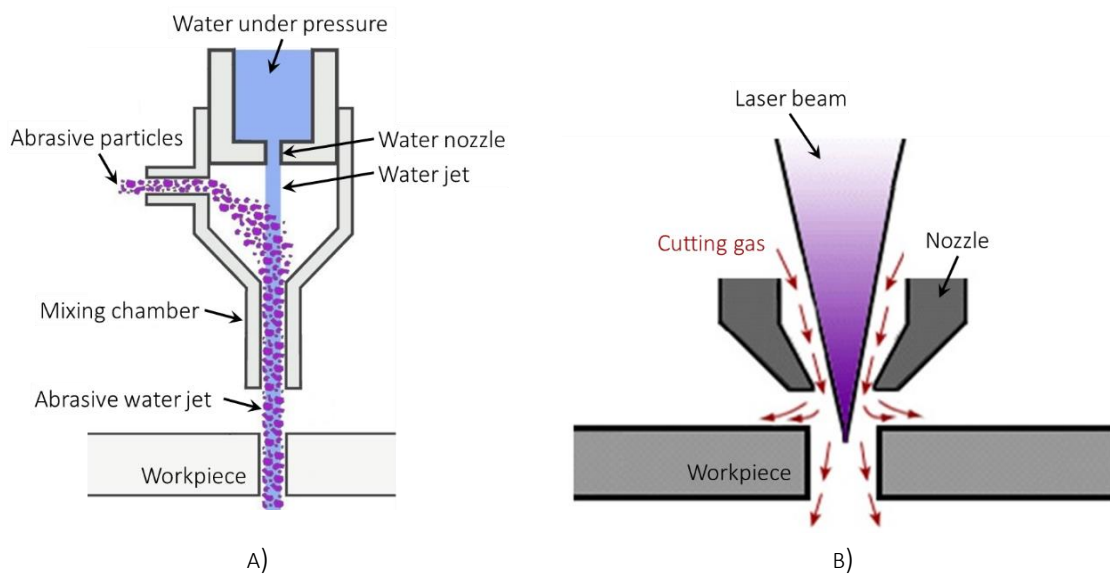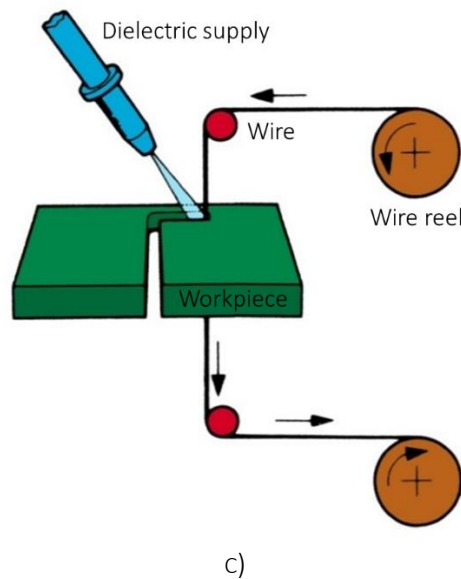
FIGURE 2.3 A) ABRASIVE WATER JET, B) LASER CUTTING MACHINING AND C) EDM

Summing up, machining is that manufacturing technique that is performed on polymers and composites when the manufacturing of holes or other features is required for instance for achieving a defined tolerance of the part that cannot be obtained by primary processes (Mazumdar, 2001). It is important to highlight that the machining operations on polymers and composites may i) compromise the performance of the part because of the reinforcement discontinuity caused by the cutting of this latter, ii) damage the part because of the high processing temperatures, which may change the mechanical properties of the material, iii) damage the cutting tool more frequently because of the abrasive nature of the fiber reinforcement.

2.2. THERMOFORMING

Thermoforming is one of the oldest forming technology and can be considered the most common method used for transforming a plastic sheet using heat and pressure (Throne, 2008).

Materials (such as metals, glass) started to be thermoformed at the beginning of the 20th century. The introduction of thermoplastics contributed to the development of this process and it continued growing during and after the Word War II, because of aircraft applications (Thompson, 2007). Research in materials and machines led to the production of parts for several other sectors, such as automotive, packaging and sporting goods (Martin, 2009), improving at the same time quality, production rate, production volumes and control systems (Ashter, 2013).

The thermoforming technique consists, basically, in the following operations Figure 2.4:

i) *Heating*: the thermoplastic material is heated, usually externally to the forming tool, until the softening temperature (glass transition temperature for amorphous polymers and melting point for semi-crystalline polymers) (Osswald and Hernández-Ortiz, 2006) by conduction, convection or radiation.

ii) *Transfer*: the pre-heated sheet is transferred into a mold where the temperature is controlled, for avoiding the cooling down.

iii) *Forming*: the material is clamped and shaped under pressure or vacuum, according to the specific requirements.

iv) *Consolidation*: the part is cooled down, so that the material maintains the mold shape.

v) *Demoulding*: the part is removed from the mold after opening the clamps.
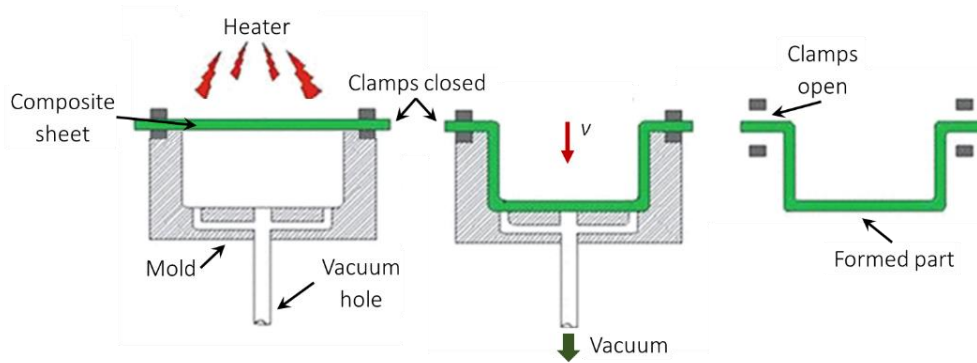
FIGURE 2.4 THERMOFORMING (BIRAT ET AL., 2015)

The scientific literature contains a wide number of studies on the thermoforming of polymers and composites. Below some of them are reported.

Lau et al. (1998) studied and measured the melt strength of different grades of PP, discussing its impact on sagging resistance during thermoforming applications. More in detail, the authors stated that the melt strength increases with decreasing temperature and increasing extrusion rate and that, to minimize the sagging, the forming temperature has to be close to the melting one.

Lessard et al. (2015) investigated experimentally the influence of the operational parameters on the thermoforming of a CF/PEEK laminate. The authors demonstrated that the most influent parameters on the part thickness and consolidation are the mold temperature and the stamping pressure. Jobey et al. (2016) predicted the thickness distribution on a multilayer ABS/PMMA sheet, investigating the influence of the bubbles. The authors proposed a method for showing how the bubble's shape can be adapted to the mould in order to improve the thickness distribution of the part. Finite element analysis are necessary for a full comprehension of the issues that may arise during the forming process of polymers and composites (deLorenzi and Nied, 1987; Nied et al., 1990; Vantal et al., 1995). Warby et al. (2003) proposed a computational model for polymeric sheets at various temperatures and for different loading conditions, stating that the material behaviour is highly strain rate dependent. Guzman-Maldonado et al. (2016) presented an approach for simulating the thermoforming of glass/PA66 thermoplastic prepreg. Thermal and forming analysis showed that the temperature modifies significantly during the process and this may have, therefore, an important impact on the mechanical behaviour of the part. Schell et al. (2016) simulated the thermoforming of a glass fiber reinforced PA6, aiming at predicting the patch movement. More recent works focused on the optimization of the thermoforming process using artificial neural networks (Leite et al., 2018) and on the use of thermoformed fiber reinforced polymeric composites for creating multifunction components characterised by an integrated intelligence (Yang et al., 2018).

Several variations of the thermoforming process exist and may be differentiated according to the method used for pressing and shaping. Vacuum forming, pressure forming, mechanical forming and drape forming belong to the thermoforming category. A brief description of these alternatives is presented below.

VACUUM FORMING

Vacuum forming is considered the simplest technique and the most widely used among the previous mentioned methods based on forming by heating. This is also due to the cost of the vacuum equipment that is cheaper than other thermoforming tools.

The process is shown in Figure 2.5: a clamped plastic sheet is heated until the softening temperature and sucked onto the cold surface of the mold that can be made of metal, wood or resin. After cooling, the formed part is removed from the mold.

A single-side tool is used, therefore just one side of the material is affected by the tool surface. Furthermore, channels are drilled into the mold for an efficient extraction of the air.
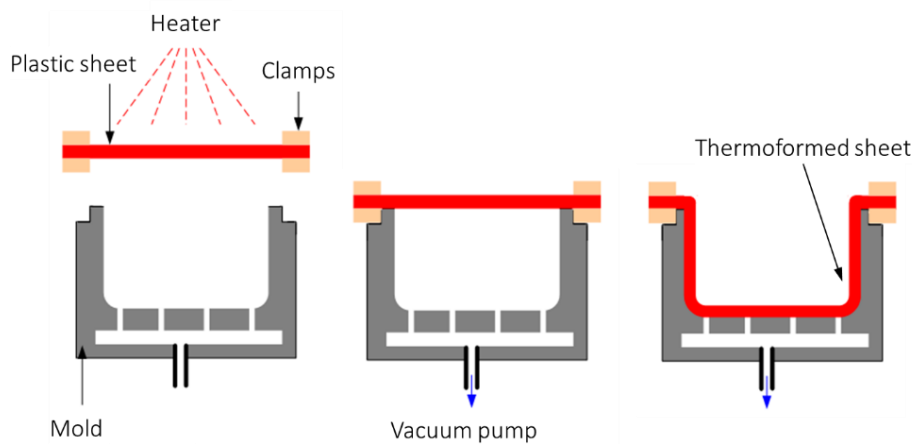
FIGURE 2.5 VACUUM THERMOFORMING (KOPELIOVICH, 2004)

PRESSURE FORMING

Pressure forming is a two-step process. The plastic sheet is clamped and heated to a specific temperature and for a specific time. By air pressure, as the name of the process suggests, the sheet

is   forced   into   the   mold   cavity   (
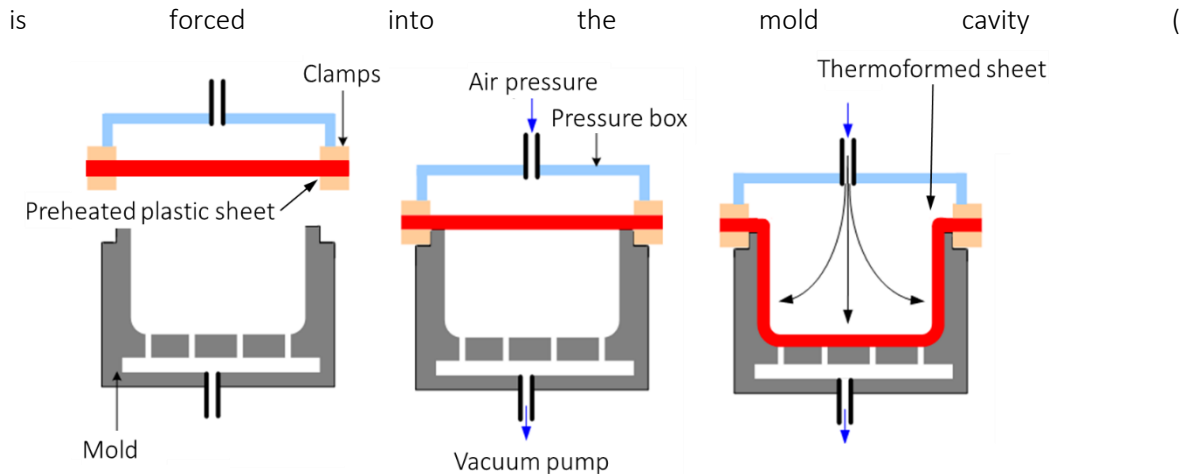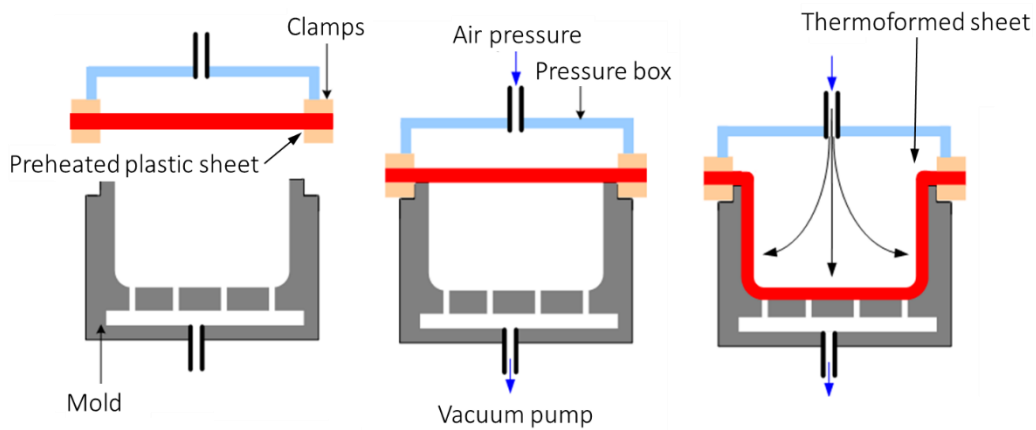
Figure 2.6).

FIGURE 2.6 PRESSURE THERMOFORMING (KOPELIOVICH, 2004)

This process is widely used by industries because it guarantees fast production cycle, short lead-time, high part definition and dimensional control. Furthermore, high pressures allow the forming of sharp edges, more complex shapes, with a good surface finishing and reproduction of details.

It is worth pointing out that this process, together with the vacuum forming, is suitable for sheet form geometries, while for deep profiles other techniques are required (Ashter, 2013; Thompson, 2007).

MECHANICAL FORMING

In the mechanical forming process, the heated plastic sheet is clamped on a female mold and the action of a male mold allows the shaping of the part (Figure 2.7).

The output is characterised by excellent dimensional accuracy and good reproduction of details (Ebewele, 2000).
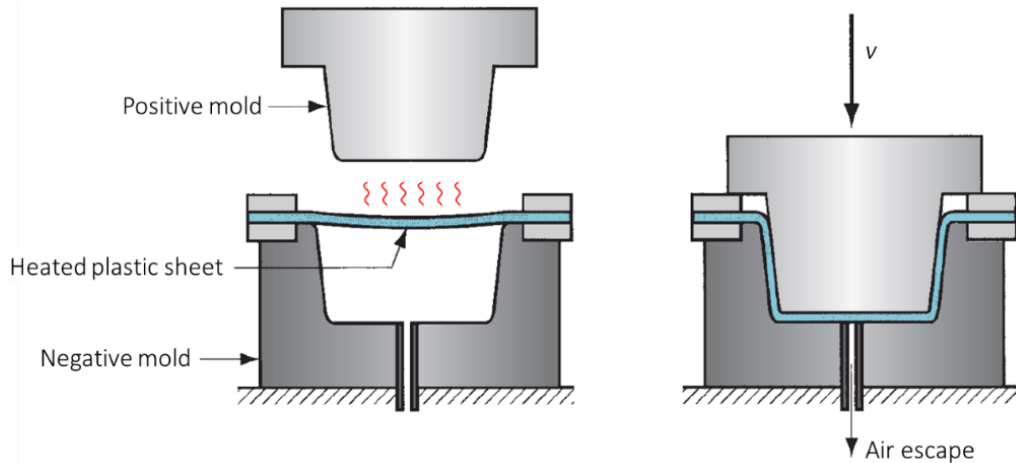
FIGURE 2.7 MECHANICAL THERMOFORMING (MIKELL P. GROOVER, 2010)

DRAPE FORMING

Drape forming is a combination of mechanical and vacuum forming, used for such products that require gradual curve or bend. Here, the pre-heated sheet is mechanically draped over a female or male mold and the vacuum is applied for providing the shape.
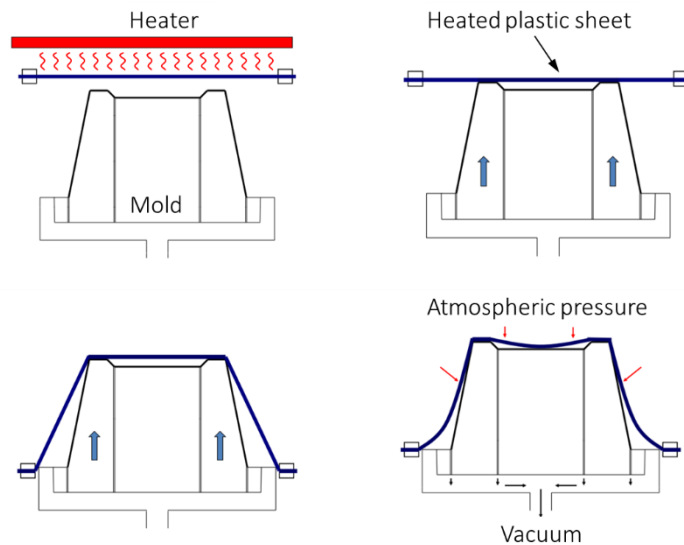
FIGURE 2.8 DRAPE FORMING PROCESS (KLEIN, 2009)

2.3. INCREMENTAL FORMING

Incremental forming processes belong to a new class of techniques that can be considered for secondary manufacturing of polymers and composites. Strong and Hauwiller (1989) designed an incremental forming method for shaping thermoplastic composite sheets. Each sheet was previously heated and then transferred on a forming area for shaping it between modular molds. Gutowski et al. (1991) introduced two diaphragms in the incremental forming process. A composite laminate was

positioned between the diaphragms, heated by an infrared source and pressed on a mold (Figure 2.9 A)). The authors asserted that the forming was mostly related to the part curvature and to the initial fiber placement. Few years later, the same authors patented a technique for reducing some issues that may arise during the composite forming, such as wrinkling. The proposed method necessitated reinforcing structures (e.g. stainless steel strips) for increasing the buckling resistance (Gutowski et al., 1991). Kaufman et al. (1997) investigated a new method for incrementally forming composites. It was based on the setting, by a cam, of a reconfigurable discrete element tool to shape the desired geometry (Figure 2.9 B)). The pre-heated composite sheet was laid first between two diaphragms and them on the reconfigurable forming tool. Walczyk et al. (2003) studied a method for manufacturing aircraft composite parts without dimples or wrinkles. A reconfigurable tool was designed aiming also at reducing the heating time and at maintaining constant the temperature during the forming.
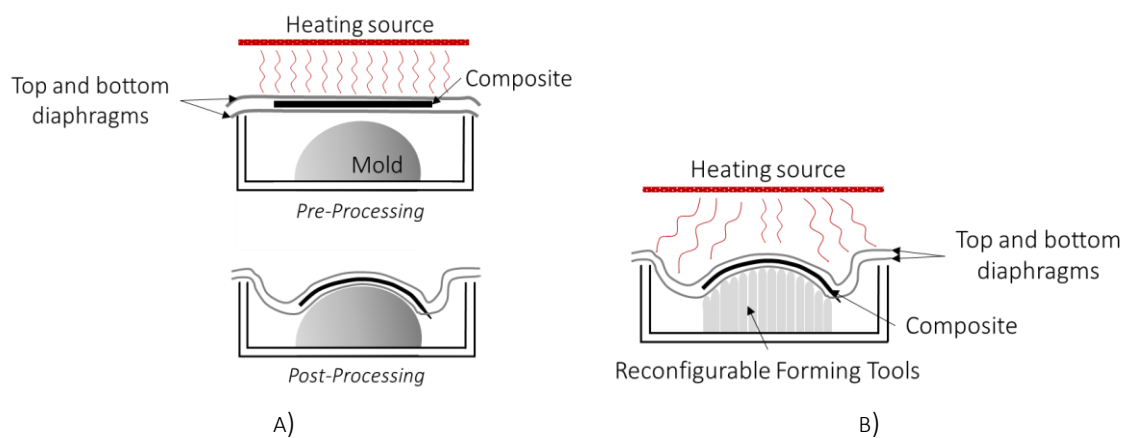
FIGURE 2.9 INCREMENTAL FORMING METHODS

An alternative incremental forming method is called Single Point Incremental Forming (SPIF).

The process consists of a progressive movement of a punch on computer numerical control (CNC) milling machine along a designed trajectory, allowing the plastic and local deformation of a sheet, clamped on the working equipment (Figure 2.10). The operation principle of this technology guarantees a high level of flexibility, moreover allows the manufacturing of complex components decreasing cost production, since no further dies and short set-up times are required. Nevertheless, a higher process time, if compared with traditional processes, limits its use just to prototypes and small production batches (Filice et al., 2002).

Initially the process was used for shaping metal sheets (Ambrogio et al., 2012; Jeswiet et al., 2005; Kim and Park, 2002). The process parameters and the properties of the formed materials have been investigated in order to understand their influence on the output (Ambrogio et al., 2011; Bouffioux et al., 2011; Fratini et al., 2004).
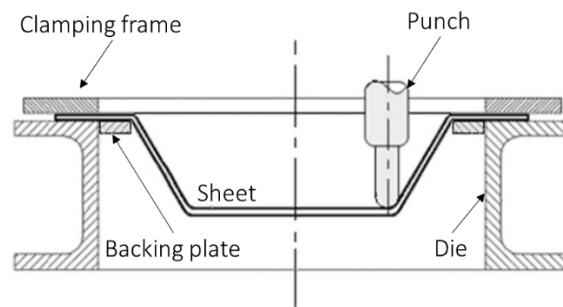
FIGURE 2.10 SINGLE POINT INCREMENTAL FORMING PROCESS (MICARI ET AL., 2007)

Recent works focused on the performance of the SPIF process on further materials, like some polymers that can be shaped at low temperature. Franzen et al. (2008, 2009) investigated this technology on commercial polyoxymethylene (POM), polyethylene (PE), polyamide (PA), polyvinyl chloride (PVC) and polycarbonate (PC) sheets, successfully demonstrating the feasibility of SPIF on materials different from metals. Furthermore, the authors identified the most influent process parameters and the main failure modes. Le et al. (2008) extended the research on polypropylene (PP), while Martins et al. (2009) on polyamide (PA), polycarbonate (PC), polyethylene (PE) and polyoxymethylene (POM).

Marques et al. (2012) proposed a methodology for i) understanding which are the influent process variables, ii) diagnosing possible failures and ii) selecting the most appropriate materials at specific working conditions. Rajenthirakumar and Sridhar (2014) investigated in their work three polymers (high-density polyethylene (HDPE), polycarbonate (PC) and polyvinyl chloride (PVC)) and analysed the effect of the set process parameters both on the springback and on the thickness distribution.

Bagudanch et al. (2015) and Bagudanch et al. (2016) assessed respectively the maximum forming force, the surface roughness and the temperature variation on PVC and the influence of SPIF variables on the energy consumption, and therefore on the production costs, aiming at minimizing them through the identification of a suitable combination of parameters. Davarpanah et al. (2015) examined experimentally the effects of the incremental depth and tool rotation speed on the failure modes, void structures and crystallinity of the *SPIFed* materials. Furthermore, they demonstrated that the formability is mainly influenced by the tool diameter, the step depth, the spindle speed and the feed rate. In a successive work (Davarpanah et al., 2016), the authors experimented the Double Side Incremental Forming (DSIF) on PVC sheets. A comparison with the SPIF process was carried out in terms of formability, voids and sheet bending and the advantages of the DSIF were highlighted.

More recently, the SPIF technology was tested also on composites, which properties depend on some factors, such as the orientation and distribution of fibers within the matrix or the proportion of phase and matrix (Altin Karataş and Gökkaya, 2018; Sakin et al., 2008). The first investigation was carried out by Fiorotto et al. (2010). The authors tested first the incremental sheet forming of Al molds to be used later to form composite parts. Plastic rollers were used for shaping composite plies placed on a mold. A second experiment allowed to perform the process directly on glass fiber and Kevlar reinforced laminates, using simultaneously diaphragms made of aluminium and PVC. Diaphragm mechanical failure, wrinkling and quality surface have been analysed and discussed. A

similar study on the manufacturing of molds to use for shaping composite prototypes or customized component was reported by Rimašauskas et al. (2014). The authors analysed the formability and the surface quality of the molds and in addition stated that the technology was characterized by low time and costs if compared with traditional processes. Lozano-Sánchez et al. (2017) processed by SPIF polypropylene reinforced with multi-wall carbon nanotubes. The performance of the outcome was analysed, stating that a little presence of the fibers does not affect the formability and besides an improvement of the mechanical reinforcement is obtained. The authors investigated also the colour variation and the influence of the thermal effect on the shaped parts.

2.4. JOINING

Joining is a widespread process that allows the assembly or connection of parts aiming at achieving specific mechanical performances. Indeed, components are manufactured separately (e.g. because of technical feasibility or structural requirements) and reach specific functionality just when attached to each other. Joints are usually considered the weakest part of a structure, because is a source of stress concentration, and for this reason static strength and fatigue, crack propagation, load resistance are always investigated (Chaves et al., 2018). The joining process can be quite difficult when dissimilar materials have to be joined due to their distinct physical and chemical properties, therefore issues may arise because, for instance, of dissimilarity in terms of expansion coefficient or galvanic properties (Amancio-Filho and dos Santos, 2009). Hybrid structures are widely used in such sectors like automotive (Sakundarini et al., 2013) and aerospace (Kapidžić et al., 2014), where innovative joining systems are continuously requested because of the need of manufacturing lighter components. Martinsen et al. (2015) reported a review of the technologies to use for joining dissimilar materials and discussed selection criteria, modelling and inspection/testing of joints.

The traditional joining techniques can be classified in three main categories: adhesive, thermal and mechanical joining. Their approach depends on the materials involved in the process and on the specific requirements.

Adhesive bonding is a permanent joining process in which the use of an adhesive substance is required. It is placed between the parts that have to be joined (called interphases regions) and solidifying the adhesive bond is produced (Figure 2.11). This process finds application in several areas (automotive, aerospace, aeronautics, electronics and packaging) for manufacturing complex-shaped structures and provides advantages compared to other traditional fastener techniques. Nevertheless, the joint typology is chosen according to the specific application of the part, to the involved materials and to the loading conditions. Furthermore, several types of adhesive bonded joints exist: single and double lap joint, step joint, single and double strap joint, scarf joint, butt joint (Mazumdar, 2001). Adhesive bonding is considered a more suitable method than others for joining metals to fiber reinforced composites (or in general plastic materials), because it guarantees a more regular distribution of the load, a low structural weight and prevent galvanic corrosion. Furthermore, the fibers are not damaged during the process so that stress concentrations are not introduced and the structural integrity is not reduced. A further and more important advantage is related to the fact that the microstructure of the joined materials does not change during the process. Nonetheless, some limitations and drawbacks have been identified and should be solved before employing the

process at large scale. They consist mainly of long surface preparation, for increasing the intrinsic adhesion between the material and the adhesive, and curing time, weight increase, easy failure due to peel stresses, poor temperature resistance and a deep control of humidity is necessary to avoid issues during the use of the component. In addition the long-term integrity cannot be guaranteed and the disassembly of the joint is quite impossible without destroying it (Amancio-Filho and Blaga, 2018; Darwish, 2010).
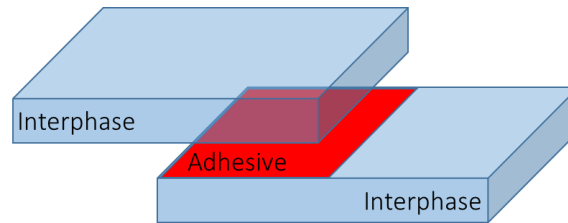
FIGURE 2.11 ADHESIVE BONDING

The *thermal joining* solutions require thermal energy to melt the material surface. This energy can be provided by several sources and this makes the main difference among the technologies. One of the most suitable technologies for hybrid structures is *ultrasonic welding*, where the parts are held together under pressure and joined through ultrasonic vibrations. Magin and Balle (2014) investigated the joining of a thermoplastic composite to aluminium and titanium, and reported a comparison between ultrasonic polymer welding and ultrasonic metal welding. Deng et al. (2015) in their work highlighted the potential applications of fusion bonding in joining composite structures, suggesting the application of a thermoplastic layer on the thermoset composite before performing the joint with metal. Lionetto et al. (2016) experimented, first, ultrasonic welding of a thermoplastic composite, stating the low energy input and the short processing time. Then, the same authors, according to the previous mentioned study, carried out a further investigation for joining aluminium to a thermoset composite, using a thermoplastic film for promoting the joining between the two dissimilar materials and for preventing the galvanic corrosion of the reinforcement (Lionetto et al., 2017). A new methodology for joining metals to composite by ultrasonic energy was developed by Helmholtz-Zentrum Geesthacht, and simply called *ultrasonic joining* (U-joining). Feistauer et al. (2016) demonstrated the feasibility of this process with titanium/glass-fiber-reinforced polyetherimide joints and presented microstructural features, mechanical properties and failure mechanisms of the hybrid joints. *Induction Spot Welding* is a further thermal joining technique characterized by a rapid heating. Mitschang et al. (2013) experimented a combination of metals and carbon fiber reinforced composite and analysed the influence of the surface treatments and of the process parameters. The *laser welding* technology belongs to the thermal joining method as well, characterized by low thermal effect and high efficiency. Investigations on plastic/composite-metal joints have been widely reported by Katayama and Kawahito (2008), Jung et al. (2013) and Jiao et al. (2017). The thermal energy can be also generated by friction. When materials belong to the metal category, the *friction stir welding* is applied (Sato et al., 2004; Uzun et al., 2005). The process has been performed also on metal matrix composites. Indeed, Periyasamy et al. (2013) in their work evaluated the performance of friction stir welding joints of AA6061/20%SiCp MMCs, aiming at understanding the relationship among the process parameters and at finding their optimal

combination in order to tensile strength, notch tensile strength and the weld nugget hardness of the joints. When polymers/composites are involved in the joint with metals, the *friction lap joining* can be performed. Nagatsuka et al. (2015) reported the direct joining of a carbon fiber reinforced thermoplastic and an Aluminum alloy. The surface roughness and the influence of the joining speed on the output were investigated. An innovative variant of friction stir welding, but that can be used for metal-composite joints, is *friction stir scribe* (FSS). Indeed, it was developed for meeting the demand of combining materials characterized by different melting regimes (Upadhyay et al., 2017).

The *mechanical fastening* solutions are applicable mainly when the materials involved in the process are difficult to weld. They present some advantages compared to the previous described techniques, such as no surface treatment, no heat or fume generation and a minimum geometrical distortion. The main disadvantages are related to the weight increase of the structure, to the stress concentration close to the holes, to the problems due to the galvanic corrosion, and to the fiber discontinuity created when holes are drilled and therefore to the exposure of fibers to chemicals.

Mechanical joints can be differentiated in two groups: without additional fastener and with additional fastener. In the first case, the joint is performed without using additional external components and just using the parts to be joined. In the second case, external fastener are required, such as rivets (in riveting) or bolts, screws, pins, studs, nuts, blots and washers (in bolded joints). These latter can be single lap joints, double lap joints or butt joints. Fasteners are classified according to the joint typology, in temporary or permanent. If temporary, removable fasteners are used and they can be removed and reinstalled; if permanent, fasteners can be used once and for removing them it is necessary to destroy the whole component. *Clinching* belongs to the processes that do not require external fasteners. It is a cold process, based on the action of a punch that pushes the material into a die or into the material positioned below, therefore a local plastic deformation occurs, without the need of drilling holes. A die is used for facilitating the interlock. This variant is also known as single-step clinching. Figure 2.12 A) shows a hole-clinching version designed by Lee et al. (2014) for joining metals and carbon fiber reinforced plastic. Cracks around the holes and delamination may occur (Pramanik et al., 2017). Lambiase and Ko (2017) presented a study on *two-steps clinching* for joining Aluminum and CFRP. A reshaping deformation was used at the end of process to improve the mechanical behaviour of the connections. Analysis on the morphology and geometry of joints were carried out to understand how the reshaping step influences joint quality and the damage produced on the CFRP sheet.

A further method that does not require holes but belongs to the mechanical joints with additional fastener is the *self-piercing rivet* (SPR) (Figure 2.12 B)). A single-step process that involves the driving of a rivet into the materials to be joined. The rivet is pressed by a punch piercing through the sheets, while a die shape allows the mechanical interlock. Fratini and Ruisi (2009) demonstrated the feasibility of joining fibreglass composite panels and aluminium blanks by this technique. Ueda et al. (2012) proposed a method for minimizing delamination, while Di Franco et al. (2012) investigated the influence of the distance between rivets in terms of tensile strength.
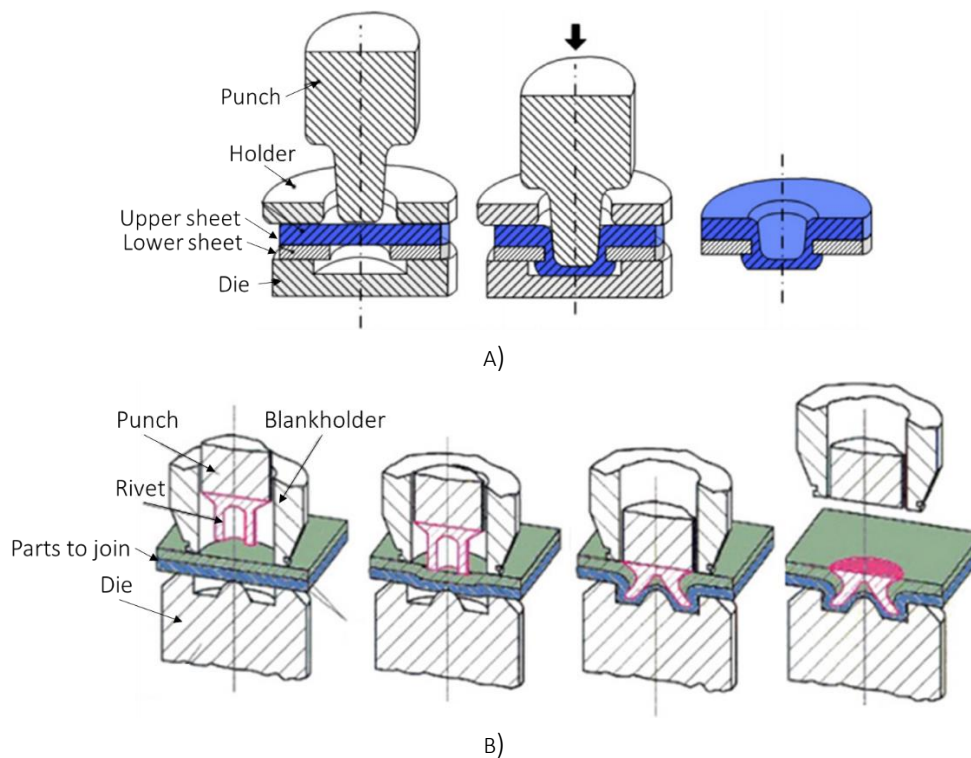
FIGURE 2.12 CLINCHING (LEE ET AL., 2014) AND SELF-PIERCING RIVET (DI FRANCO ET AL., 2013)

Researchers, aiming at improving the joint quality, have developed new techniques, sometimes combining or innovating existing methods (Lopez-Cruz et al., 2017). The Helmholtz Zentrum Geesthacht (WO/2001/036144) developed *friction spot welding* (FSpW) for offering advantages, such as shorter welding times, less wastes, good surface quality, over the conventionally used welding technologies. The heat generated by the friction between the rotational tool and the workpiece causes the molecular interdiffusion across the interface for welding. Gonçalves et al. (2015) demonstrated successfully the feasibility of this method on woven reinforced thermoplastic composite evaluating through mechanical testing and optical microscopy. *Friction spot joining (FSpJ)* is a new technique investigated for joining lightweight metals with high-performance engineering thermoplastics and composites (Figure 2.13 A)). A metallic partner is plasticized and deformed due to the generated frictional heat and applied force. A metallic nub is created and inserted into the composite. Simultaneously, a thin layer of polymer matrix is molten and displaced around the joining area. After the consolidation of the polymeric molten layer, the joint is completed (Esteves et al., 2015; Goushegir, 2016).

Amancio-Filho (2011) patented a new joining process called *friction riveting* (Figure 2.13 B)). A rotating cylindrical metallic rivet is used to connect thermoplastic-metal parts plasticizing and deforming the tip of the rivet heated by frictional forces. The process involves two phases: during the first one, the metallic rivet rotates and pierce through the components to be joined (heating phase); at the end of this phase, the rotational speed decelerates and the rivet is pushed into the materials to be connected (forging phase). Rotational speed, friction time and friction pressure, forging time and forging pressure, are the main process parameters to set and that have to be combined properly for improving the quality of the connection. Borges et al. (2012) attempted the

simulation of this typology of joint using the commercial code Abaqus™. The feasibility of this method on thermoplastic composites was proved on plastic matrices reinforced with short fiber by Altmeyer et al. (2014), on laminates by Blaga et al. (2013) and also on high-performance plastics (Altmeyer et al., 2014; Blaga et al., 2015). Furthermore, Borba et al. (2018) demonstrated the direct friction riveting of titanium rivets and carbon fiber reinforced polyether-ether-ketone laminates, stating that is it a competitive method for aircraft applications. The main defects that may be detected when reinforced thermoplastics are involved in the process are the generation of voids and porosity, the fiber-matrix debonding and the thermal degradation of the matrix (Amancio-Filho and Blaga, 2018). A further defect was reported by Su et al. (2006) and defined as broken stir zone. Seidlitz et al. (2016) investigated an innovative thermo-mechanical technique, called *flow drill joining*, for connecting sheet metals and reinforced thermoplastic composites. A rotating mandrel shapes a bushing from the metal material, plasticizing locally. At the same time, the composite material melts locally and the moveable fibers are deviated. The authors stated the feasibility of the process.
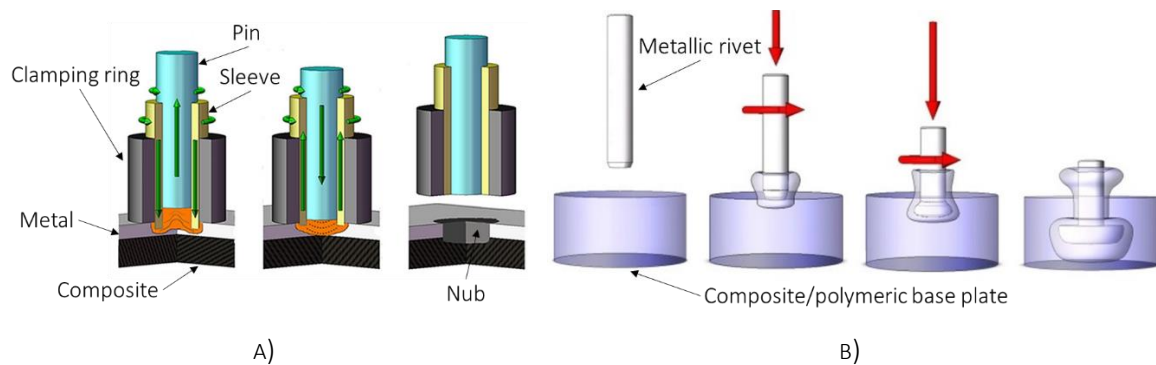
FIGURE 2.13 FRICTION SPOT JOINING AND FRICTION RIVETING

An experimental comparison of mechanical bolts, adhesive bonds and hybrid joints, in terms of mechanical properties, has been carried out by Mariam et al. (2018). The materials involved in the investigation were Aluminum and glass fiber reinforced composites. The stiffness, the failure modes and the fatigue damage mechanism have been widely discussed.

CHAPTER 3

SINGLE POINT INCREMENTAL FORMING

"No amount of experimentation can ever prove me right;
a single experiment can prove me wrong"

Albert Einstein

3.1. SINGLE POINT INCREMENTAL FORMING PROCESS

Single Point Incremental Forming (SPIF) has been widely investigated on metals. As reported in Chapter 2, recently, some works have proved the feasibility of the process on polymers. More in detail, the processed thermoplastic materials are characterized by glass transition temperatures close to the room one and, therefore, SPIF has been performed without external thermal source, taking advantage mostly of the friction heat generated during the forming phase. Edwards et al. (2017) applied additional heat by an air gun for reducing the springback effect on a *SPIFed* polycarbonate sheet, but after the forming and while the specimen was kept in the forming fixture. The reached temperature was approximately 55 °C, therefore far from the glass transition temperature of the material (around 145 °C).

In this work a first preliminary experimentation has been carried out on polypropylene (PP), the second investigation on poly(methyl methacrylate) (PMMA) and the third on polyamide 6 (PA6) reinforced with short glass fibers.

3.1.1. EXPERIMENTAL EQUIPMENT

As widely described in the previous chapter, Single Point Incremental Forming (SPIF) is a technology performed on sheets for manufacturing simple and complex shapes, through the action of a punch, which locally and plastically deforms the material. The part geometry is designed and set on a CNC machine. The punch follows the imposed trajectory moving on the three directions. The sheet to form has to be adequately clamped to avoid changing of position during the process. Spindle speed (S) , forming velocity (F), tool diameter (D), step depth (d) and wall angle (α) are the main process parameter to set. To the aim of the investigations carried out and presented in this thesis, a further factor has to be taken into account, the temperature (T_i).

According to that, a specific apparatus has been designed, manufactured (Figure 3.1) and installed on a Mazak Nexsus 410 A vertical CNC machine.

A)

B)
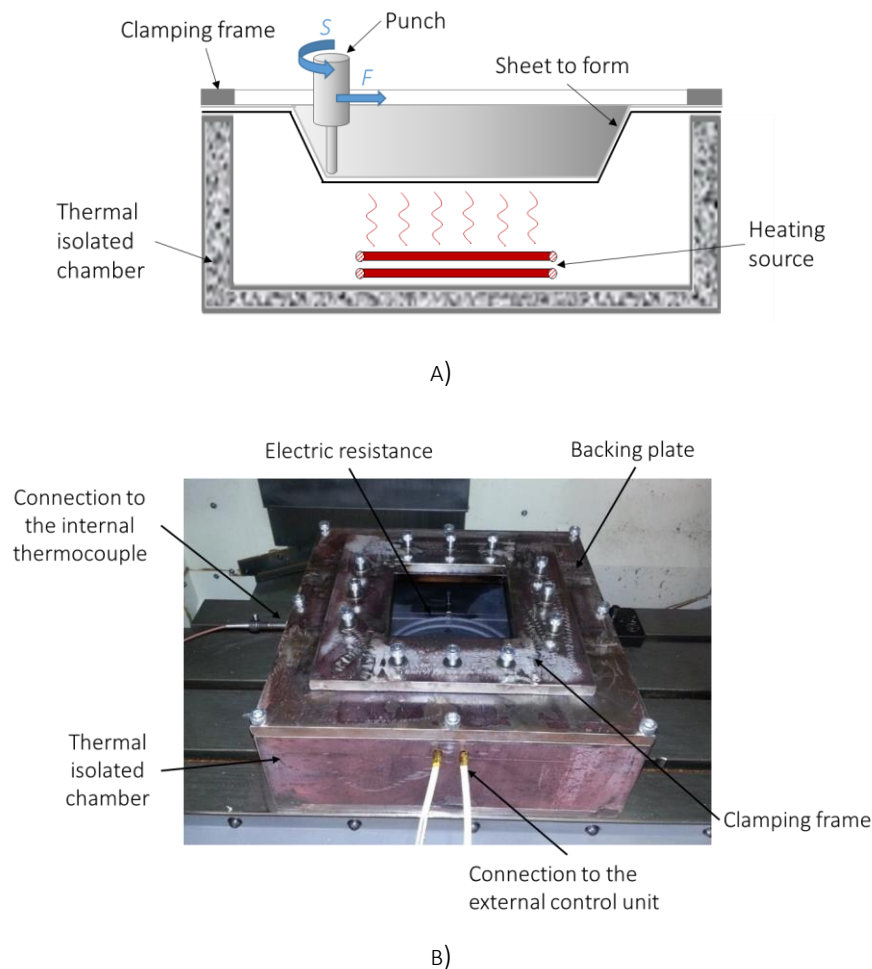
FIGURE 3.1 A) A SCHEMATIC OF THE PERFORMED SPIF PROCESS AND B) THE MANUFACTURED EQUIPMENT

As shown in Figure 3.1 B) a thermal isolated chamber was built internally coating the metallic structure with refractory material and an electric resistance of 2 kW was installed inside and connected to an external control unit in order to heat up the air and reach the necessary temperature for deforming the material. To control the working temperature a thermocouple was placed into the chamber as well, and connected to the same external control unit. A second

thermocouple was instead used during the process for monitoring the temperature on the upper surface of the worked material. In addition, a thermographic camera was also employed for a further control of the temperature and its emissivity was calibrated using the above mentioned thermocouple. Finally, a clamping frame and a backing plate allowed to fix the sheets, a hemispherical punch was used for the tests and mineral oil was applied on the material as lubricant.

All the experimental investigations described in the next paragraphs of this chapter have been performed on the described apparatus. Details of the materials, working conditions and process parameters are provided in each specific section.

3.1.2. PRELIMINARY EXPERIMENTAL INVESTIGATION ON POLYPROPYLENE (PP)

MATERIAL AND METHOD

This preliminary investigation was carried out on 1 mm thickness sheet blanks of polypropylene (PP) (see Chapter 1 for details on the material), produced by compression molding and characterized by a T_g of around 8 °C, measured by the Dynamic Mechanical Analysis (DMA). Each blank sheet (150 x 150 mm^2) was placed between the clamping frame and the backing plate, as shown in Figure 3.2. The selected geometry for these first tests was a truncated cone characterized by a big diameter of 130 mm, a wall angle of 55° and a final desired height z of 30 mm. That shape has been largely used as a test specimen for incremental sheet forming polymers and metals. In order to reduce friction, lubricant was applied on the upper surface of the sheet. A thermographic camera was used for acquiring the temperature variation during the working operation.

A preliminary 2^{4-1} factorial design of experiment was prepared. The process parameters values considered for the experimental tests are summarized in Table 3.1, distinct respectively in fixed (tool diameter D, wall angle α, forming velocity F) and variable (spindle speed S, step depth d, temperature T_i). They were set according to previous tests reported in the literature (Franzen et al., 2009, 2008; Le et al., 2008), except the temperature, which manual increase was not investigated before because the cited authors performed the cold forming.

The heat-assisted SPIF has been here investigated aiming at understanding the influence of the local temperature increase on the formability. The initial temperature has been considered a variable parameter: when tests required an initial temperature T_i higher than the room one, the heating source was turned on through the external control unit and the desired temperature was reached.

TABLE 3.1 PROCESS PARAMETERS_PP

Constant parameters		
D [mm]	α [°]	F [mm/min]
8	55	1500
Variable parameters		
S [RPM]	d [mm]	T [°C]
200	0.5	room
2000	1.0	75

FIGURE 3.2 EXPERIMENTAL SETUP

RESULTS

The following figures show the obtained samples and the process temperature at the same production phase. It is worth pointing out that the measurement of the temperature by thermographic camera was not easy due to the tool rotation and movement along the set trajectory and to the continuous temperature variation on the forming zone.

| A) | B) | C) |
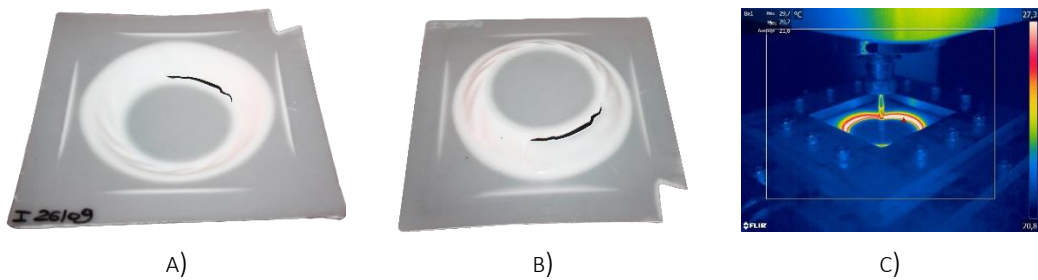
FIGURE 3.3 TEST PP_1 (S=200 RPM, d=0.5 mm, ROOM TEMPERATURE)

| A) | B) | C) |
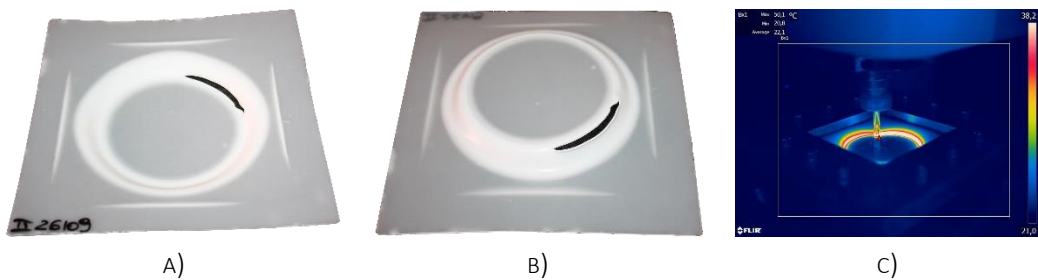
FIGURE 3.4 TEST PP_2 (S=2000 RPM, d=0.5 mm, ROOM TEMPERATURE)

A) B) C)
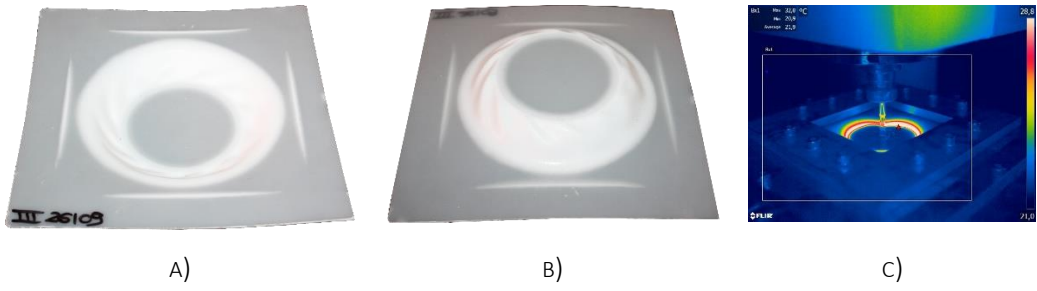
FIGURE 3.5 TEST PP_3 (S=200 RPM, d=1 mm, ROOM TEMPERATURE)

A) B) C)
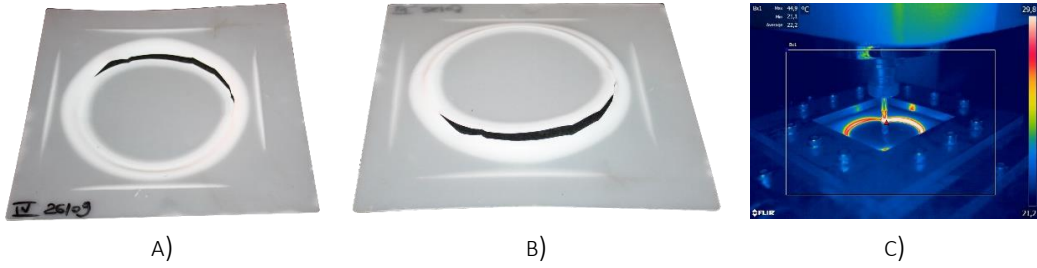
FIGURE 3.6 TEST PP_4 (S=2000 RPM, d=1 mm, ROOM TEMPERATURE)

A) B) C)
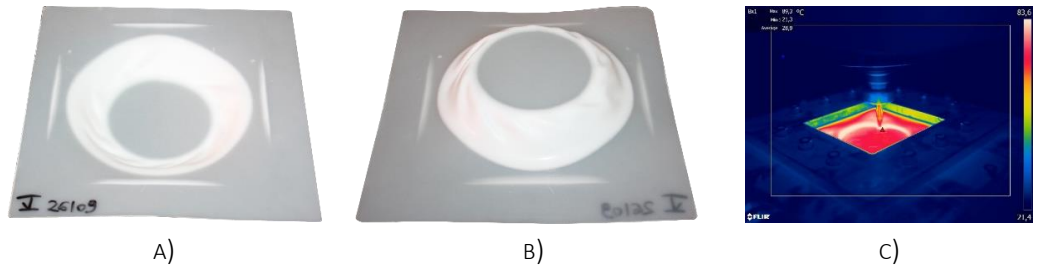
FIGURE 3.7 TEST PP_5 (S=2000 RPM, d=1 mm, T_I=75 °C)

A) B) C)
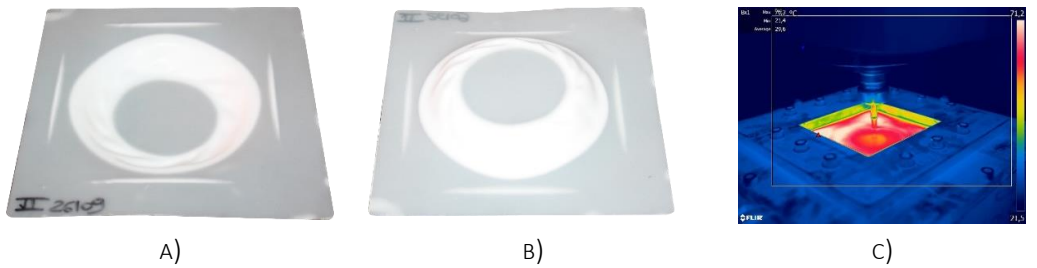
FIGURE 3.8 TEST PP_6 (S=200 RPM, d=1 mm, T_I=75 °C)

A) B) C)
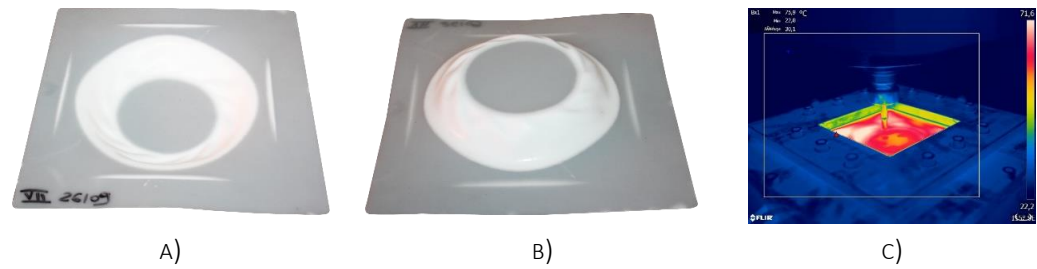
FIGURE 3.9 TEST PP_7 (S=200 RPM, d=0.5 mm, T_I=75 °C)

A)   B)   C)
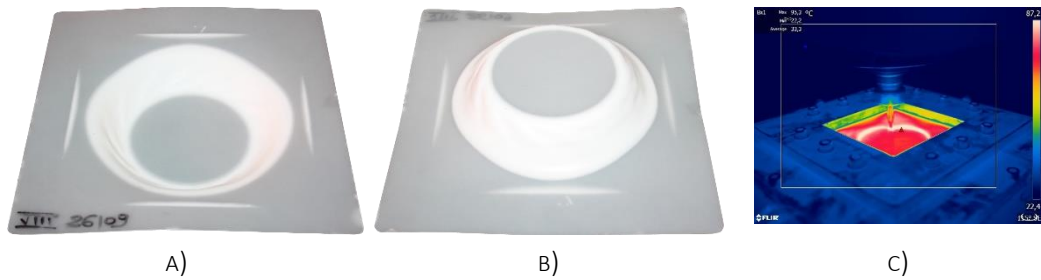
FIGURE 3.10 TEST PP_8 (S=2000 RPM, d=0.5 mm, T$_i$=75 °C)

Looking at the pictures it is possible to notice that the manufactured truncated cones whiten after forming, both inside and outside. This effect was also observed by Marques et al. (2012) who investigated other thermoplastic materials and it was attributed to the concentration of crazes in the deformed surface due to the forces exerted on the sheet.

Table 3.2 reports the obtained results of this preliminary investigation in terms of process temperature (T$_p$), maximum achieved height, failure occurrence and failure mode.

TABLE 3.2 EXPERIMENTAL RESULTS ON PP

# Test	S [RPM]	d [mm]	T$_i$ [°C]	T$_p$ [°C]	Max height [mm]	Failure
Test PP_1	200	0,5	room	29,7	20,43	Yes, crack at z=-27 mm
Test PP_2	2000	0,5	room	50,1	14,74	Yes, crack at z=-19 mm
Test PP_3	200	1	room	32	19,31	No, wrinkling
Test PP_4	2000	1	room	44,9	10,00	Yes, crack at z=-10 mm
Test PP_5	2000	1	75	89,3	23,10	No, wrinkling
Test PP_6	200	1	75	76,3	22,25	No, wrinkling
Test PP_7	200	0,5	75	75,9	21,94	No, wrinkling
Test PP_8	2000	0,5	75	95,3	25,77	No, wrinkling

In general terms, it can be observed that in all the cases of high working temperature T$_p$ (Test PP_5-6-7-8)), due to the external heating source, no cracks occurred but wrinkles along the inclined angle appeared, following the rotational movement of the forming tool. The wrinkling effect was also caused, likely, by the geometrical difference between the sample to shape and the clamping frame. In the all other cases of failure, the crack appeared along the circumferential direction.

Previous studies reported that the spindle speed has a great influence on the formability of polymers, due its relation to the increase in forming temperature (Marques et al., 2012). The investigation described in this paragraph highlights the impact of this parameter on the springback, measured in terms of maximum height of the final truncated cone. The friction between the tool and the sheet is not so high to get the material to the flow state; therefore, the final height can be explained considering that the material is still in the rubbery state (for the thermo-behaviour of thermoplastics see Figure 1.4). The influence of the temperature was also investigated in terms of surface roughness. According to Bagudanch et al. (2014), who reported a study on the incremental sheet forming process performed on PVC and PC, an increase in temperature, due to the spindle speed setting, results in a higher surface roughness. In the current study, the surface analysis was carried out evaluating the mean roughness R$_a$ measured considering two values of mean peak spacing (AR - the average distance between measured peaks), 1 mm and 5 mm, recording three

measurements for each sample. As already specified above, in this case, the temperature T_i was a process parameter and therefore the process temperature T_p was not only affected by the spindle speed value. The obtained results on PP, displayed in Figure 3.11, show that the surface roughness at low and high temperatures are comparable, therefore a substantial difference has been not detected.
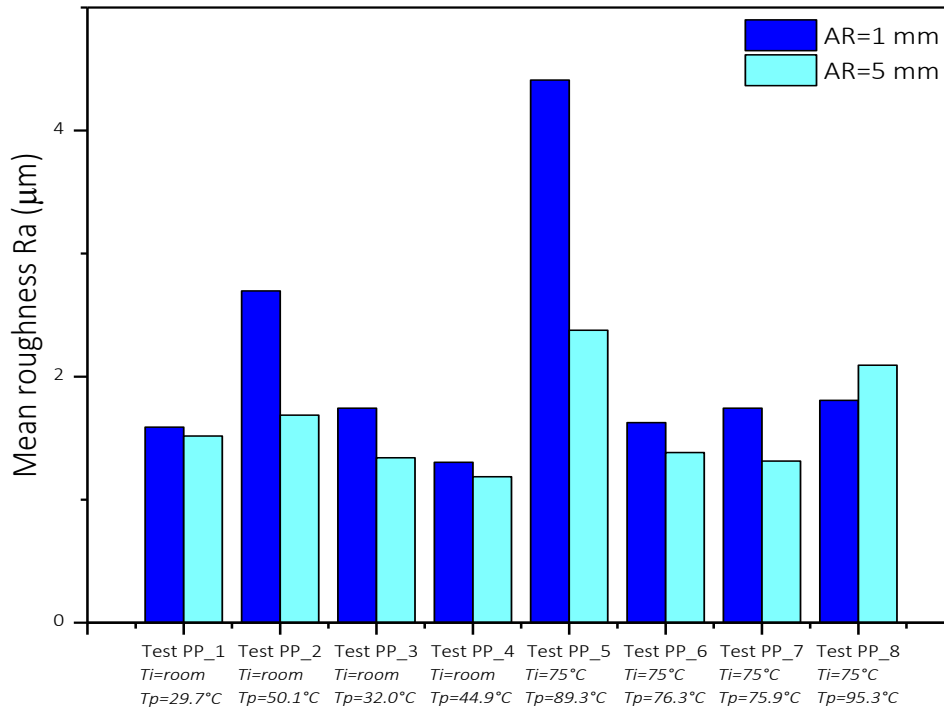
FIGURE 3.11 INFLUENCE OF T_I AND T_P ON MEAN ROUGHNESS

3.1.3. EXPERIMENTAL INVESTIGATION ON PMMA

MATERIAL AND METHOD

The experimental analysis presented in this paragraph was performed on extruded commercial poly(methyl methacrylate) (PMMA) sheets. The investigated material is characterized by a glass transition temperature of 114 °C, determined by calorimetric measurements. This means that the processed polymer is far from its rubber-like state at room temperature with the amorphous phase relatively *glassy,* therefore, consistent deformations are not feasible without the occurrence of brittle ruptures.

Each PMMA sheet (185 x 185 mm^2) was placed on the equipment, clamped and processed after being heated from its lower side and having reached temperatures close to its T_g. The temperature on the upper surface of the sheet was monitored by a thermographic camera, properly set by matching its readings with the ones extracted by a thermocouple put in contact with the sheet. Mineral oil was applied as a lubricant. At the end of the forming phase, the material was air-cooled at room temperature and, then, unclamped.

A benchmark profile, namely a frustum of cone, characterized by a big diameter of 130 mm and a final desired height z of 30 mm and a slope angle of 30° was the geometry to shape.

Details of two experimental investigations carried out on PMMA are provided below.

Aiming at understanding the influence of the working temperature on the *SPIFability* of PMMA and on the accuracy of the formed parts, a first full 2^3 factorial plan was designed and executed without any type of reduction. Each configuration was repeated three times. The experimental plan was developed taking into account the main factors that affect the investigated response and which values have been set according to the literature (Fiorotto et al., 2010; Franzen et al., 2008; Martins et al., 2009) and after a screening investigation. Four parameters were set as fixed (sheet thickness t, step depth d, tool diameter D and wall angle α) and three were varied on two levels (spindle speed S, forming velocity F, initial temperature T_i). The values are reported in Table 3.3. As concerns the initial temperature T_i, never considered as a process variable in previous studies, its values were chosen after a preliminary experimental investigation and it was carefully monitored during the forming process.

TABLE 3.3 PROCESS PARAMETERS_1° INVESTIGATION ON PMMA

Constant parameters		
t [mm]	d [mm]	D [mm]
2	2	10
Variable parameters		
S [RPM]	F [mm/min]	T_i [°C]
100	1000	80
6000	5000.0	100

A second experimental plan, based on a Design of Experiments (DOE) method, was later designed for an in-depth analysis and for an integrated comprehension of the effects of all the factors influencing the incremental sheet forming of PMMA, that is intrinsically brittle at room temperature and exhibits a super-plastic behaviour at temperatures close to the glass-rubber transition region (Abdel-Wahab et al., 2017). Six main factors, listed in Table 3.4, were considered and qualitative and quantitative outputs were evaluated as response variables, by micro and macro observations. Taking into account the no-linearity of the phenomena, each factor was varied on three levels for a full understanding of potential no-linearity in the investigated aspects. Considering the set input-output conditions, a full factorial experimental plan (3^6 test configurations) resulted unfeasible, therefore a small face-centred Central Composite Design (CCD), which consisted of 40 configurations, was adopted and evaluated according to the Response Surface Methodology (RSM).

TABLE 3.4 VARIABLE PROCESS PARAMETERS_2° INVESTIGATION ON PMMA

t [mm]	D [mm]	d [mm]	S [RPM]	F [mm/min]	T_i [°C]
2	6	0.5	100	1000	80
4	8	1.25	3000	3000	90
6	10	2	6000	5000	100

RESULTS

Performing the heat assisted SPIF on PMMA according to the first experimental plan (Table 3.3), three types of outcomes were observed: *broken* when a brittle fracture occurred, *sound* when the sheet was properly formed and *springback* when the sheet lost considerably the imposed shape (Figure 3.12).

On the *sound* samples, the thickness distribution was measured and an average thinning of about 8% was experimentally obtained.

A)   B)   C)
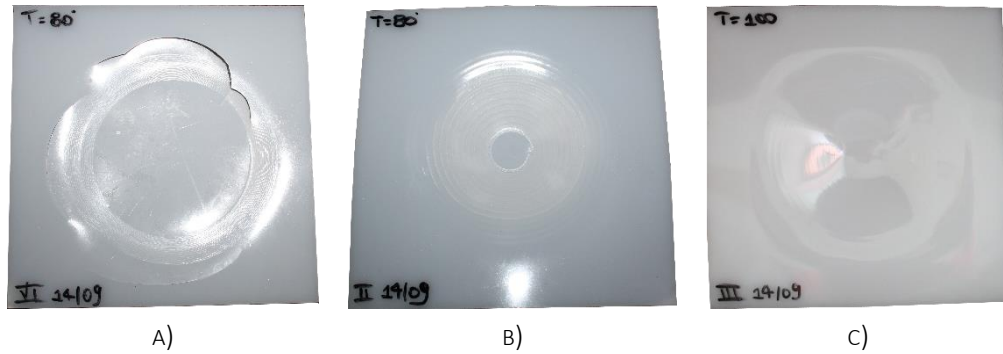
FIGURE 3.12 PMMA SAMPLES. OUTCOME TYPOLOGIES: A) BROKEN, B) SOUND AND C) SPRINGBACK

A graphical report of the interaction between the investigated process parameters (S, F, T_i) and workability output, measured in terms of final height, is shown in the following Figure 3.13, where units are omitted for the sake of simplicity.

A)
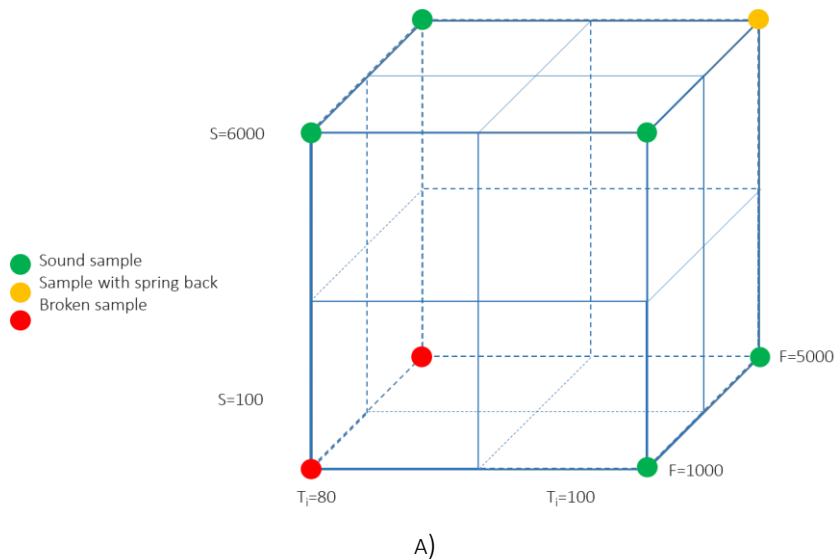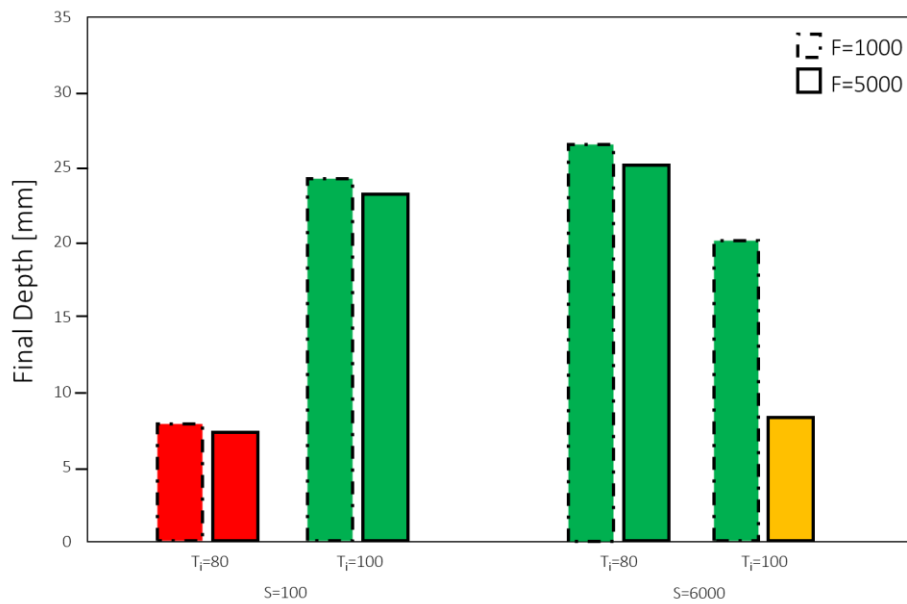
B)

FIGURE 3.13 IMPACT OF THE INVESTIGATED PARAMETERS ON THE WORKABILITY OF PMMA BY SPIF

From the bar graph, it can be observed that the spindle speed and the initial temperature are the parameters that affected considerably the process results, while the forming velocity seems to have a marginal influence, at least for the investigated input ranges. In detail, regardless the F, broken tests were obtained setting low values of T_i and S. On the contrary, high values of these parameters brought to considerable springback, which becomes relevant for the fastest condition (S=600 RPM, T_i=100 °C, F=5000 mm/min), shown with the yellow bar, where the recovery of the imposed plastic deformation returned a component close to the not deformed planar shape. Sound specimens were, instead, produced calibrating properly the combination of T_i and S, i.e. T_i=80 °C and S=6000 RPM (here defined as Sample 1) and T_i =100 °C and S=100 RPM (here defined as Sample 2). Although the final depth is a satisfactory index of the part accuracy, it has to be taken into account that a conical shape was manufactured starting from a square frame, therefore the accuracy can be improved.

The influence of T_i and S was observed also in terms of working temperature. The previous mentioned Sample 1 and Sample 2, manufactured at the same forming velocity F=1000 mm/min, were compared mainly to understand how the spindle speed affects the temperature during the process, due to the friction forces and, consequently the friction heating. Therefore, considering the two tests, Sample 1, characterized by higher S and lower T_i than Sample 2, was processed at a more elevated working temperature (about 135°C vs about 104°C), as detected by the thermographic camera (Figure 3.14). This means that the friction heating influences the overall working temperature significantly and has to be taken into account in the process setting considering the importance of the forming temperature in relation to the T_g of the processed material.

A)   B)
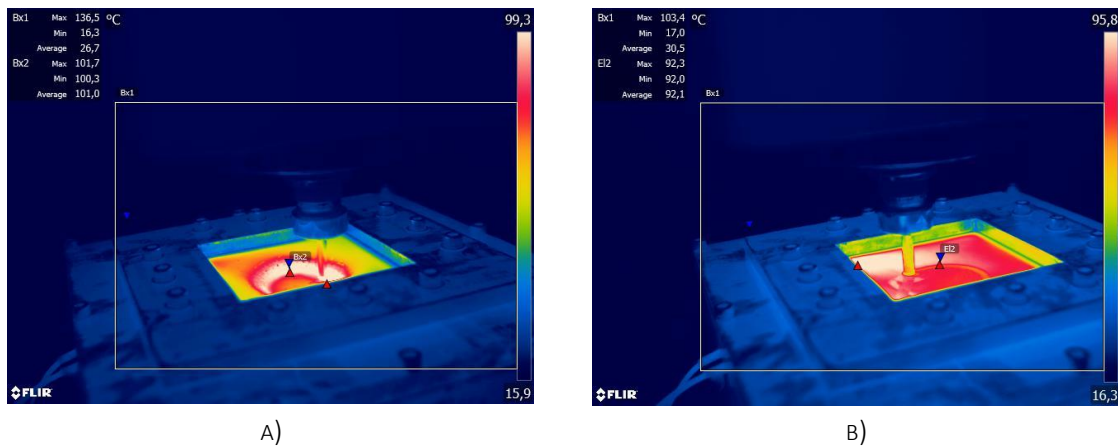
FIGURE 3.14 WORKING TEMPERATURES OF A) SAMPLE 1 AND B) SAMPLE 2

A further analysis was carried out on the surfaces of Sample 1 and Sample 2 for investigating how their quality was affected by the initial temperature (external electric heating) and by the spindle speed (friction heating). The surfaces, on the side directly subjected to the forming tool, were examined by scanning electron microscopy (SEM) and reported in Figure 3.15. As visible to the naked eye and as clearly shown in the low magnification micrographs the surface of the Sample 1 results to be damaged severely and this effect can be attributed reasonably to the high friction induced between the tool and the material surface. This is mainly due to the rubbing between the material and the forming tool at a high S value. Furthermore, this damage can be emphasized by the initial temperature (80 °C) lower than the glass transition of the analysed PMMA (114 °C). In fact, the high spindle speed promotes a local overheating of the loaded surface and, hence, an increase of its maximum tolerable stress. On the other hand, it is probable that the corresponding temperature of the surface in contact with the spindle is such that its glassy behaviour prevails on the rubbery one, increasing the stress state of the same. As regards Sample 2, the mild conditions of forming, due to a lower S and a higher T_i, allow to obtain a smooth surface, apparently featureless to the touch but characterized by traces generated by the slow spindle movement, as shown by the SEM micrograph collected at high magnification of 5000 x (Figure 3.15 B)). The SEM morphological observations confirm that, under the considered constant parameters, the effect of the electric heating (related to external heating source) on the part quality is more pronounced than the friction heating (related to the spindle speed). In fact, by operating with relatively low spindle speeds on surfaces conditioned at temperatures very close to the glass transition, it is possible to obtain items with high aesthetic quality surface and probably with satisfying mechanical properties, as long as brittle fractures and springback effects are controlled.

A)   B)
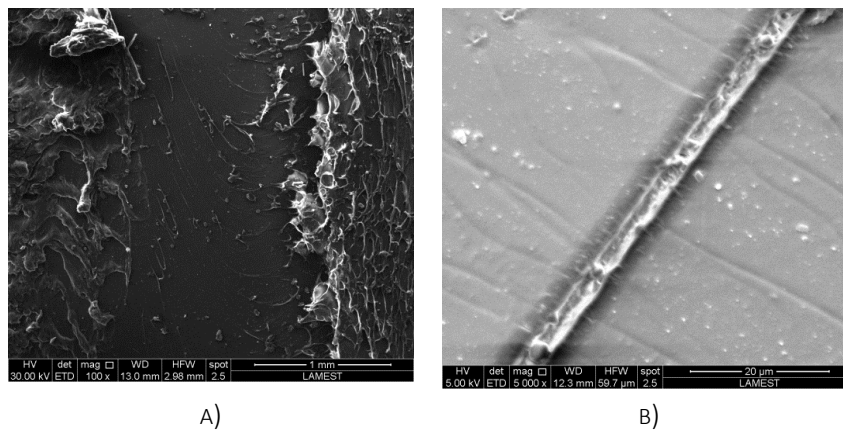
FIGURE 3.15 SURFACE MICROGRAPHS OF A) SAMPLE 1 AND B) SAMPLE 2

Summing up, the results obtained from the first experimental phase allow to conclude that the temperature plays a relevant role for properly incrementally forming thermoplastic materials. The analysis of the influence of three process parameters on the material temperature distribution during the process demonstrated that the forming velocity has a low effect on the temperature variation. Furthermore, the formed surfaces were studied and it was observed that they are damaged severely for higher spindle speed values. Consequently, an external heating source which allows the incremental forming of the material at temperatures very close to its T_g without increasing the spindle speed was judged as the most valuable solution for secondary forming sheets of thermoplastic materials with a T_g higher than the room temperature.

The successive experimental plan (Table 3.4) aimed at investigating the influence and interaction of various working parameters on the product soundness, process temperature and accuracy error of the formed parts. Furthermore, the study focused also on microscopic observations of the integrity grade of the samples surface.

A first examination was carried out quantifying the geometrical discrepancy between the expected and the obtained profiles by measuring the sound parts by a Minolta Laser scanning system and compared into CAD virtual environment with an ideal profile. Figure 3.16 reports the comparison between a real and an ideal profile of the specimen with the best dimensional accuracy obtained within this experimental campaign. An average geometrical error equal to 3.2 mm was measured on the overall surface, while a value of 1.8 mm was detected on the bottom of the specimen.
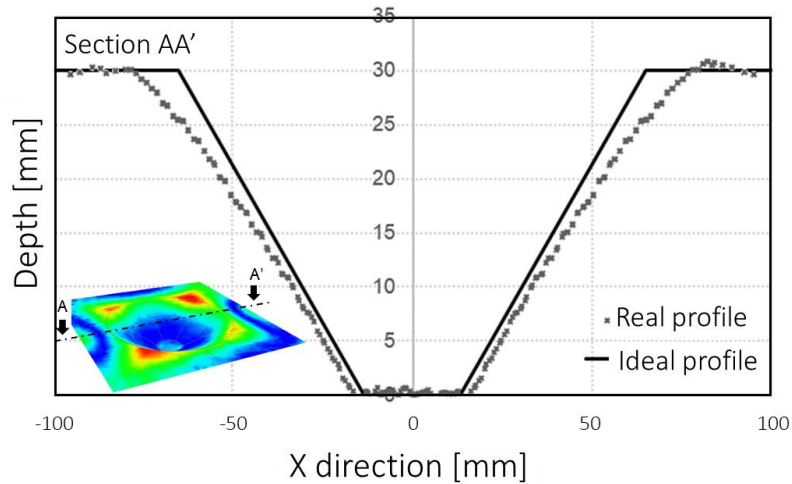
FIGURE 3.16 COMPARISON BETWEEN REAL AND IDEAL PROFILE OF A SOUND SPECIMEN

The results obtained from the small CCD-Face centred experimental plan were first analysed at a macroscale level, by Response Surfaces Methodology (RSM) techniques, aiming at emphasizing the manufacturing process optimization, and then the same tests were validated by means of an empiric approach at a microscale level to clarify the temperature effect on the quality of the post-processed parts, mainly to verify if the material degradation occurred.

Concerning the macroscale analysis, three responses were considered and discussed:

I) the product/process soundness, evaluated as a binary factor (0 for broken and springback outputs, 1 otherwise).

A preliminary regression analysis based on the t-test of single effects showed that a significant linear dependence between the product soundness and the spindle speed S and the initial temperature T_i exists (Figure 3.17 A)). At the same time, the one-factor analysis explained the type of dependence and the opposed role played by S and T_i (Figure 3.17 B)).

A)

B)
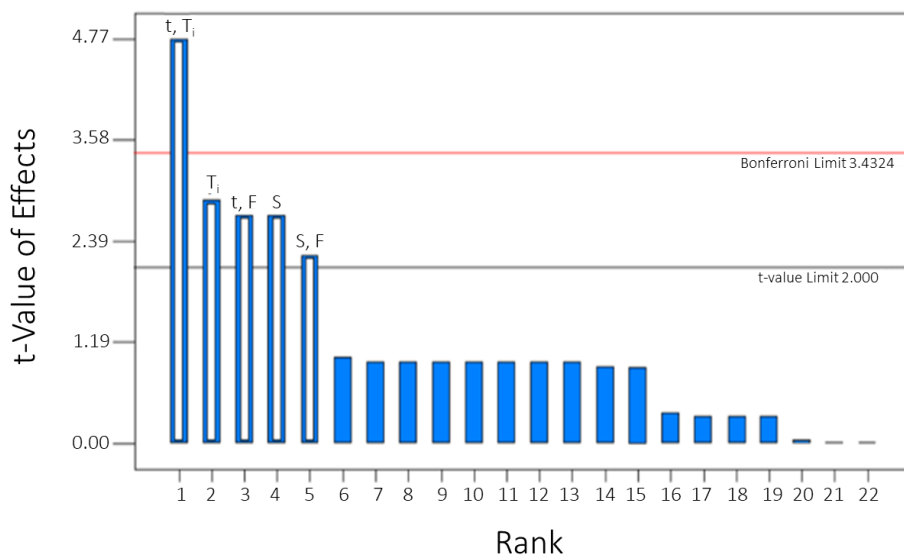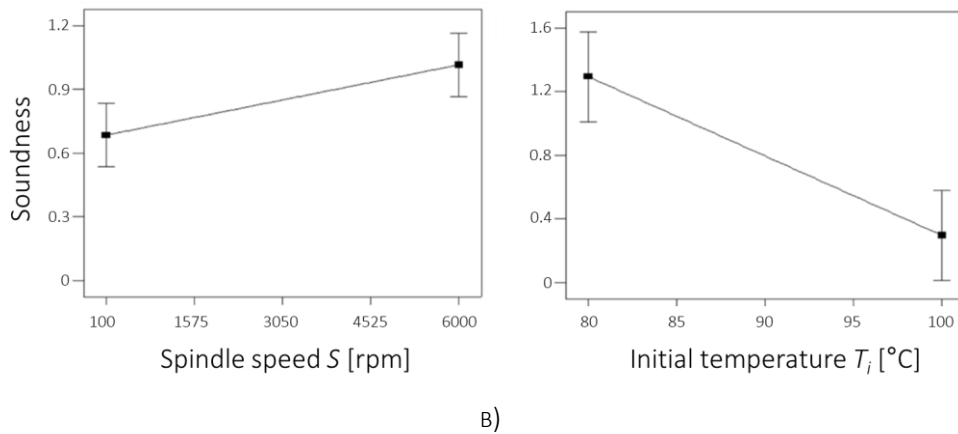
FIGURE 3.17 A) T-VALUE OF EFFECTS AND B) ONE-FACTOR ANALYSIS FOR BINARY SOUNDNESS RESPONSE

Accordingly, the best process performance has been reached finding the right compromise between these two variables. Furthermore, the t-test established a very strong influence due to the correlation between the sheet thickness t and the forming velocity F. This result is reasonably explicable considering the adopted heating system, as detailed in the next Table 3.5 where the results obtained from the numerical simulations are shown.

II) The process temperature, measured by the thermographic camera.

III) The accuracy error, measured by comparing the imposed height to the obtained one after unclamping the sheet.

Concerning these quantitative results, they have been considered as key performance indicator (KPIs). The first one was chosen since the workability of the PMMA changes according to the material temperature during the process and even small variations of this parameter, in the glass transition region, can lead to significant variations in the results. The process temperature T_p is not controlled and a priori fixed, but it results from the combination of the investigated parameters. This is important to understand how much each of the parameters and their correlation influence the temperature during the process to perform optimized forming sequences. For this reason, the maximum temperature T_{max}, reached for each configuration, was measured by the thermographic camera.

The second KPI, the part accuracy, was assessed by the following ratio:

$$Accuracy\ error = \frac{H_f - H_{after\ unclamping}}{H_f}$$

where H_f is the final depth reached by the punch at the end of the forming phase and is equal to 30 mm for sound parts or less when a crack occurs. $H_{after\ unclamping}$ is the final height of the component after its unclamping, when the elastic deformation is recovered. According to that, values of this ratio close to 1 are synonymous of a not satisfactory result and therefore this has to be avoided.

For a full comprehension of the investigated responses, the RSM was adopted starting from the ANOVA analysis. For both of the investigated responses, a reduced factorial model of the first order was adequate to justify the obtained evolution trend.

Concerning T_{max}, the slope of the diagrams reported in Figure 3.18 suggested a significance of the first order factor. Looking at the trend slopes, the spindle speed S and the initial temperature T_i are the variables, which mainly affect the process temperature on the upper surface of the sheet. These variables are, therefore, the most important to guarantee suitable forming conditions avoiding brittle fractures and excessive springback of the parts.
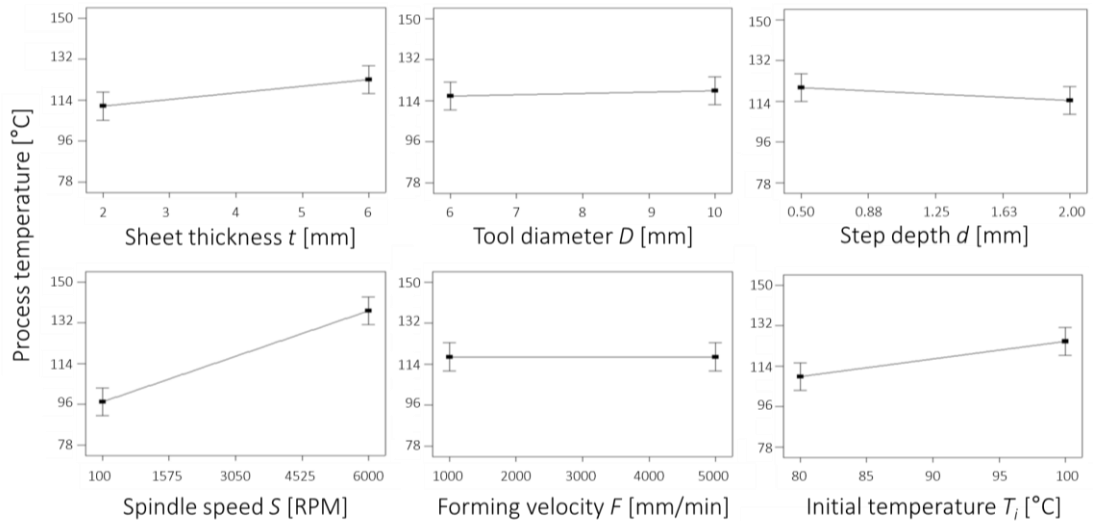
FIGURE 3.18 INFLUENCE OF THE INVESTIGATED PARAMETERS ON THE PROCESS TEMPERATURE

The influence of the investigated parameters on the loss of the shape once the process finished, was also investigated by RSM. The results are graphically shown in the one-factor diagrams reported in the following Figure 3.19.
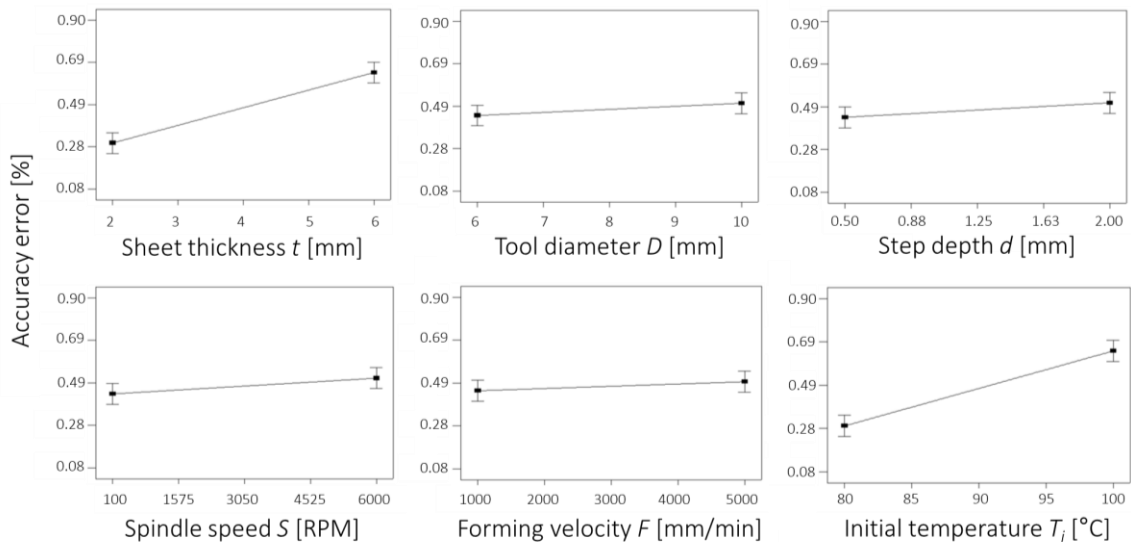
FIGURE 3.19 INFLUENCE OF THE INVESTIGATED PARAMETERS ON THE ACCURACY ERROR OF THE FORMED PARTS

The final height of the specimen resulted to be dependent on T_i, S and t. The influence of the first two variables is expected due to their effect on the temperature variation during the process as demonstrated in the first experimental investigation, while the relevance of the sheet thickness for the springback was explained considering the temperature gradient at different thickness values.

79

Indeed, the target value on the upper side of the surface was obtained setting a higher temperature inside the heated chamber. Because of this, part of the material from the bottom side of the sheet is viscous and the stiffness of the worked parts is reduced. When the forming tool moves back at the end of the process, the height of the truncated cone results more reduced when the sheet has a bigger thickness. To verify the hypothesis the thermal gradient generated during the process along the sheet thickness was numerically estimated. The model was implemented by Altair Hyperworks 14.0 and transient thermal analyses at various working temperatures were performed. The model was meshed by bricks with a density of 2 elements for each millimeter along the sheet thickness (http://altairuniversity.com/). The PMMA thermal properties were set in the material model, while isotropic structural properties were considered since the analyses based just on the heat flow inside the plate. The boundary conditions were defined according to the experiments. Specifically, the sheet was surrounded on its top and bottom side by two fluids to simulate the interaction between air and sheet. Superficial elements were defined for both the faces of the sheet to simulate the heat exchange by convection between fluid and material. The initial temperature, set at 20 °C for both fluids, remains constant on the upper side, while progressively increases on the lower side following trends derived by experimental evidences. The peripheral edges of the sheet were set as adiabatic being the parts in contact with refractory materials. Once the temperatures monitored during the experiments on the upper face of the sheet were reached, the simulations were stopped and the value on the bottom surface was determined, as reported in Table 3.5. The computational time depends both on the imposed temperature and on the thickness of the formed sheets, but few minutes were required for each configuration.

TABLE 3.5 TEMPERATURES ON THE TOP AND BOTTOM SURFACES AT DIFFERENT SHEET THICKNESSES

	Sheet thickness [mm]								
	2	2	2	4	4	4	6	6	6
Input data from experiments									
Top surface temperature [°C]	80	90	100	80	90	100	80	90	100
Chamber temperature [°C]	185	205	230	205	220	235	230	240	255
Output data from numerical model									
Bottom surface temperature [°C]	85	96	107	92	105	106	98	111	122

The differences among the calculated gradients resulted consistent. These discrepancies can affect the obtained results and, therefore, have to be taken into account. The designed heating system showed not promising results if the thickness of the sheet is greater than a specific value. Indeed, on PMMA sheets that are thick 6 mm, consistent springback phenomena seem to be unavoidable unless different heating solutions are considered.

Since the formability cannot be the only analysed aspect for evaluating the soundness of the PMMA manufactured samples, the integrity grade of the surface was also investigated, considering that side where the material was in contact with the forming tool. Therefore, microscopic observations were necessary for understanding if some specimens had to be considered production waste because of their surface degradation.

Four different conditions, depicted in Figure 3.20, were identified and defined as *cold*, *sound*, *hot* and *burned* surfaces. The initial temperature and the spindle speed can be considered the most relevant process parameters that affect the surface quality, because of the link between the temperature and the stress state and the flexural strength. The other investigated variables showed a negligible influence on the surface. More in detail, if the process parameters lead to cold conditions, the stress state exceeds the material ultimate strain and breaking points appear randomly on the surface (Figure 3.20 A)). Increasing the temperature during the forming phase, the material gets into its viscous or rubbery state, the flexural strength is reduced significantly and a surface without defects, or sound, is detectable (Figure 3.20 B)). On the other side, the more the process temperature is higher than the PMMA glass transition, the bigger the micro bubbles, which appear on the surface, become (Figure 3.20 C)). Emphasizing this phenomenon with critical conditions (i.e. high spindle speed), large-scale surface damages appear (Figure 3.20 D)). In this last case, the plastic undergoes a general degradation, named as *burned* surface, with a generalized damage that affects both the mechanical and aesthetic quality of the formed parts.

A)

B)

C)

D)
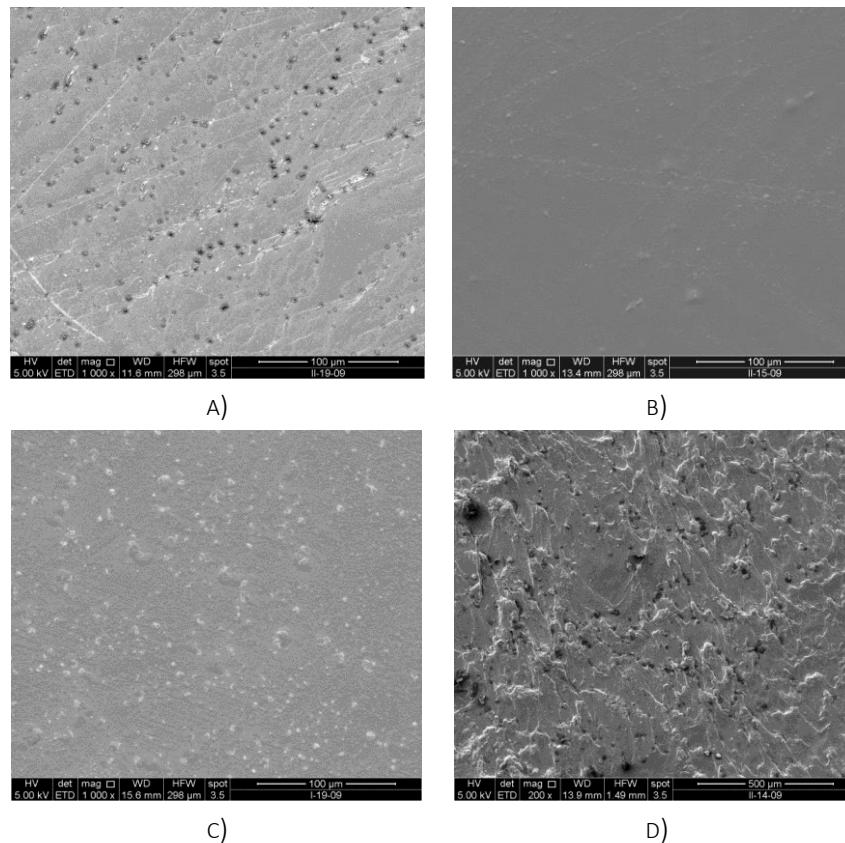
FIGURE 3.20 SURFACE INTEGRITY ANALYSIS: A) COLD, B) SOUND, C) HOT AND D) BURNED

To further prove that the surface integrity is mostly influenced by the initial temperature and by the spindle speed, micrographs of samples have been analysed. Specifically, the samples were manufactured setting the same process parameters (t=2 mm, d=0.5 mm, D=6 mm, F= 5000 mm/min), except the initial temperature and the spindle speed (varied from 100 °C to 80 °C and from 100 RPM to 6000 RPM, respectively). The maximum process temperature T_{max} was comparable, having been detected equal approximately to 105 °C for the first case (Figure 3.21 A)) and to 110 °C

for the second one (Figure 3.21 B)). Observations highlighted that the surface integrity is clearly different and that an increment of the spindle speed worsens the surface, which appears to be stirred.

A)   B)
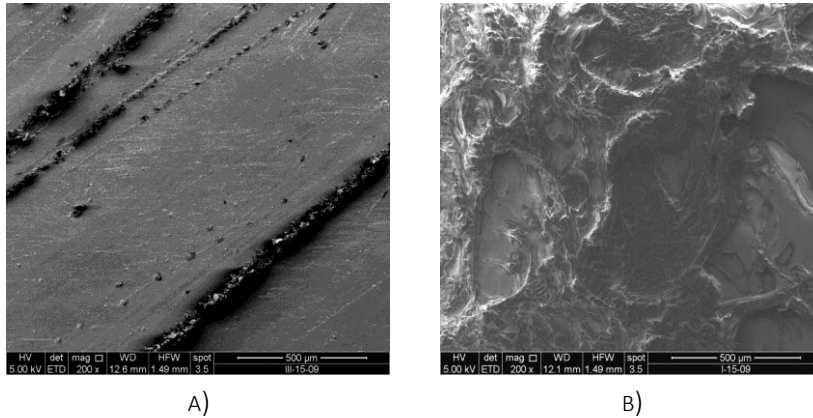
FIGURE 3.21 PROCESS CONFIGURATIONS WITH COMPARABLE MEASURED WORKING TEMPERATURE T_{MAX}: A) T_I=100 °C, S=100 RPM, B) T_I=80 °C, S=6000 RPM

Summing up, satisfactory results were achieved especially when PMMA sheets with smaller thickness were considered, whereas the adopted equipment is not suitable to form sheets with thickness greater than a certain threshold.

Macroscale evidence demonstrated that the initial temperature and the spindle speed are the main process parameters to take into account for a sound sheet formability. Their values have to be balanced to find suitable conditions and to guarantee the process feasibility.

As regards the microscale observations, four conditions were identified and defined. The initial forming temperature and the spindle speed, being correlated to the process temperature, were still identified as the most relevant parameters, which strongly affect the quality of the results. Furthermore, microscopic observations revealed that elevated spindle speeds damage the surface integrity, significantly. In fact, in spite of similar forming temperatures, tests carried out with higher spindle speed were characterized by more deteriorated surfaces. The other investigated parameters, resulted to be less significant because the initial temperature and the spindle speed hide their influences.

Finally, the hot-assisted incremental forming of polymers with a glass transition temperature higher than the room one is feasible by maintaining the forming temperature in a suitable range during all the phases of the process. The analysis of the experimental plan pointed out that heating the material by means of an external source up to the adequate forming temperature is the best solution for incrementally shaping this thermoplastic material within certain values of thickness.

3.1.4. EXPERIMENTAL INVESTIGATION ON GLASS FIBER REINFORCED PA6

MATERIAL AND METHOD

The investigations discussed in the previous paragraphs proved the feasibility of SPIF on thermoplastic materials. The obtained results allowed to extend the research on thermoplastic matrix based composites. To this aim, the selected material was polyamide 6 (PA) reinforced with 12% of short glass fibers, used to produce lightweight components for the mechanical engineering, as well as for aircraft and automobile constructions. This material is characterised by high stiffness and strength, low specific weight, long-term application temperature (140°C) and a good chemical resistance. Furthermore, it has a continuous working temperature between -20°C and 140°C, can withstand high temperature peaks up to 180°C and is characterized by a crystalline grain melting range of about 220 °C (Table 3.6). Machining and laser cutting are examples of the only tested secondary processing techniques (Hendel, 2003).

TABLE 3.6 FIBERGLASS REINFORCED PA 6

Properties	Value	Unit
Density	1,22	g/cm^3
Yield stress	105	MPa
Tensile modulus of elasticity	5400	MPa
Service temperature, long term	-20 ÷ 140	°C
Service temperature, short term	180	°C
Heat deflection temperature	190	°C

Tests were carried out on square sheets (150 x 150 mm^2) 1 mm thick. The geometry to shape was a truncated cone characterized by an initial diameter of 130 mm and a final height of 30 mm. Furthermore, since the T_g of the studied material is higher than the room temperature, the external heating source was necessary to perform the process in *hot* conditions.

1° EXPERIMENTAL INVESTIGATION

Taking into account the previous experimental plans on polymers, the following constant parameters were set, while for this preliminary analysis the values of the variable parameters were defined step-by step. They are summarized in Table 3.7.

TABLE 3.7 PROCESS PARAMETERS_GLASS FIBER REINFORCED PA6

Constant parameters			
D [mm]	d [mm]	S [RPM]	F [mm/min]
10	1	100	5000

Variable parameters	
α [°]	T [°C]
30	80
40	150
-	200

2° EXPERIMENTAL INVESTIGATION

After having proved the feasibility of the process with the above described first experimental plan, the research was extended for a better understanding of the main parameters that affect the process and the quality of the manufactured outcomes. For this reason, a further parameter was set as variable (step depth d) and together with the wall angle α and the initial temperature T_i were varied on two levels according to preliminary screening tests (Table 3.8), while the other constant factors are the same listed in Table 3.7. A full orthogonal experimental plan was designed, therefore 8 (2^3) different configurations were defined, and three replications were executed for each test configuration to prove the repeatability and to ensure the robustness of the results.

TABLE 3.8 VARIABLE PROCESS PARAMETERS_ GLASS FIBER REINFORCED P6A

d [mm]	α [°]	T_i [°C]
1	30	150
2	40	200

RESULTS

RESULTS OF THE 1° EXPERIMENTAL INVESTIGATION

The preliminary investigation carried out on glass fiber reinforced PA6 aimed at assessing the SPIF feasibility and to characterize the formability limits of the material, including the temperature influence on the global sheet formability.

The first two tests were performed setting a wall angle α=30° and changing the processing temperature. Figure 3.22 shows the first sample manufactured at a temperature of 80 °C. It presents a crack along the working trajectory, which occurred when the specimen was almost half-shaped. The low temperature caused both the failure of the part and the surface degradation with a noticeable whitening of the lower part (Figure 3.22 B)). This phenomenon could be due to the stretching of the polymeric chains for their low mobility, which has to be ascribed to the combination of low forming temperature and the presence of included glass fibers.

A)   B)
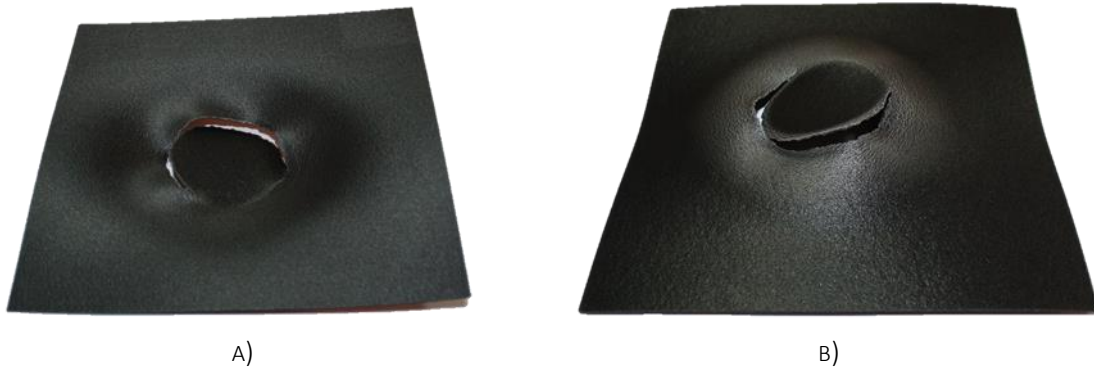
FIGURE 3.22 A) FRONT AND B) BACK SIDE OF THE SPECIMEN SHAPED AT α=30° AND T$_I$ =80 °C

The second test is shown in Figure 3.23 and was performed increasing the temperature up to 150 °C. A crack occurred because of the rubbery state reached by the sheet, due to the high temperature. The material, in fact, reduced its stiffness sharply and a consistent springback was also observed. However, a different result on the back surface of the sample was detected. In fact, the surface whitening did not appear and this was attributed to a more elevated energy related to the higher working temperature, which allows the polymeric chains to move easier at the molecular level.

A)   B)
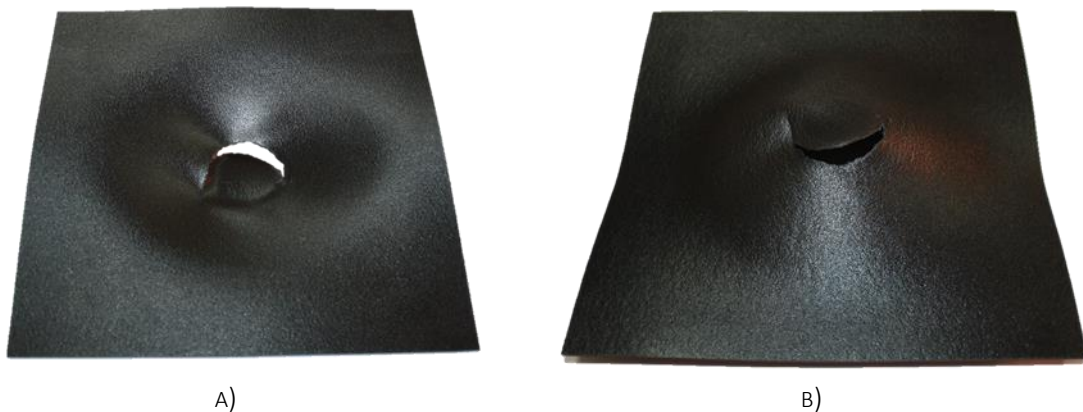
FIGURE 3.23 A) FRONT AND B) BACK SIDE OF THE SPECIMEN SHAPED AT α =30° AND T$_I$=150 °C

Observations on these first two samples led to conclude that SPIF cannot be used to form composite sheets regardless the imposed working conditions. In fact, if a low temperature is set, the polymeric chains cannot arrange during the punch passage and the sheet breaks easily. On the other side, increasing the temperature, a viscous behaviour of the material is evident, which does not allow a proper shaping of the part.

To overcome this issue and to examine in detail the formability of the investigated material, an aluminium sheet (AA-1050) (150 mm x 150 mm x 1 mm) was used during the process. Metal and composite were fixed together by the clamping frame and the punch acted directly on the aluminium, deforming at the same time the under laid composite. A lubricant emulsion was supplied on the Aluminum sheet during the process to reduce friction. Furthermore, to control and measure the temperature on the upper surface of the composite during the process by means of a thermocouple, a small hole was drilled in the centre of the aluminium sheet (Figure 3.24).

FIGURE 3.24 DRILLED ALUMINIUM SHEET LAID ON THE COMPOSITE ONE

The same test of Figure 3.23 was repeated superimposing the metal sheet on the composite one. The obtained result showed that in this case, the sample was well shaped and no tearing and no bottom surface degradation occurred.

A)   B)
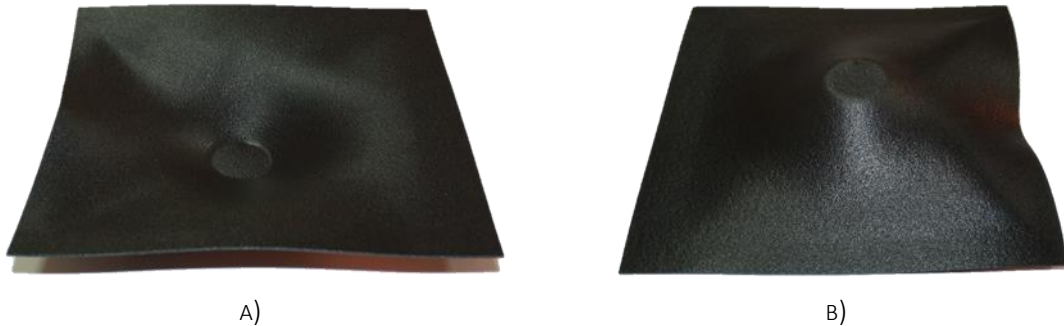
FIGURE 3.25 A) FRONT AND B) BACK SIDE OF THE SPECIMEN SHAPED AT α=30° AND T_I=150 °C SUPERIMPOSING AN AL SHEET ON THE COMPOSITE ONE

To deeply assess the formability, the wall angle value was increased to 40° maintaining the temperature at 150 °C. As shown in Figure 3.26, increasing the forming limit a crack occurred almost at the end of the process. Its typology was different from the previous ones where the crack was tangential to the tool path (Mode 1). In this last case instead, the composite was ripped by the punch movement and the crack spread radially (Mode 2). The different behaviour can be explained considering that in Mode 1, the break is linked to a material softening with a loss of its load-bearing properties, while in Mode 2, the deformation of the aluminium sheet stretches the composite circumferentially bringing the material to rupture.
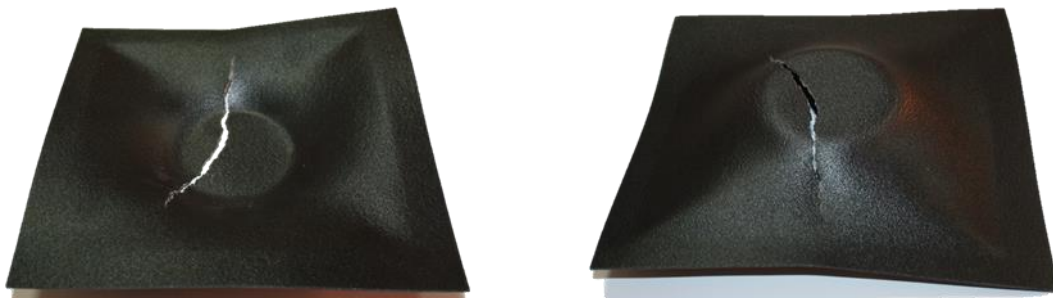
A)   B)

FIGURE 3.26 A) FRONT AND B) BACK SIDE OF THE SPECIMEN SHAPED AT α =40° AND T$_i$=150 °C SUPERIMPOSING AN AL SHEET ON THE COMPOSITE ONE

A further configuration was tested setting α=40° and T$_i$=200 °C aiming at understanding the relation between these two parameters. Figure 3.27 shows that the part was successfully processed confirming that, if properly set, SPIF can be used to shape the composite sheet using the temperature variation to change the forming limits.

A)   B)
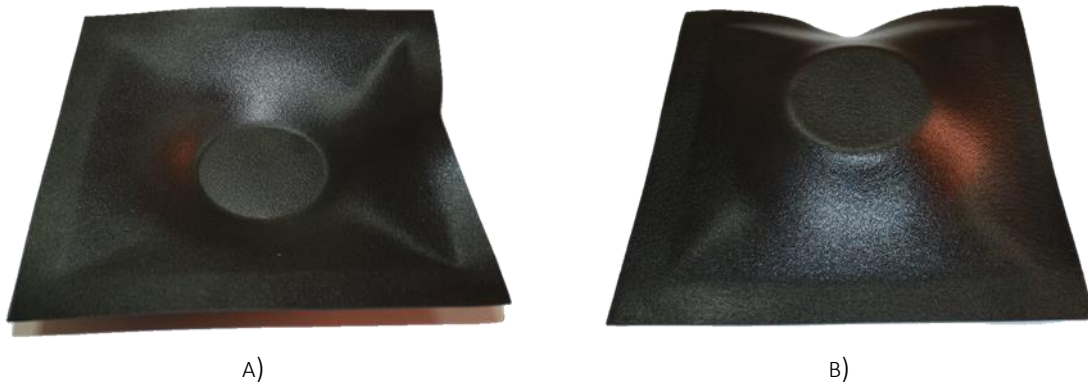
FIGURE 3.27 A) FRONT AND B) BACK SIDE OF THE SPECIMEN SHAPED AT α=40° AND T$_i$=200 °C SUPERIMPOSING AN AL SHEET ON THE COMPOSITE ONE

Summarizing, this preliminary study on PA6 reinforced laminates demonstrated that SPIF cannot be applied in the conventional way (direct contact of the punch on the sheet), but an additional low-cost-high-formable material blank is required for facilitating the process and sustaining the composite deformation.

RESULTS OF THE 2° EXPERIMENTAL INVESTIGATION

The second investigation was carried out to extend the analysis on the SPIFed composite sheets and more in detail to evaluate the material formability, the thickness distribution and the part accuracy. All tests were performed using the aluminium sheet support and mineral oil was applied as lubricant.

Concerning the material formability, all the test configurations gave back sound components (an example in reported in Figure 3.28 A)), except one processed setting α=40°, d=1 mm and T$_i$=150 °C (Figure 3.28 B)). The low value of d combined with a low value of T_i caused a fracture that proceeded tangentially to the tool path. Furthermore, a distortion out of the forming area was observed and this can be probably attributed to high residual stresses in the sheet and could be reduced using a backing plate that fits with the sample geometry.

A)   B)
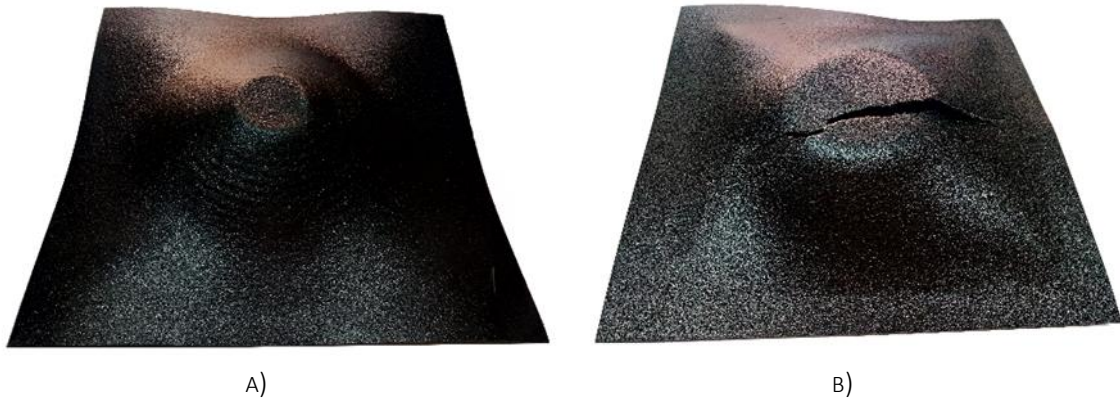
FIGURE 3.28 A) SOUND SPECIMEN AND B) BROKEN SPECIMEN

As regards the analysis on the thickness distribution, it was measured after the unclamping phase and along the two orthogonal planes perpendicular to the clamping zone. Figure 3.29 A) reports the obtained values for the experiments carried out with a wall angle of 40° and changing the other process parameters. The trends shows that a reduced sheet thinning can be observed for lower step depth. This allows to conclude that i) the composite deformation mechanics has the same characteristics observed on SPIFed metals and therefore the deformation results strongly localised to the contact zone between the punch and the sheet, and ii) comparing the curves with the same α and d but changing T_i, the overlapping is quite fitting. This suggests that, within the investigated range, the temperature does not influence the thinning phenomenon. Figure 3.29 B), instead, displays curves of samples manufactured setting the same initial temperature (T_i=150 °C). Comparing the samples characterized by the same step depth d, it is possible to observe that the higher the slope of the cone is, the more consistent the thinning is.

A)   B)
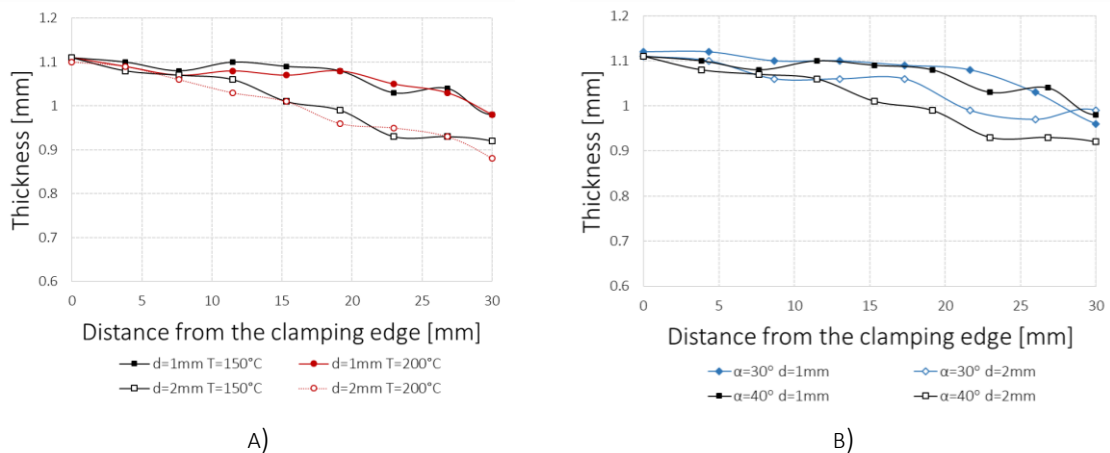
FIGURE 3.29 THICKNESS DISTRIBUTION_PA6 REINFORCED WITH SHORT GLASS FIBERS

The last goal of this second investigation was to evaluate the part accuracy, measured both in terms of springback, by comparing the final height reached after the manufacturing phase with the ideal geometrical height of 30 mm, and in terms of the 3D profile, by acquiring the geometry of the

manufactured sample by a 3D Minolta Laser Scanning System (Figure 3.30) and comparing it with the ideal profile.

FIGURE 3.30 3D LASER SCANNING SYSTEM

Concerning the springback, Figure 3.31 shows that the best results are obtained processing the material at higher T_i and higher d. Nevertheless, the part accuracy represents the main drawback of the process, indeed the 60% of the samples has a final height less than 25 mm, and therefore this weakness cannot be neglected.
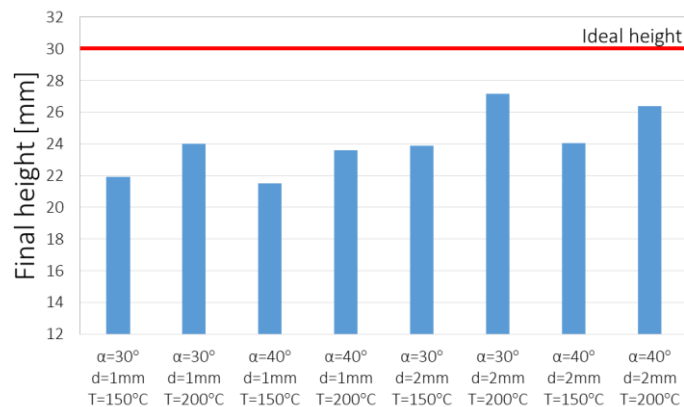
FIGURE 3.31 FINAL HEIGHT_ PA6 REINFORCED WITH SHORT GLASS FIBERS

As regards the 3D profile, the used technique allowed to obtain a cloud of points of every single manufactured sample and each one was then uploaded into a virtual environment and aligned to the 3D ideal profile. The punctual geometrical errors and the relative average value were quantified and measured as the orthogonal minimum distance between each point and the ideal surface. An example is reported in Figure 3.32, which displays a sample processed setting α=30°, d=1 mm and T_i=150 °C. A significant geometrical deviation between the two profiles can be observed, especially on the lateral surface, with an average geometrical error of 2 mm.

A)   B)
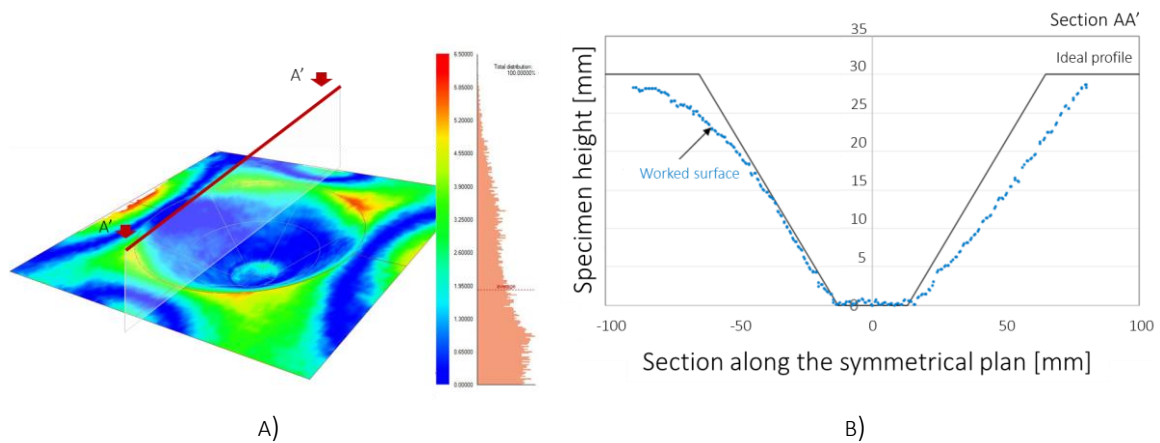
FIGURE 3.32 A) GEOMETRICAL ERROR ANALYSIS AND B) COMPARISON BETWEEN IDEAL AND REAL PROFILES

The detected geometrical distortion can be mainly attributed i) to the springback and residual stresses because stretching is the main deformation mechanism, ii) to the absence of the backing plate which makes the material more free to bend and iii) to the imposed thermal gradient that can affect the material behaviour, making it softer or stiffer.

To examine in depth the part accuracy, aiming at reducing the above described effect, a further experimental investigation was designed. A hexagonal pyramid with a lateral wall angle α of 40°, a major diagonal of 130 mm and a final height of 40 mm was chosen as geometry to shape (Figure 3.33 A)). A backing plate was added to the equipment to properly lock the bottom part of the sheet (Figure 3.33 B)), as prescribed by Jeswiet and Young (2005). All the new tests were performed setting the same constant process parameters reported in Table 3.7 and keeping fixed d and T_i as well, chosen considering the worst conditions of the previous reported experimental investigation (d=1 mm and T_i=200 °C). The idea was to test four different thermal cycles for evaluating the effect of the thermal gradient for the heating and cooling phases, maintaining constant the duration of the working phase (Figure 3.33 C)). Therefore, the variability was defined modifying:

- the power setting of the electrical heater for a fast, medium or slow heating reached respectively after 5 min, 10-12 min and 55-60 min
- the cooling mode which could be in air for 15 min or in cold water for 1 min.

A)   B)

c)
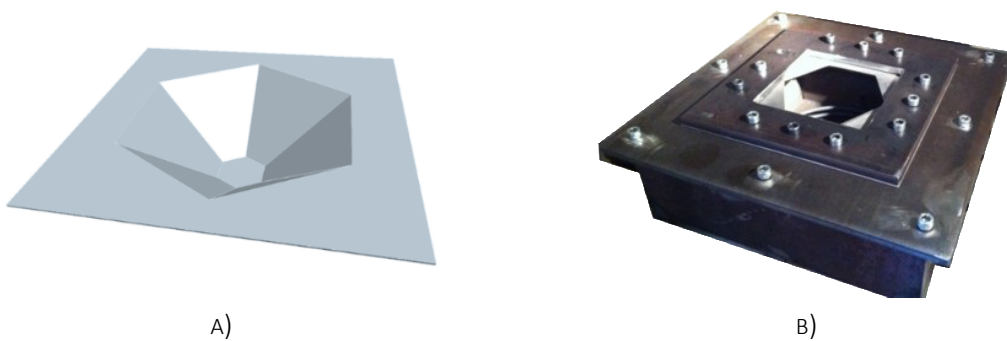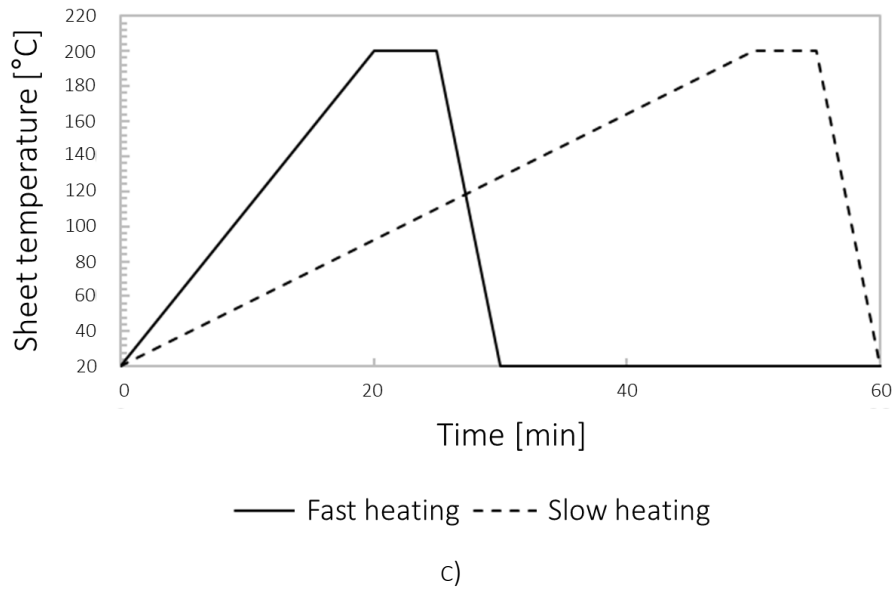
FIGURE 3.33 A) HEXAGONAL PROFILE, B) NEW BACKING PLATE, C) TEMPERATURE LAWS WITH A DIFFERENT GROWTH GRADIENT

All the manufactured specimens were classified as *sound*, as actually expected, even if a remarkable difference in terms of shape accuracy was observed. The same method of comparing the 3D scan of each sample to the ideal profile was used. Table 3.9 summarizes the test conditions and for each one displays both the manufactured sample and the measured geometrical error.

TABLE 3.9 ACCURACY ANALYSIS OF HEXAGONAL SAMPLES

Test condition	Manufactured sample	Geometrical error
Test 1: Fast heating Air cooling		
Test 2: Medium heating Air cooling		

Test 3:
Slow heating
Air cooling
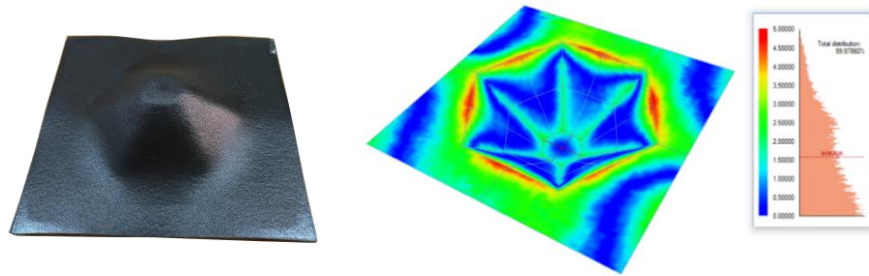
Test 4:
Slow heating
Water cooling
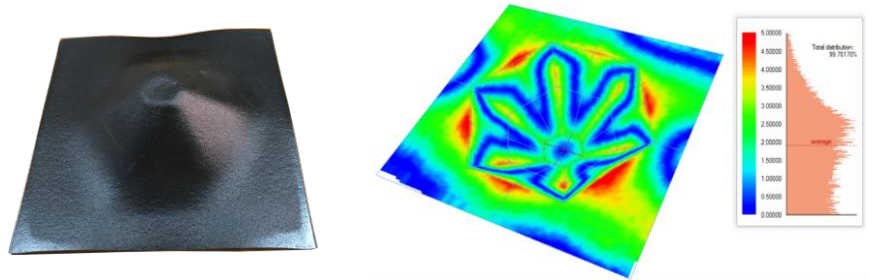
The 3D profiles of *Test 1* and *Test 2* reproduce better the desired geometry, as visible from the coloured maps. The distribution of the geometrical error along the whole profile and the relative average error are graphically represented next to the coloured map. *Test 1*, characterized by fast heating and air cooling mode, presents the smallest value of average geometrical error (about equal to 1 mm) and the best accuracy. On the other side, the slower heating strongly affects the part accuracy with an increase of the average geometrical error up to 1.5 mm. The worst condition can be observed for the *Test 4*, where the slow heating is combined with the faster cooling in water.

For sake of completeness, the thickness distribution and final height of the hexagonal based pyramid samples were measured as well. The results are shown in the following table.

TABLE 3.10 FINAL HEIGHT AND THINNING OF HEXAGONAL SAMPLES

Heating mode	Cooling mode	Final height [mm]	Average thickness [mm]	Minimum thickness [mm]
Fast	Air	40	0.84	0.51
Medium	Air	38	0.85	0.38
Slow	Air	38	0.95	0.56
Slow	Cold water	38	0.95	0.52

Although the previous observations on the part accuracy based on the 3D profile analysis, the appearance of small inhomogeneity on the worked product were observed measuring the final height and thinning. These effects, considering the previously mentioned absence of chemical and physical degradations of the investigated material, can be attributed to local macromolecular rearrangements that could happen due to both low thermal conductivity and long structural relaxation times, typical of polymers. Moreover, the presence of rigid glass fibers into the plastic matrix could further constrain the macromolecular structure, determining the mentioned inhomogeneity visible on the sheet surface.

For a full understanding of the material behaviour, morphological observations were executed on the material surface and along the sample thickness by scanning electron microscopy (SEM), which provides high-resolution micrographs at different length scales. The analysis, carried out on the truncated cone samples, aimed mainly at studying if and how the process parameters may affect the glass fibers or may degrade the thermoplastic matrix.

First of all, an as-received piece of material was analysed in order to compare these results with those obtained from the analysis on the SPIFed samples. Figure 3.34 A) shows the fibers orientation due to the primary manufacturing process, while Figure 3.34 B) displays a random distribution of fibers along the thickness.

A   B
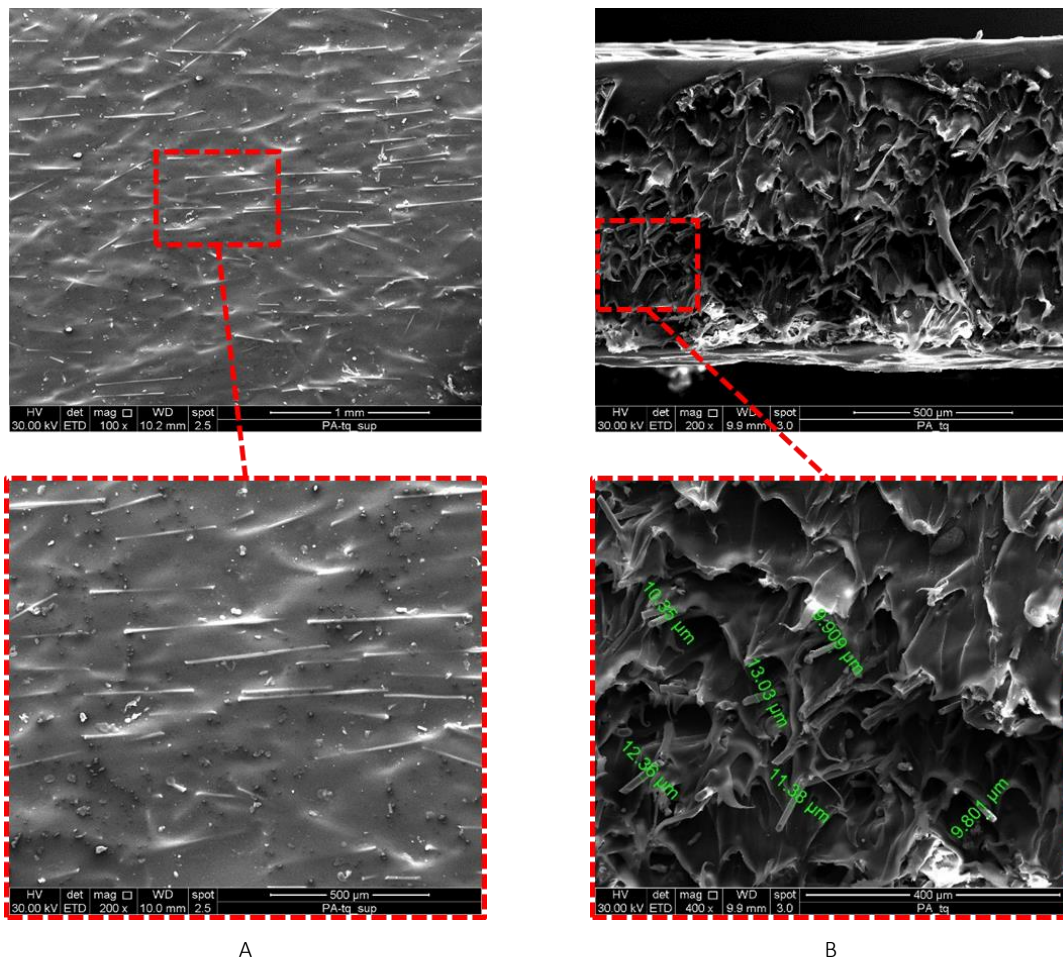
FIGURE 3.34 SEM IMAGES OF THE AS-RECEIVED MATERIAL: A) ON THE SURFACE AND B) ALONG THE THICKNESS

The SEM analysis carried out on the manufactured samples did not show any material alteration or fibers distortion. This can be observed on Figure 3.35, which displays micrographs of the surface (on the left) and along the thickness (on the right) of four different test configurations.

α=30°, d=1mm, T_i=150°C
α =40°, d=1mm, T_i=150°C
α =40°, d=1mm, T_i=200°C
α =40°, d=2mm, T_i=200°C
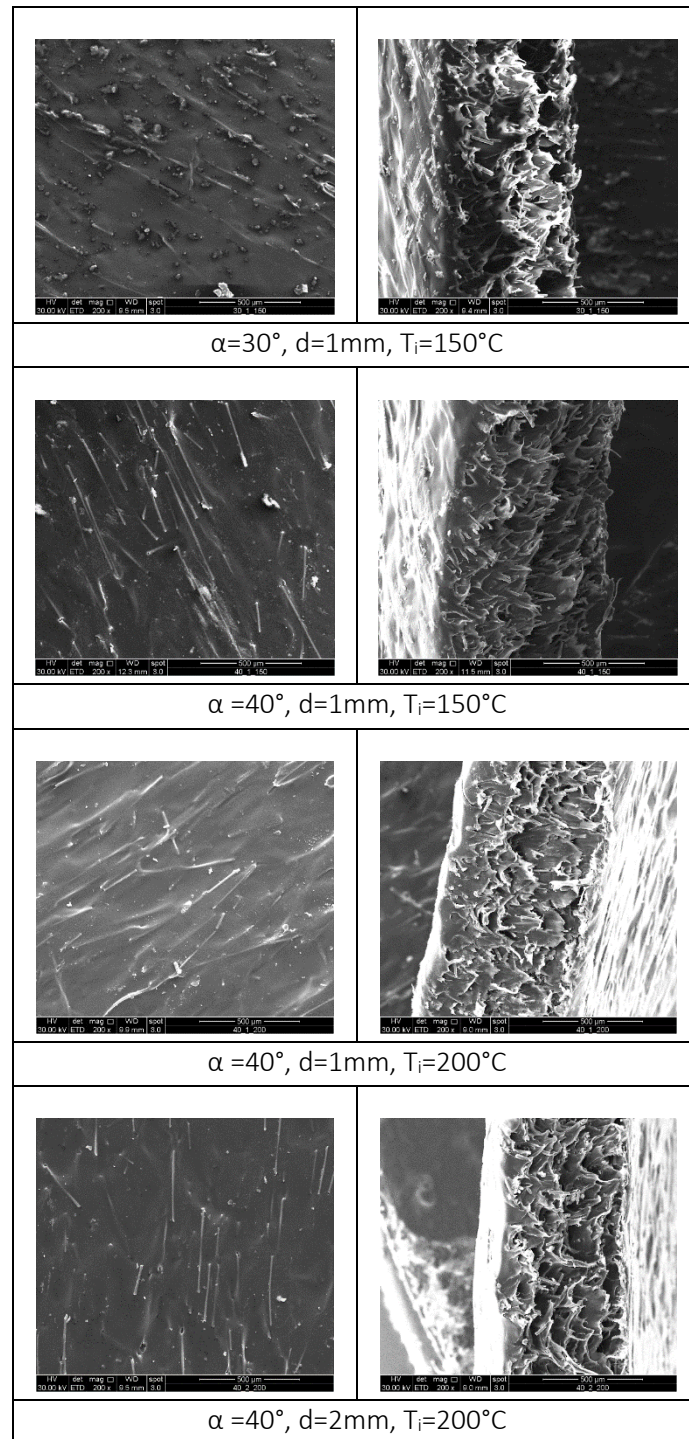
FIGURE 3.35 SEM ANALYSIS OF THE MANUFACTURED SAMPLES AT DIFFERENT WORKING CONDITIONS

Summing up, the designed and performed experimental investigations demonstrated the feasibility of SPIF on thermoplastic composites reinforced with short glass fibers, using macroscopic (part soundness, thinning and accuracy) and microscopic (fibre distortion and polymer degradation) indexes for the evaluation. Furthermore, an accuracy optimization was tested considering the thermal gradient effect. This demonstrated a significant improvement of the part geometry working with fast blank heating and regular air-cooling.

CHAPTER 4

JOINING TECHNIQUES

*"If we knew what it was we were doing,
it would not be called research, would it?"*

Albert Einstein

The increasing need of hybrid structures is pushing industries to design new technological solutions for ensuring their accuracy, reliability and environmental sustainability. As widely described in Chapter 2 joining techniques are the main processes involved in the connection of dissimilar materials for improving their performance but the joint may become very difficult and complicated when the materials are characterized by different chemical and mechanical properties.

In this research, two main techniques have been experimentally investigated, focusing the attention on lightweight engineering materials.

4.1. FRICTION RIVETING

Friction Riveting is classified as a spot joining technique, which requires a rivet and sheets to be performed. The rotating cylindrical rivet is inserted into clamped sheets following two main phases that may affect the connection quality and the material properties. The first one is called *friction phase*: the rotational speed and the applied axial force generate heat by friction increasing the ductility of the metallic pin plasticizing the materials. The second one is known as *forging phase*:

when the friction phase finishes, the spindle rotation is stopped and the axial force is increased allowing the tight placement of the rivet into the sheets.

The rotational speed, the friction and forging times, and the friction and forging pressure are the main factors to consider for assessing the obtained connections. Specifically, a right compromise between the reached temperature (that determines the resistance to the rivet penetration) and forging force needs to be found for each combination of rivet and sheets.

A sketch of the process performed to the aim of this research is displayed below.
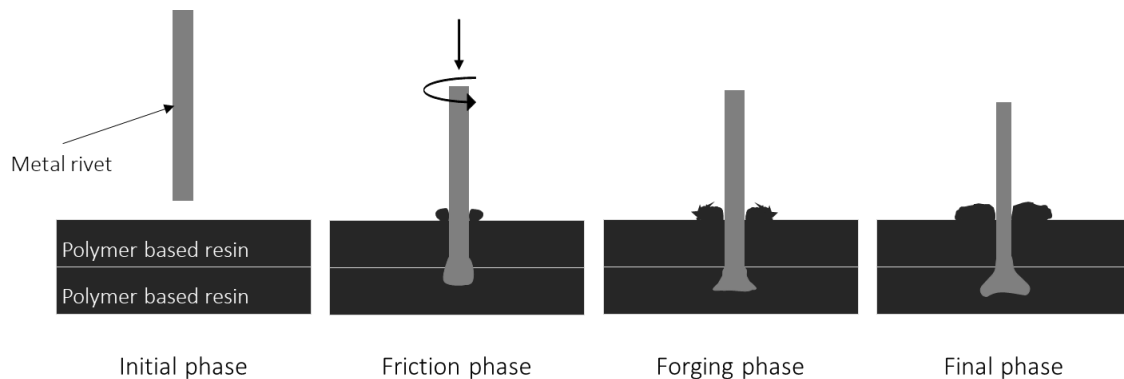
FIGURE 4.1 FRICTION RIVETING PROCESS

4.1.1. EXPERIMENTAL EQUIPMENT

To prove the feasibility of Friction Riveting a specific equipment has been designed and located inside the working volume of a traditional milling machine. The sheets needed to be solidly secured during the joining phase in order to avoid their detachment. The equipment and its components are shown in Figure 4.2. Specifically, for the purpose of this research a speed multiplier has been connected to the mandrel in order to obtain rotational speeds higher than 40000 RPM. In fact, the rivet rotation is an important variable for getting the desired temperature increment during the heating phase. Furthermore, a dynamometer was placed under the equipment for monitoring the loads during the process and a thermographic camera and a thermocouple were used for controlling, globally and locally, the temperature of the material during the joint forming. More in detail, the thermocouple was embedded in a pre-defined position chosen considering the results obtained by Amancio-Filho (2011), who stated that the temperature trend, locally measured, presented consistent differences according to the position of the thermocouple along the specimen thickness. To the scope of this investigation, the thermocouple was embedded in the middle of the lower sheet height. Concerning the thermographic camera, an emissivity of 0.95 was set for the plastic material. This value was validated by using a thermocouple.

Speed multiplier

Thermocouple

Dynamometer
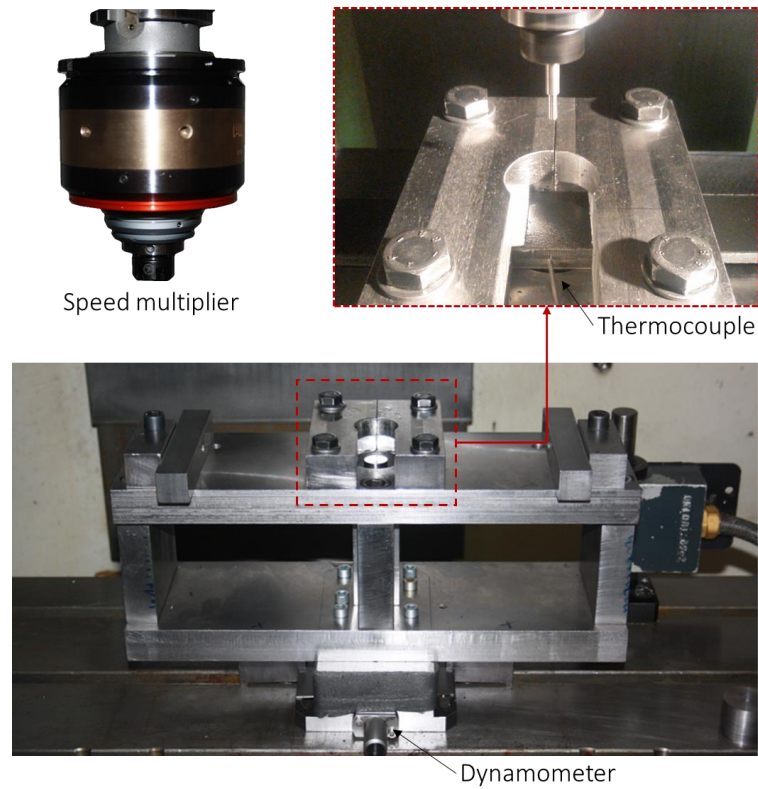
FIGURE 4.2 FRICTION RIVETING EXPERIMENTAL EQUIPMENT

4.1.2. EXPERIMENTAL INVESTIGATION

MATERIAL AND METHOD

For the first joining investigation based on Friction Riveting, two categories of materials have been selected: polymers and metals. As concerns the first group, sheets of pure and reinforced polyamide 6 (PA6) have been chosen and provided by the German company Lanxess. These polyamide based resins are commercially known as Durethan B30S (white virgin grade PA6) and Durethan BKV30 H (black grade PA6 containing 30 wt% of glass fibers). Both have been molded in 5 mm thick sheets under the temperature and pressure profiles shown in Figure 4.3 and by using a Lab Press Colin GmbH. To carry out the joining tests they were cut in the laboratory in stripes 60 mm width.
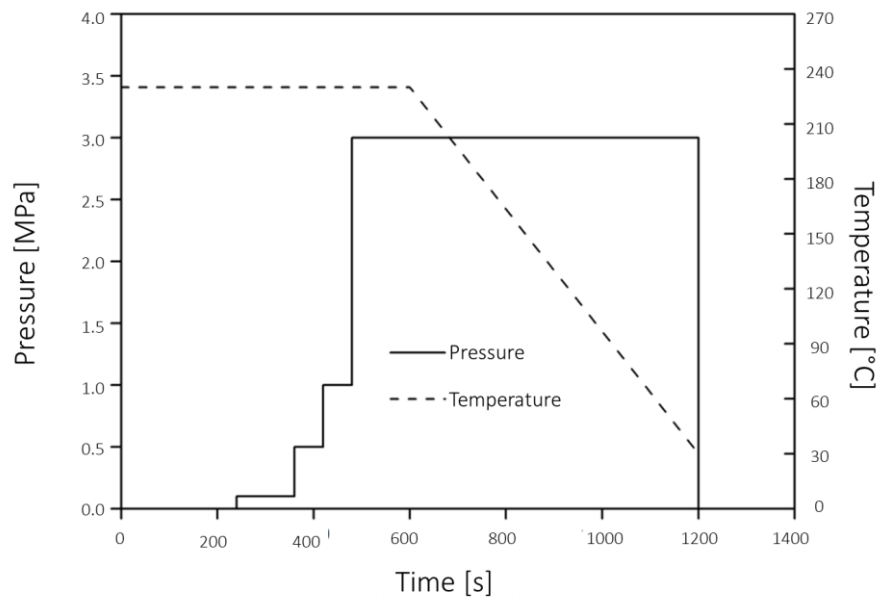
FIGURE 4.3 COMPRESSION MOLDING CONDITIONS OF POLYAMIDE BASED RESINS

Regarding the second group, and according to previous studies (Altmeyer et al., 2014; Amancio-Filho and dos Santos, 2009), bars of commercial pure titanium (Ti) Grade 2 and of aluminium AA 6060 have been utilized as rivets. They are characterized by a diameter of 5 mm and a constant length of 60 mm.

The following Table 4.1 reports the main mechanical and thermal properties of the above-mentioned categories of materials.

TABLE 4.1 MECHANICAL AND THERMAL PROPERTIES OF INVESTIGATED MATERIALS

Material	ρ [g/cm3]	E [GPa]	Strength [MPa]	Thermal Cond. [W/mK]	Spec. Heat Cap. [J/g °C]	T_{melt} [°C]
B30S	1.14	1.10	60	0.33	1.70	222
BKV30 H	1.36	6.10	100	0.30	1.00	220
Ti Grade 2	4.51	102	430	16.4	0.523	1660
AA6060	2.70	68.9	215	2.2	0.896	659

To perform the joint, two stripes of material (thick 5 mm each one) were superimposed and put into the working area. As already mentioned, a hole needed to be drilled into the lower sheet side for inserting the thermocouple and allowing the monitoring of the temperature during the process. A distance of around 1 mm between the thermocouple tip and the rivet was fixed.

An illustration of the process at the end of the forging phase is provided below (Figure 4.4).
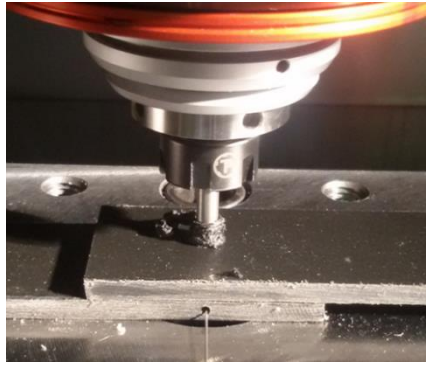
FIGURE 4.4 JOINING OF POLYMERIC BASED RESINS BY FRICTION RIVETING

To measure the maximum pulling strength of the joint an Instron testing machine with a traverse speed of 1 mm/min at room temperature and with a load cell of 5 kN was used. The connected parts were tested fixing them in a sample holder made of two bolt-connected rigid plates, while the rivet was clamped to the moving traverse and pulled out from the sheets. The tensile machine and a sketch of the performed test are shown in Figure 4.5. Due to the complex geometry of the deformed rivet, the determination of a real cross-sectional rivet area was very difficult and the joint strength was presented only in terms of tensile force.

A)

B)
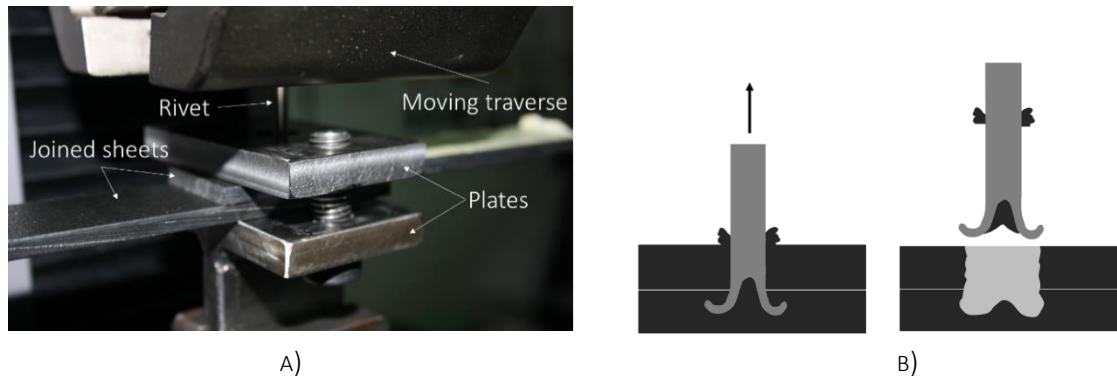
FIGURE 4.5 A) SAMPLE FIXED ON THE CUSTOMIZED TENSILE MACHINE AND B) SKETCH OF THE TENSILE TEST

1° EXPERIMENTAL INVESTIGATION

A first experimental analysis, aiming at assessing preliminarily the quality of the connections obtained combining sheets and rivets made of different materials, was performed setting the following material combinations and process parameters.

TABLE 4.2 GEOMETRICAL AND PROCESS PARAMETERS_1° INVESTIGATION

Sheet material	Rivet material	Total linear stroke [mm]	Forging linear stroke [mm]	Rotational speed [RPM]
B30S	Ti Grade 2	7.5	40%	20000
BKV30H	AA6060	9.5	60%	35000

2° EXPERIMENTAL INVESTIGATION

Considering the results obtained from the just described investigation, a second experimental plan was designed to improve the quality of the joints and to better understand the link between the process outputs (reached temperature, forging load and pulling strength) and the process parameters. In this case, to join pure and reinforced PA6 sheets, the only rivet used was that one in titanium Grade 2.

The variable factors considered in this second performed analysis are reported below in Table 4.3. The forging linear stroke was the only investigated stroke variable, because the friction and forging strokes are actually related. A total stroke of 9 mm was considered.

TABLE 4.3 GEOMETRICAL AND PROCESS PARAMETERS_2° INVESTIGATION

Forging Linear Stroke [mm]	Friction Linear Velocity [mm/s]	Forging Linear Velocity [mm/s]	Rotational speed [RPM]
3.0	1.0	1.0	15000
4.5	2.0	2.0	25000
6.0	3.0	3.0	35000

To reduce the number of experiments, a fractional design was used instead of a full factorial design, allowing therefore to save a considerable amount of time and costs. The number of required experiments was reduced utilizing a mathematical procedure. The main steps of the implemented approach are:

1) *Definition of the process domain*: the set of factors that influence each key performance indicator is determined in accordance with literature (Altmeyer et al., 2014; Amancio-Filho, 2011; Amancio-Filho et al., 2008; Blaga et al., 2013; Goushegir et al., 2015). As a result, the process parameters indicated in Table 4.3 were selected and the range of values to consider was defined.

2) *Definition of the Design of Experiments*: a crucial role on the quality of a predictive model is given by the choice of the design of experiments. A Taguchi design was used since it offers a good trade-off between accuracy and costs.

3) *Feature selection*: the collected data are used to identify the set of process parameters that influence any output response. The Regressional ReliefF (RReliefF) (Robnik-Šikonjalgor and Kononenko, 2003) method was used for this task.

4) *Definition of the optimal process configuration*: the configuration that maximizes the quality of the obtained joint is identified. Different configurations could be defined according to the required constraints that the user has to take into account for the specific application. Each step of the proposed procedure is described in the following section, where it is presented how the methodology was applied on the case study.

To perform the statistical investigation it was necessary to define the sampling strategy to collect a set of data to test and train the model. Instead of a full factorial design (Eriksson et al., 2000), a fractional design was used to decrease significantly the number of the required data saving a considerable amount of time and costs. For this purpose, the Taguchi method (Zhang et al., 2007)

uses a special design of orthogonal arrays to study the entire space of parameters with a small number of experiments. A set of fractional factorial designs ignores the parameter interactions and focuses the attention on the estimation of the main effects. This design is particularly suitable for initial analysis in which the main goal is a first understanding of the system and a screening of the most relevant variables for each process indicator. The steps included in the Taguchi methodology are:

1) selecting the proper orthogonal array (OA) according to the number of parameters;
2) running experiments based on the selected OA;
3) analyzing data;
4) identifying the optimum process conditions.

The array chosen for this application is the L$_{27}$ (Zhang et al., 2007), which has 27 rows corresponding to the number of tests and can be used to analyze a number of parameters up to 13. The design was performed with two replications to check the process replicability carrying out a more reliable statistical analysis. The number of experiments performed was therefore equal to 54.

In addition, to the aim of this research, a feature selection technique has been utilized to identify the most influent process parameters. Feature selection focuses on eliminating redundant and irrelevant data and is a crucial part of pre-processing step to determine more accurate input-output relationships. Feature selection improves the quality of the data and increases the performance of metamodel algorithms by reducing the space and time complexity. The RReliefF technique was here used to select the relevant features of each investigated process objective. Relief algorithms are general and successful attribute estimators. They are commonly considered as feature subset selection methods applied in a pre-processing step before the model is learned and are among the most successful pre-processing algorithms. RReliefF algorithm estimates the quality of attributes by how well their values distinguish between patterns that are near to each other. It was assumed that examples $I_1, I_2, .., I_n$ in the instance space are described by a vector of attributes A_i , $i = 1,...,a$, where a is the number of attributes, and are labelled with the target value τi. The main idea of the algorithm is to calculate the importance of each attribute *W [A]*. The value *W [A]* is calculated based on the estimation of $P_{diffA}, P_{diffC}, P_{diffC|diffA}$ which are defined as:

$$P_{diffA} = P(\text{diff value of } A | \text{nearest instance})$$

$$P_{diffC} = P(\text{different prediction} | \text{nearest instance})$$

$$P_{diffC|diffA} = P(\text{different prediction} | \text{diff value of } A \text{ and nearest instance})$$

The value of *W [A]* is calculated based on Bayesian rule as:

$$W [A] = \frac{P_{diffC|diffA} P_{diffA}}{P_{diffC}} - \frac{(1 - P_{diffC|diffA}) P_{diffA}}{1 - P_{diffC}}$$

The algorithm presented below contains the weights for different prediction, different attribute, different prediction and different attribute, denoted respectively as N_{dC}, $N_{dA}[A]$, $N_{dC\&dA}[A]$:

Algorithm RReliefF

Input: for each training instance a vector of attribute values *x* and its predicted value τ(*x*)

Output: vector W of estimations of the qualities of attributes

> **Set** all N_{dC}, $N_{dA}[A]$, $N_{dC\&dA}[A]$, $W[A]$ to 0
>
> **for** i:=1 to m **do begin**
>
>> randomly select instance R_i;
>>
>> select k instances I_j nearest to R_i;
>>
>> **for** j:=1 to k **do begin**
>>
>>> $N_{dC} := N_{dC+}\text{diff}(\tau(\cdot), R_{i,,}I_j)\cdot d(i,j)$;
>>>
>>> for A:=1 to #attributes do begin
>>>
>>>> $N_{dA}[A]:= N_{dA}[A]+\text{diff}(A, R_{i,,}I_j)\cdot d(i,j)$;
>>>>
>>>> $N_{dA\&dA}[A]:= N_{dA\&dA}[A]+\text{diff}(\tau(\cdot), R_{i,,}I_j)\cdot\text{diff}(A, R_{i,,}I_j)\cdot d(i,j)$;
>>>
>>> end
>>
>> end
>
> end
>
> **for** *A*:=1 to #attributes **do**
>
>> $W[A]= N_{dA\&dA}[A]/ N_{dC}-(N_{dA}[A]- N_{dA\&dA}[A])/(m- N_{dC})$;

The value $\text{diff}(A, Ri,,Ij)$ is calculated as:

$$\text{diff}(A, Ri,,Ij) = \frac{|value(A, R_i) - value(A, I_j)|}{\max(A) - \min(A)}$$

The term $d_{i,j}$ calculates the distance between the two instances R_i, and I_j. The ratio is that closer instances should have a greater influence, so the influence of the instance I_j with the distance from the given instance R_i is exponentially decreased:

$$d(i,j) = \frac{d_1(i,j)}{\sum_{l=1}^{k} d_1(i,l)}$$

$$d_1(i,l) = e^{-\left(\frac{Rank(R_i,I_j)}{\sigma}\right)^2}$$

where, $Rank(R_i, I_j)$ is the rank of the instance I_j in a sequence of instances ordered by the distance from R_i and σ is an algortithm predefined parameter used to control the influence of the distance. The final estimation of the relevance of each attribute *W[A]* is finally computed through the expression in line 14 of the algorithm.

The threshold value to select the relevant features can be determined by Chebyshev's inequality for a given confidence level α (where α is the probability of accepting an irrelevant feature as relevant) and it is equal to $\frac{1}{\sqrt{\alpha\cdot m}}$. However it is stated that a much smaller value could be used (Robnik-Šikonjalgor and Kononenko, 2003). Therefore, we define as *secondary relevant parameters* the features with a value *W[A]* in the range $\left[\frac{1}{2\sqrt{\alpha\cdot m}}, \frac{1}{\sqrt{\alpha\cdot m}}\right]$.

RESULTS

RESULTS OF THE 1° EXPERIMENTAL INVESTIGATION ON FRICTION RIVETING

A section of the obtained joints and a deformed rivet pulled out by the tensile test are shown in the following Figure 4.6.

A)   B)

C)
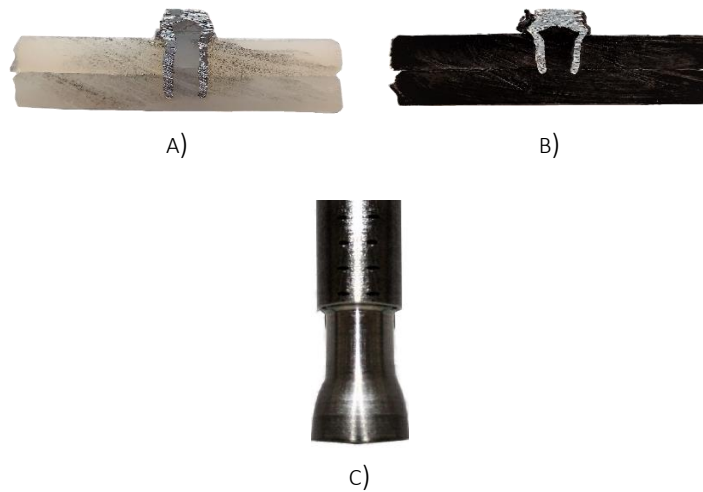
FIGURE 4.6 PERFORMED JOINTS USING A) B30S (PA6) AND B) BKV30H (REINFORCED PA6); C) DEFORMED RIVET PULLED OUT BY THE TENSILE TEST

The preliminary performed joining tests (
Table 4.2) were analysed in order to understand the influence of the friction and forging lengths on the joint quality, and therefore on the processing temperature, quantifying the anchoring of the rivet into the polymer based sheets. Furthermore, the strain distribution around the joining area was assessed as well.

As regards the influence of the joint length, here defined as *linear stroke*, and of the friction phase percentage on the connections (measured by tensile test) and on the temperature (measured by the thermographic camera), the obtained trends are displayed below:

A)   B)
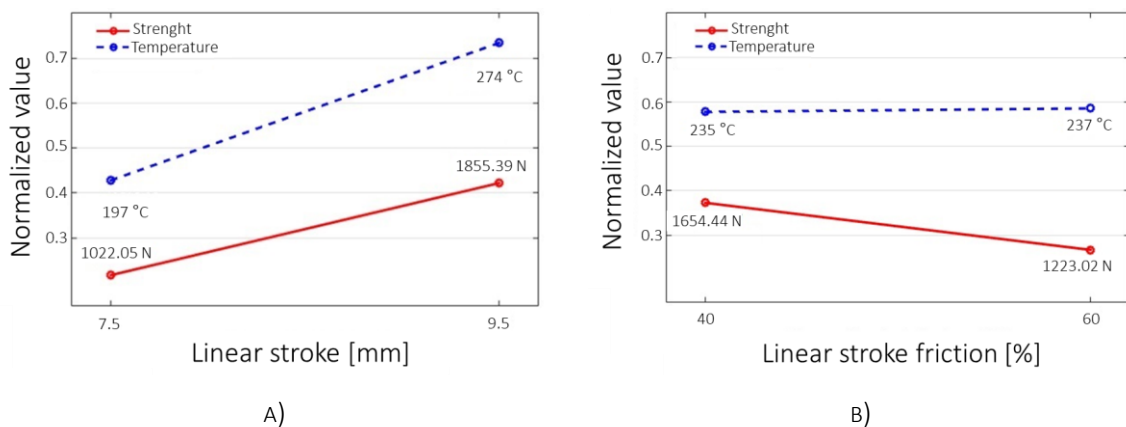
FIGURE 4.7 INFLUENCE OF THE LINEAR STROKE AND OF THE FRICTION PHASE ON THE JOINT

Looking at the graph in Figure 4.7 A), it is evident that the strength of the connection increases if the total linear stroke increases. This means that the Friction Riveting technique is more promising when thicker parts have to be joined. If the heating and forging phases are longer, more heat is generated and the forging loads are more elevated, therefore, the rivet is able to better deform inside the plastic matrix and, consequently, the rivet anchorage is stronger. Taking into account that the process length includes two process phases, the temperature monitored by thermographic camera increases slightly if the friction percentage increases, while the joint strength decreases. This last evidence is due to the reduction of the forging phase and, consequently, to a lower compression load which causes a reduction of the rivet deformation.

Further observations are related to the influence both of the glass fiber percentage contained inside the polymeric matrix and of the rivet material on the measured process outputs. Concerning the first factor, the graph in Figure 4.8 A) demonstrates that the percentage of glass fibers has a considerable impact on the quality of the joints and on the temperature variation. In fact, the strength required to pull the rivet was higher for the sheets reinforced with 30% of glass fibers. This was due to the interaction between metal and glass fibers that caused higher heat generation and forging forces and therefore a more consistent rivet deformation occurred as well. As regards the rivet, Figure 4.8 B) shows that a different material does not affect the values of the joint strength. This evidence has to be considered just for the range of variables utilized in the performed research and for the two types of materials analysed. Indeed, the pulling force depends on the deformations of the rivet within the matrix. The deformation level could reach different values if the mechanical properties of the dipped material were dissimilar.

A)   B)

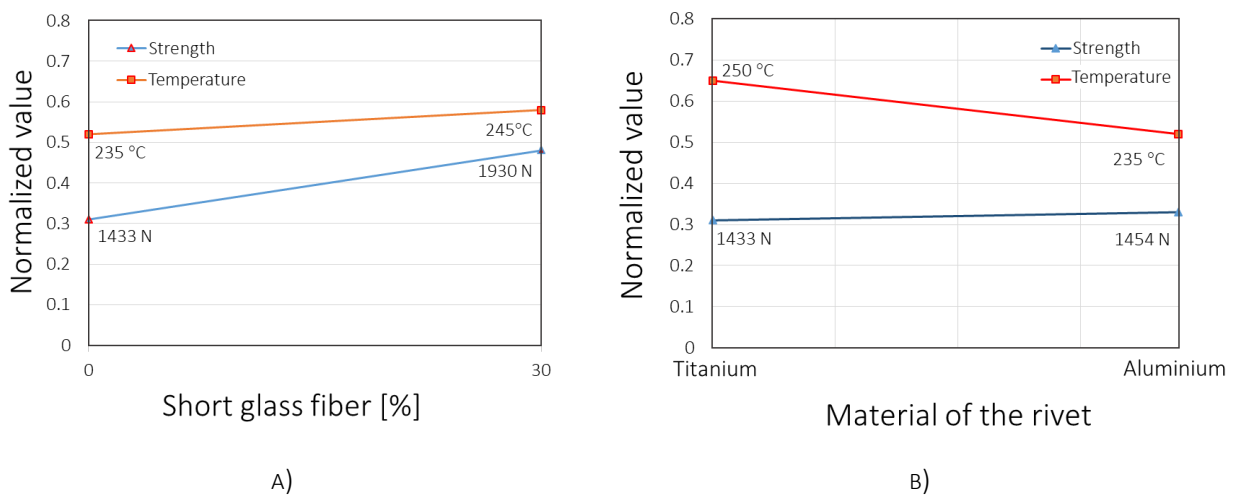FIGURE 4.8 STRENGTH AND TEMPERATURE TRENDS OF THE TWO INVESTIGATED MATERIALS OF A) SHEET (PURE AND REINFORCED PA6) AND B) RIVET (TITANIUM AND ALUMINIUM)

The influence of the rotational speed of the mandrel was investigated too. It is considered an important process variable because it affects the friction phase, increasing both the process temperature and the registered strength of the joints (Figure 4.9).
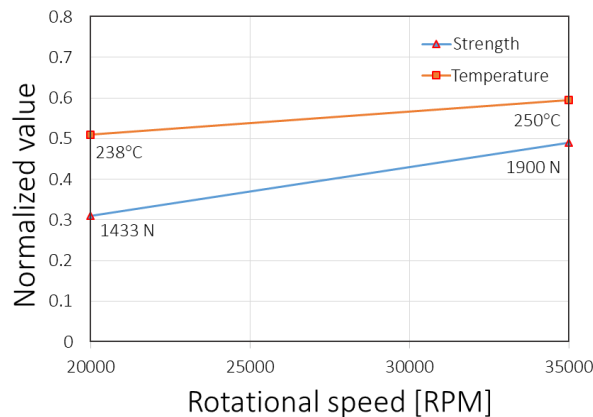
FIGURE 4.9 INFLUENCE OF THE ROTATIONAL SPEED ON THE INVESTIGATED PROCESS OUTCOMES

Finally, the strain distribution and the surface quality on the upper side of the joined sheets, and therefore around the joining area, were analysed using Electronic Speckle Pattern Interferometry (ESPI) (Pagliarulo et al., 2015). The caught area for both configurations are displayed in Figure 4.10. The surface of the sheet without reinforcement does not show any lack of uniformity and the strain level fluctuates concentrically to the joining hole. On the other hand, in the case of reinforced PA6 the deformation is reduced and has a different direction (shown using the red arrow), proving a no uniformity of the deformations on the surface of the sheet around the rivet.

A)   B)
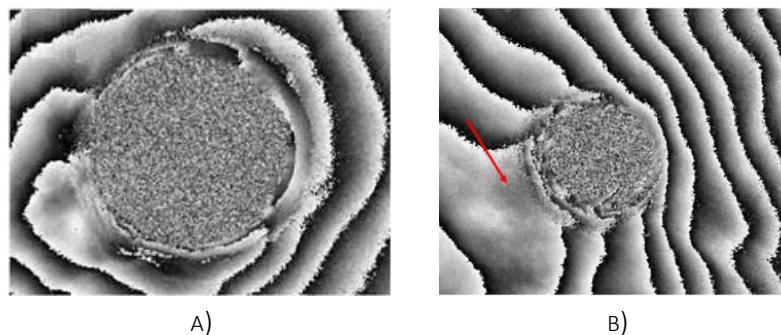
FIGURE 4.10 PHASE-CONTRAST MAP BY ESPI PERFORMED ON A) PURE PA6 AND B) REINFORCED PA6

RESULTS OF THE 2° EXPERIMENTAL INVESTIGATION ON FRICTION RIVETING

The second experimental plan allowed to deeply understand the rivet behaviour, the temperature and the variable parameters influence on the performed joint.

The rivet, entering into the thermoplastic material, deformed and became an anchoring system to connect the sheets. The extraction of the rivet led to observe a more or less pronounced barreling deformation, while externally no rivet distortion was noticeable (Figure 4.11 A)). Regarding the upper surface of the joined sheets, the processed thermoplastic material surrounded the stick of the rivet forming a flash that can have a different shape and aspect. Indeed, during the process, the plastic is firstly stirred and locally heated and then, during the forging phase, compressed. According to the

reached working temperatures, the polyamide reached different levels of viscosity and, therefore, the surface of the flash appeared grainier or shinier (Figure 4.11 A) and B)).

A)   B)   C)

FIGURE 4.11 A) EXTRACTED RIVET AND B) GRAINY AND C) SHINY POLYMERIC SURFACES

Regarding the temperature monitored during the process, the thermographic camera measured the values all around the working volume stating that the flash area was, as expected, the hottest zone (Figure 4.12). Considering the low conductivity of the polymeric matrix and the short heating phase, the flash temperature provided by the thermographic camera, can be fairly assumed as the tem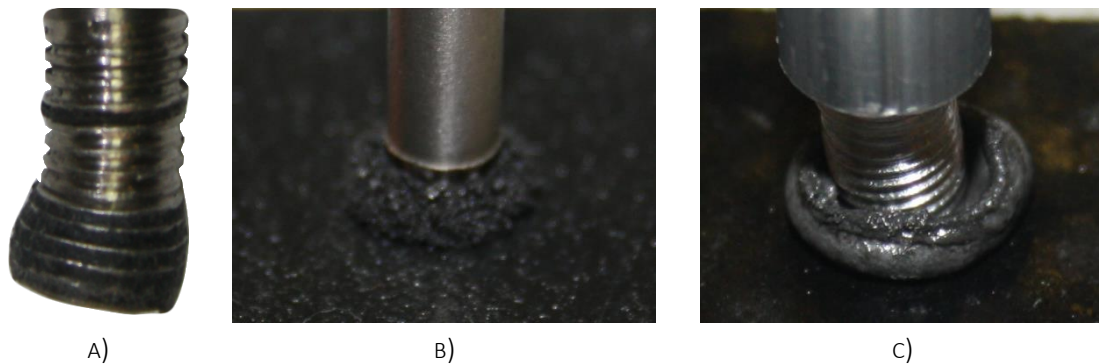perature of the plastic in contact with the rivet inside the working volume (Amancio-Filho, 2011). Specifically, temperature peaks of more than 300°C were recorded for various process configurations.

FIGURE 4.12 THERMOGRAPHIC IMAGE AT THE END OF FRICTION PHASE

As already mentioned before, the temperature was also monitored by means of a thermocouple that provided information about the temperature trend inside the joined sheets. The obtained values were quite different from those recorded by the thermographic camera and this can be explained considering that the temperature values obtained by the thermocouple depend on their position inside the joining volume (Amancio-Filho, 2011). Furthermore, monitoring the effective temperature on the rubbing area is very complicated, as confirmed also Meyer (2003), and its measurement cannot provide useful temperature trends to understand the influence of the process temperature on the matrix thermal degradation. Due to the wider recorded spectrum, the data obtained by the thermographic camera were used for the optimization of the process conditions. The main results (minimum and maximum value of each monitored output), achieved through the designed

experimental plan, are reported in Table 4.4 and can be explained through the mathematical procedure presented in the previous method section.

TABLE 4.4 EXPERIMENTAL RESULTS OF THE DOE

Process outcomes	Minimum value	Maximum value
Forging Load [N]	2438	4728
Temperature [°C]	302	456
Strength [N]	147	2429

More in detail, the RReliefF was performed using a number of iteration m equal to 27 (number of data) and a level of confidence of 90% (α=0.1). Therefore, a main threshold equal to ≈0.2 and a secondary limit equal to ≈0.1 were fixed. The importance of each attribute $W [A]$ and the main effects have been reported for all the three process output in Table 4.5 and in Figure 4.13 where the displayed plots consider a normalized value in the range [0,1] in order to avoid different units.

TABLE 4.5 RELEVANCE OF THE INVESTIGATED VARIABLES ON THE MONITORED OUTPUTS

Process Parameter	Forging Load	Strength	Temperature
Friction linear velocity [mm/s]	0.069	0.067	0.205
Forging linear velocity [mm/s]	0.061	0.091	0.203
Friction linear stroke [mm]	0.297	0.122	0.056
Rotational speed [RPM]	0.088	0.272	0.118
Short glass fibers [%]	0.135	0.209	0.080
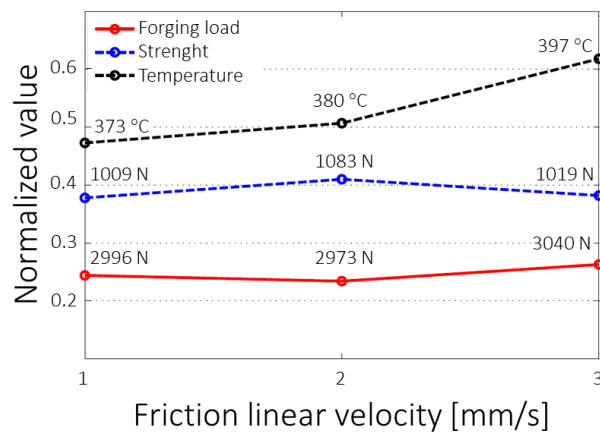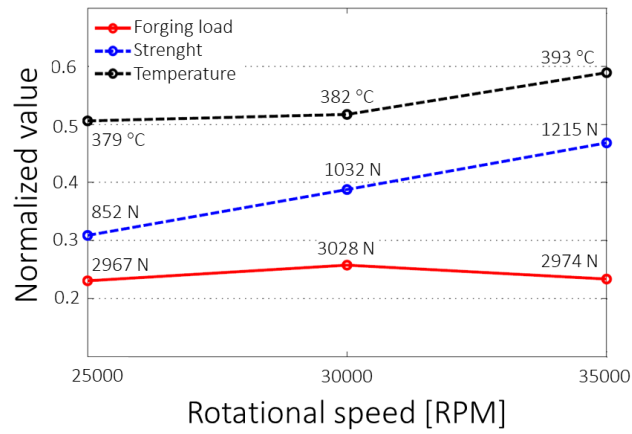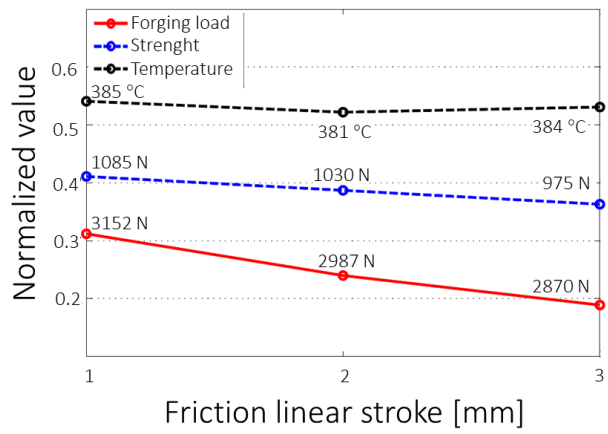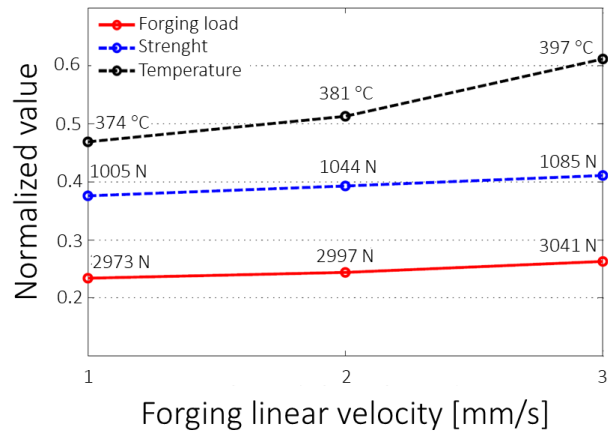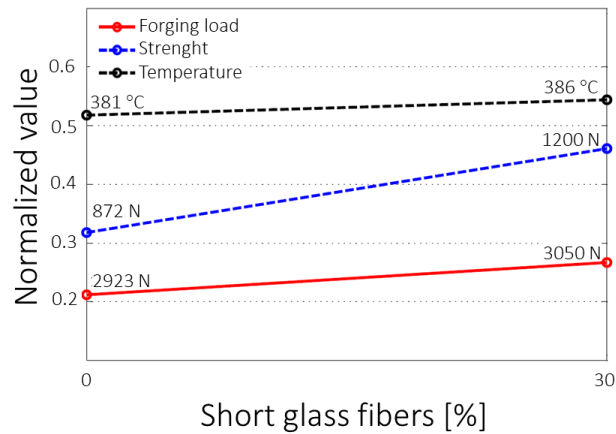
FIGURE 4.13 INFLUENCE OF THE INVESTIGATED VARIABLES ON: FORGING FORCES, RECORDED TEMPERATURE AND MAXIMUM STRENGTH

Comments on each single process output are below presented.

As concerns the *forging load*, the statistical analysis demonstrated that this variable is mainly influenced by the rivet stroke. As above highlighted, this process parameter includes the friction phase and the forging phase. The required force increases if the forging stroke increases and, consequently, the friction phase is shorter. As expected and as shown in Figure 4.14, the force is low during the friction phase and increases rapidly once the punch pierces through the composite sheets during the forging phase.
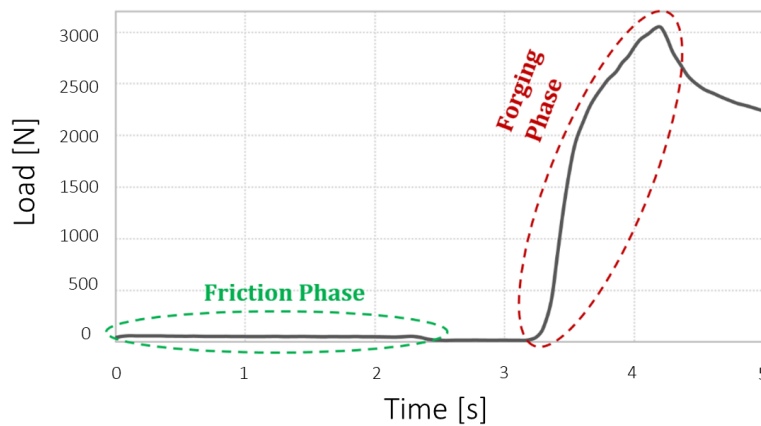
FIGURE 4.14 FORCE TREND DURING THE JOINING PROCESS

The sheet material, in this case pure PA6 or glass fiber reinforced PA6, is the secondary variable that has to be considered to control the process force. This latter increases when Durethan BKV30H sheets are joined. The other monitored inputs have a reduced influence on the forging load as clearly highlighted in Table 4.5.

Regarding the *strength*, the tensile strength required to pull out the rivet from the composite sheets depends on the joined material. This is a result that can be explained taking into account the observed type of fracture. Specifically, the rivet is completely removed cracking the polymeric matrix

around the anchoring zone. This is a fracture typically observed in joints with high ductility (Amancio Filho et al., 2008). The other relevant input that affects the joining quality is the rotational speed, important to heat the metallic part and to improve the material formability. Indeed, at least for these first reported evidences, the linear velocity of the rivet during the friction phase has a relevant effect on the temperature variation monitored by the thermographic camera. The reduced influence of this variable on the tensile strength of the joint can be explained taking into account that, if this velocity increases, the contact time between the molten polymer and the rivet decreases proportionally and this causes a reduction of the metal temperature before its forming. Finally, the stroke of the rivet during forging results to be significant for the quality of the connection. This is understandable taking into account the link between stroke and forging force. An increment of the last variable, due to a longer forging phase, leads to a more consistent rivet deformation.

Finally the last investigated process output is the *temperature* that is a function of the heat produced during the friction phase. Looking at Figure 4.13 and Table 4.5, both the friction linear velocity and friction linear stroke affect the recorded temperature peaks. Specifically, the friction linear velocity was the most meaningful variable. This result could be explained because, if the heating phase is reduced due to the velocity increment of the joining tool, the heat dispersion decreases. This effect is further increased if elevated forging linear velocities are set. The rotational speed is the other variable that contributes meaningful to the temperature variation. A higher spindle speed increases the revolutions of the rivet inside the plastic matrix, increasing the heat produced by friction and therefore the temperature variation. Even for this process output, the other monitored inputs do not show a considerable influence.

The statistical analysis highlighted the consistent impact of the glass fiber percentage and of the rotational speed on the monitored process outputs. Considering this result, these two variables were considered to understand their influence on the out of plane displacements around the joining area. This further investigation was carried out by ESPI and optical microscopy

The strain distributions on the upper sheet surface of specimens based on pure and glass fiber filled polyamide, processed under same conditions, are reported in Figure 4.15. In this case, no substantial differences were induced in terms of deformations and no cracks were revealed on the edge if elevated spindle speed (35000 rpm) was utilized (Figure 4.15 A) and B)). This consideration was confirmed by optical micrographs (Figure 4.15 C) and D)).

A)   B)

C)   D)
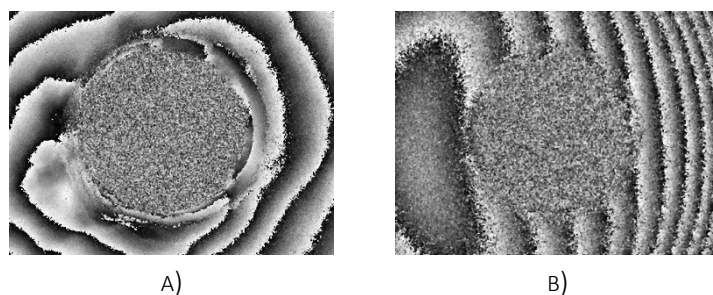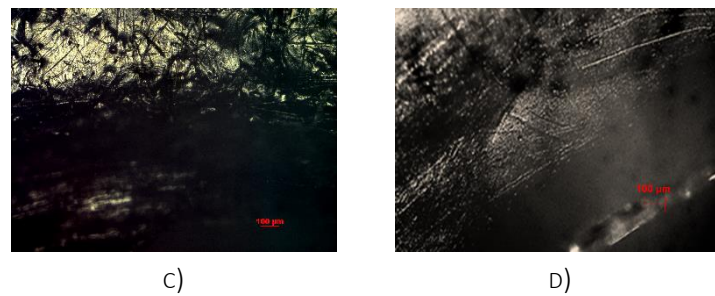
FIGURE 4.15 PHASE-CONTRAST MAP OBTAINED BY ESPI AFTER A THERMAL STIMULATION: A) PURE PA6 AND B) 30% GF REINFORCED PA6 SPECIMENS. IMAGES FROM OPTICAL MICROSCOPE: C) PART OF THE EDGE OF PURE PA6 SHEET AND D) PART OF THE EDGE OF A 30% GF REINFORCED PA6 SHEET

Figure 4.16 displays images related to specimens containing 30% of glass fibers and processed at different rotational speed. Specifically, Figure 4.16 A) and B) show the phase contrast maps obtained by ESPI on specimens processed setting spindle speeds of 20000 RPM and 35000 RPM, respectively.

The analysis shows a notable influence of the rotational speed parameter on the quality of the obtained holes. In fact, while the one in Figure 4.16 B) appears with a good quality, in the case of a lower spindle speed, Figure 4.16 A), the red arrow highlights an inhomogeneous deformation around the hole edges. The microscope image shown in Figure 4.16 C) confirms in such zone, shown in the red circle, the presence of a mass thickening. This effect could be ascribed to the moving and adjustment difficulties of the plastic matrix during the rivet insertion due to a higher material viscosity caused by the fiber presence and by lower working temperatures. This conclusion was supported by observations carried out on pure PA sheets joined at any spindle speeds that did not show any inhomogeneity.

A)   B)

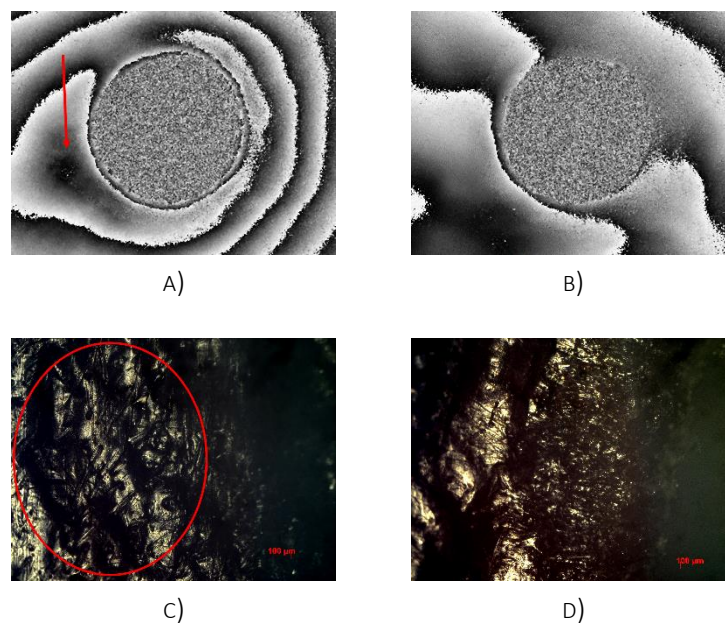C)   D)

FIGURE 4.16 PHASE-CONTRAST MAP OBTAINED BY ESPI AFTER A THERMAL STIMULATION AT A) 20000 RPM AND B) 35000 RPM. CORRESPONDENT OPTICAL MICROSCOPE IMAGES FOR SPECIMEN PROCESSED SETTING A SPINDLE SPEED EQUAL TO C) 20000 RPM AND D) 35000 RPM

Summing up, the Friction Riveting experimental investigations allow to conclude that:

- the partition of the rivet stroke between friction and forging phase affects the required process loads with an increment of the thrust forces on the rivet if the forging part increases. This result influences the joint strength due to a higher deformation of the rivet inside the polymeric matrix;

- the temperature measurement in the working area is complicated due to the short process time and the low material conductivity. A local monitoring of this variable can lead to no significant results. Therefore, the temperature of the flash surface measured by thermo-camera can be considered as an average temperature of the polymeric matrix close to the rubbing area. The monitored temperature increased for higher linear velocities of the rivet;

- the rotational speed affects considerably the joint performances. In fact, this is the process variable that mainly influences the anchoring force of the rivet inside the connected parts;

- the mechanical performances of the joint improve if the PA6 is reinforced with short glass fibers, as observed by tensile tests;

- a strong relation between spindle speed and material properties was also shown looking at the strain distribution on the upper joined surface. Specifically, the material strain around the rivet area is characterized by different degrees of no uniformity depending on the spindle speed values and on the used percentages of glass fibers.

4.2. JOINING BY A FRICTION STIR FORMING BASED TECHNIQUE

On the basic principle of the Friction Stir Welding (FSW) process, widely discussed in Chapter 2 a new method called Friction Stir Forming (FSF) was developed by Nishihara (2003) for the micro-forging of some aluminium alloys. The FSF prototype was installed on a milling machine and, exactly like for the FSW, a rotating tool, made of a probe and a shoulder, heated up the workpiece due to the friction and stirred the mating materials.

Ohashi et al. (2017) implemented the same approach of the FSF process to fabricate cylindrical extrusions from A5083P-O aluminium alloy plates and investigated the length of each extruded outcome considering the main process parameters: spindle speed, tool feed rate and step depth.

According to the aim of this thesis and starting from this latter mentioned study, the feasibility of a variation of the Friction Stir Forming process has been proposed and investigated as a new approach for joining metal sheets and fiber reinforced composites without using additional external parts or materials. The process concept is based on two subsequent steps:

I.   the Friction Stir Forming process is performed on an aluminium plate, so that material is forced to flow through a steel plate with holes laid under the plate and pins are formed;

II. the aluminium plate with pins is placed on a composite sheet, pressed on it and a locking head is formed on the part of the pins that stick out through the composite (Figure 4.17). In this basic study, the composite is not pierced by the pins but drilled.
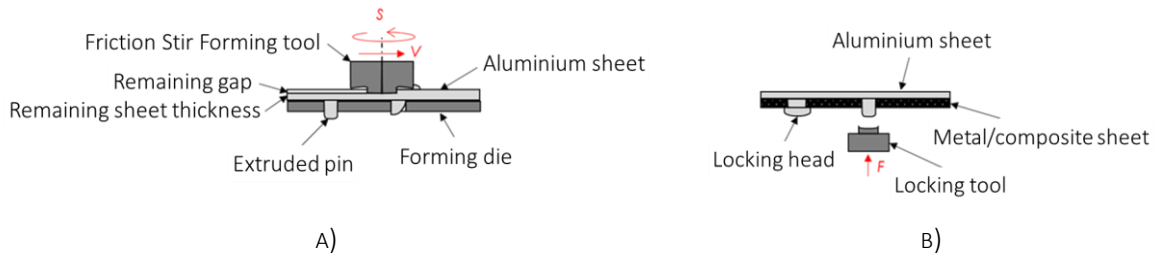
FIGURE 4.17 FSF TECHNIQUE: A) PIN FORMING AND B) JOINING AND LOCKING PHASES

4.2.1. EXPERIMENTAL EQUIPMENT

Figure 4.18 A) shows the designed and manufactured experimental equipment used during the first step. It was mounted on a general purpose milling machine with a slope angle of 5° to increase the effect of the friction, to minimize the overrun of material and to guide it into the holes. Figure 4.18 B) displays the die section through which the pins have been extruded. Two heat shields under the thin forming die stop the heat flow from the die into the holes and prevent that the flowing material cools down rapidly. Figure 4.18 C) depicts the bevel of the mold in the cavities of the forming die that assists the material flow and the ejecting process.

A)

B)

C)
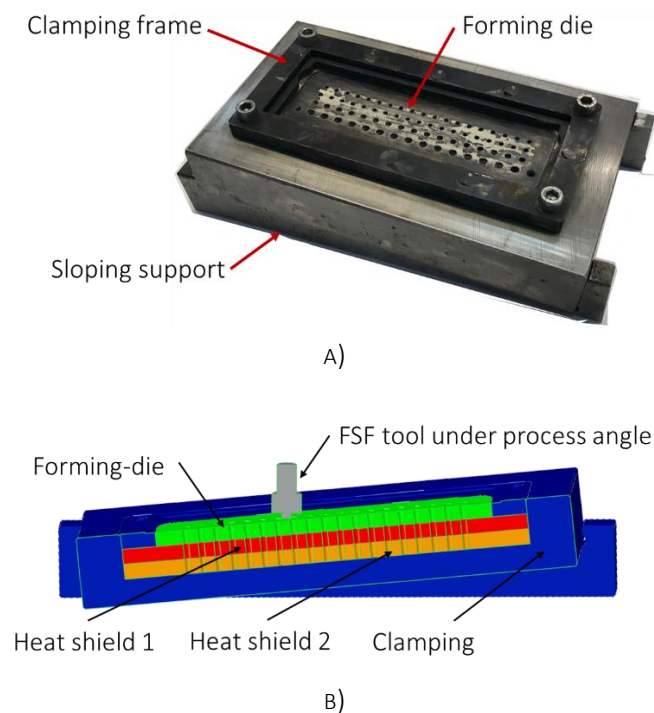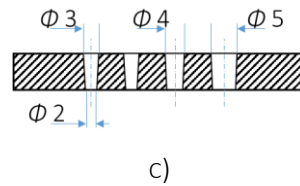
FIGURE 4.18 A) FSF SETTING IN THE HORIZONTAL MACHINING CENTRE, B) A SECTIONAL VIEW OF THE DIE-SETUP WITH TOW HEAT SHIELDS AND C) FORMING DIE DETAILS

As regards the forming tool, a punch characterized by a shoulder of 15 mm, a probe of 5 mm and 2.5 mm long stirrer was designed and manufactured. A penetration depth of 0.2 mm was set. All details are shown in Figure 4.19.

A)   B)   C)
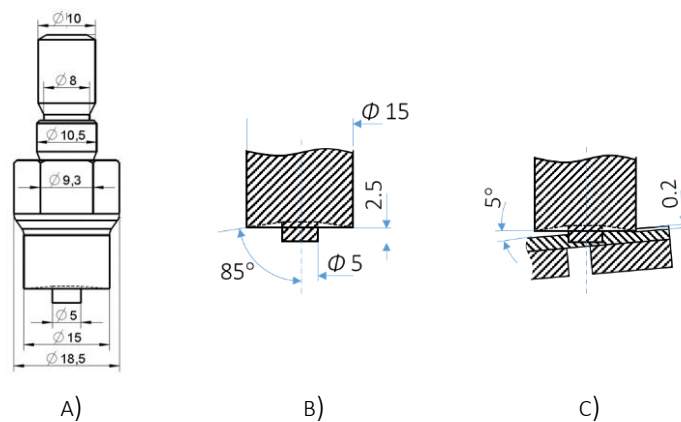
FIGURE 4.19 FSF TOOL DETAILS

Since the friction interferes with the material flow, the forming tool and the die were lubricated.

4.2.2. EXPERIMENTAL INVESTIGATION ON ALUMINUM AND GLASS FIBER REINFORCED PA6

MATERIAL AND METHOD

The first step of the innovative method, that consists on the pin manufacturing, was performed on an aluminium metal sheet EN AW-1050A-H111 of 3 mm thickness. It is characterized by very good deformability and weldability, as well as by high thermal and electrical conductivity, low mechanical properties and high corrosion resistance. For the forming process a good formability (Ag=30 %) was indeed required. The high thermal conductivity offered a commensurately low temperature distribution in the aluminium sheet. This property had an advantage for the tools, which were exposed to heat and temperature gradients. Disadvantages were the mechanical properties with a low Young's modulus E=69000 N/mm², yield point σy=30 N/mm² and tensile strength UTS=65-90 N/mm², but they fitted nearly perfectly the mechanical properties of the composite. Regarding this latter, a polyamide 6 (PA 6) matrix reinforced with short glass fibers (12% volume fraction) was chosen for the joining purpose. It is characterized by a crystalline grain melting range of about 220°C and a short-term service temperature of 180°C. Two laminated of 1.1 mm and 3 mm thickness were

selected for the tests. To carry out the preliminary tests, necessary to prove and validate the feasibility of the joining technique, different holes with a diameter of 3 mm, 4 mm and 5 mm were drilled in the composite. It is worth pointing out that a hole in this material causes a notch effect, which means a stress concentration.

TABLE 4.6 MECHANICAL AND THERMAL PROPERTIES OF THE INVESTIGATED METAL

Material	Young's Modulus [GPa]	Yield Strength [Mpa]	Tensile Strength [Mpa]	Elongation [%]	Thermal Conductivity [W/mK]	Spec. Heat Capacity [J/Kg °C]
EN AW-1050A-H111	69	30	65-90	30	230	900

RESULTS

The FSF process was performed and pins were manufactured according to the process parameters used by Ohashi et al. (2017). For the current research, four lines of pins were extruded by repeating four subsequent steps of the FSF process on the same blank. Due to the variable size of the holes on the die, the extruded pins were characterized by diameters which range from 4 mm to 2 mm as far as a variable number of pins were obtained along each line (Figure 4.18 C)). Except for the first line (those characterized by pins of 4 mm diameter), the others were manufactured as soon as the previous one was completed. Therefore, it is worth pointing out that the process temperature was not the same during the FSF process.

Figure 4.20 shows the front and back side of an aluminium plate obtained at the end of the FSF phase. The displayed pins were obtained setting a spindle speed of 2480 RPM, a tool feed rate of 50 mm/min and a penetration depth of 0.2 mm. To heat the sheet by friction up to about 250 °C, the FSF stirred the metal before starting its working path through the aluminium. The temperature in the forming area increased continuously up to approximately 500 °C while the surrounding sheet reached a value of about 300 °C.

A) B)
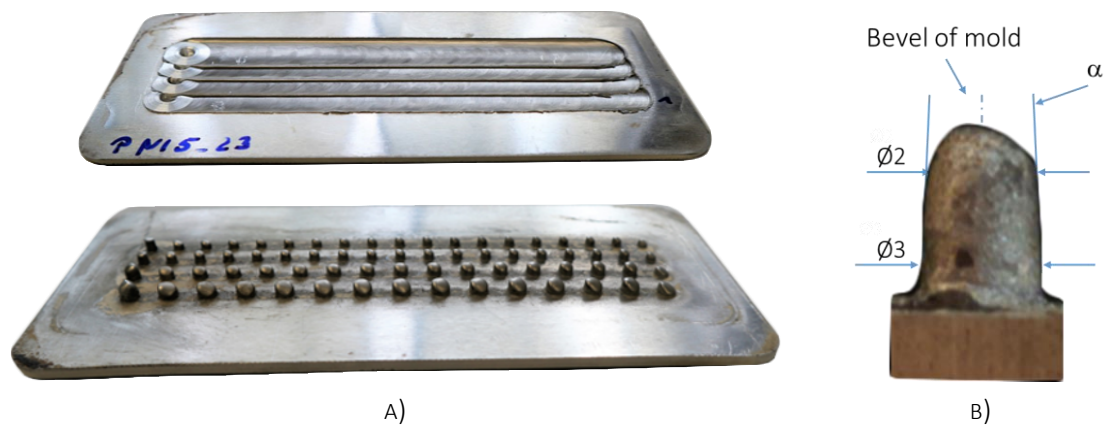
FIGURE 4.20 A) FRONT AND BACK SIDE OF A FSFED SHEET AND B) PIN GEOMETRY DETAILS

In order to evaluate the pin extrusion process and to establish the initial joining conditions, the pin length distribution was analysed and the results are provided in terms of average length and standard deviation (Figure 4.21).
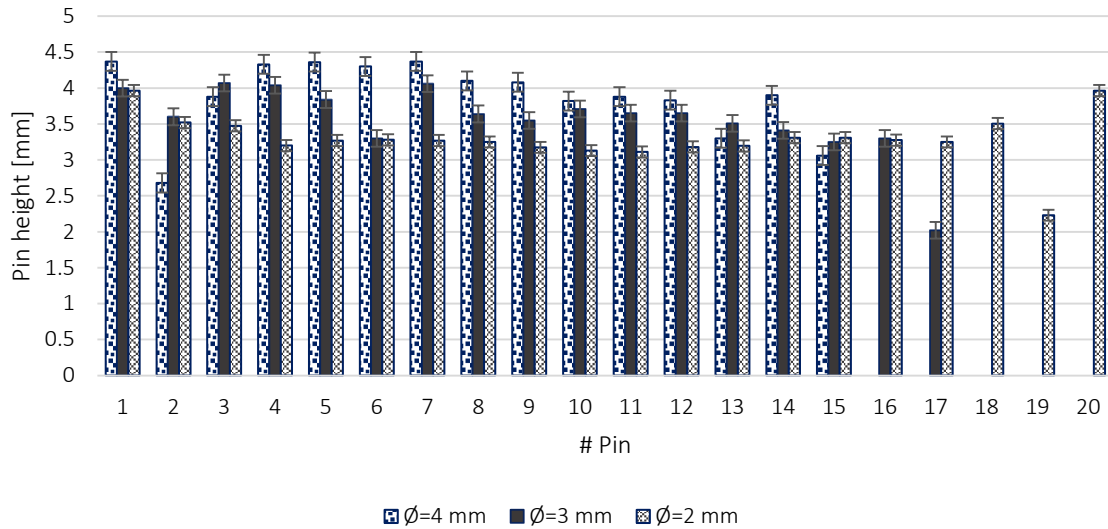
FIGURE 4.21 PIN HEIGHT DISTRIBUTION

Pins with a diameter of 3 mm were used to perform the first joining tests and according to their average length, the final pin height was headed to match the composite thickness of 1.1 mm or 3 mm.

An example of the joint is shown in the following Figure 4.22 A). The materials result successfully joined demonstrating that the proposed method might be used to obtain a joint that does not require any additional external material. It can be observed in Figure 4.22 B) that the aluminium sheet thickness did not remain constant and a point of overclosure was detected.

FIGURE 4.22 A) EXAMPLE OF A PERFORMED JOINT AND B) PIN GEOMETRY AFTER JOINING

To assess the mechanical behaviour of the joints produced by Friction Stir Forming, tensile shear tests were carried out according to DIN 53 281. More in detail, the tests aimed at determining the performance of the grooved composite, the shear that can be transmitted by the aluminium pins and the peeling tendency of the joint. To perform the tests the following values have been taken into account: the thickness of the aluminium sheets varied between 3 mm in the initial state and 2.5 mm, the incrementally measured gauging length $l_{gauging}$ started with ~20 mm and the velocity of the cross head of the testing machine remained constant during the test and was equal to 0.1 mm/s.

To analyse the static tensile performance, the cross-section A_{comp} of the notched glass fibre reinforced polyamide composite was considered. The width b of the composite was 19 mm, the thickness t was 1.1 mm and the diameters of the four pins were 3 mm. The calculation of the average tensile stress of σ = 49 N/mm² referred to the smallest initial cross-section A_{comp}= 14.3 mm².

Looking at Figure 4.23 B), it is possible to observe that the crack occurred on the surface of the hole and grew to the edges. To shift the failure mode of the composite from tensile to peeling, the width of the composite was increased, while the cross section of the aluminium pins remained constant.
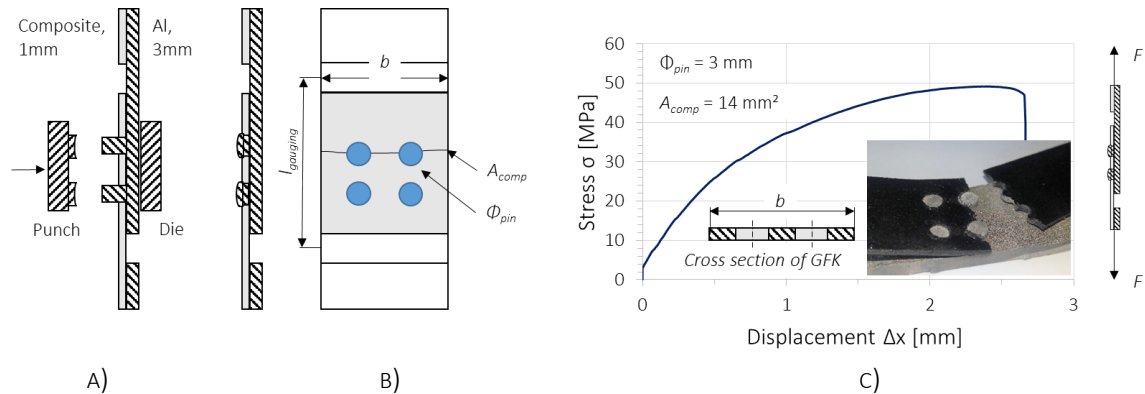
FIGURE 4.23 A) JOINING BY HEAD LOCKING OF THE PINS, B) GEOMETRY OF THE OVERLAPPING AREA AND C) TENSILE SHEAR TEST OF THE JOINED AND NOTCHED COMPOSITE

The cross section ratio (CSR) of the composite and the pin characterize the crack. The CRS was estimated as follows and failure behaviours are reported in Figure 4.24.

$$CSR = \frac{A_{comp}}{A_{pin}} = \frac{4t_{comp}\left(b_{comp} - n_{pin}d_{pin}\right)}{\pi n_{pin}d_{pin}^{2}}$$

FIGURE 4.24 A) STRESS-DISPLACEMENT CURVE OF NOTCHED COMPOSITE AND B) FAILURE MODES

A CSR of 4.2 marked the point where a combined failure of tensile crack and peeling occurred. For a bigger CSR only peeling was expected. According to the obtained results and in order to use

117

the full performance of the joining method, some design rules for the mechanical construction can be established for a composite 1.1 mm thick:

- CSR over 4.2 leads to peeling and should be avoided
- CSR between 1 and 3 leads to tensile crack in the composite

The critical CSR will change with the thickness because it depends on the bending stiffness of the composite sheet.

The mechanical strength of the pins was analysed by the tensile shear test. To investigate the elastic-plastic flow behaviour of the aluminium, the composite thickness was raised to 3 mm and two configurations of respectively one and two pins with a diameter of 3 mm were considered. For each configuration, more than one sample was tested in order to evaluate the repeatability. Since the pins had a maximum length of 4.3 mm, the closing head was not very effective. By using some additional clamping, pure shear could be induced. The following Figure 4.25 shows the shear stress displacement curve based on the initial cross section of the aluminium, which starts with an elastic behaviour to fit the remaining tolerances due to the contact stiffness in the joining.
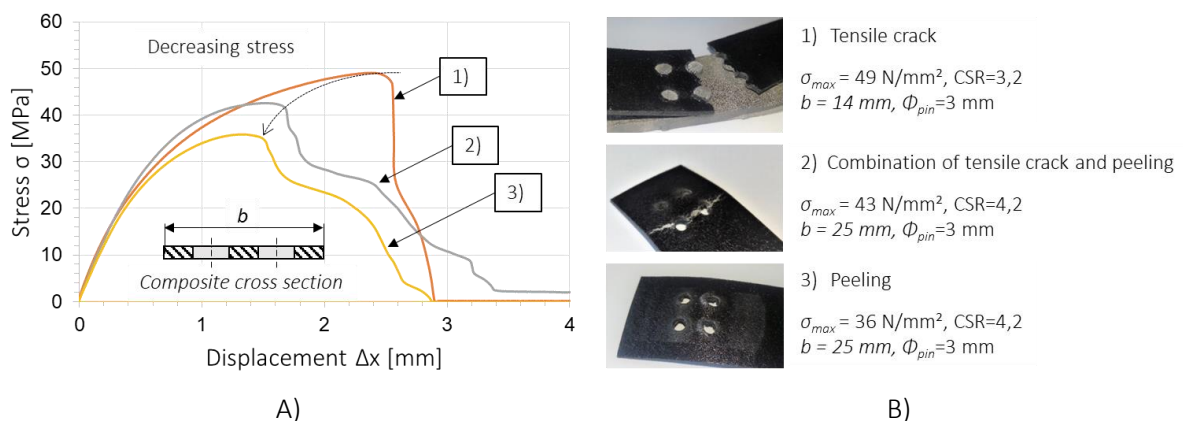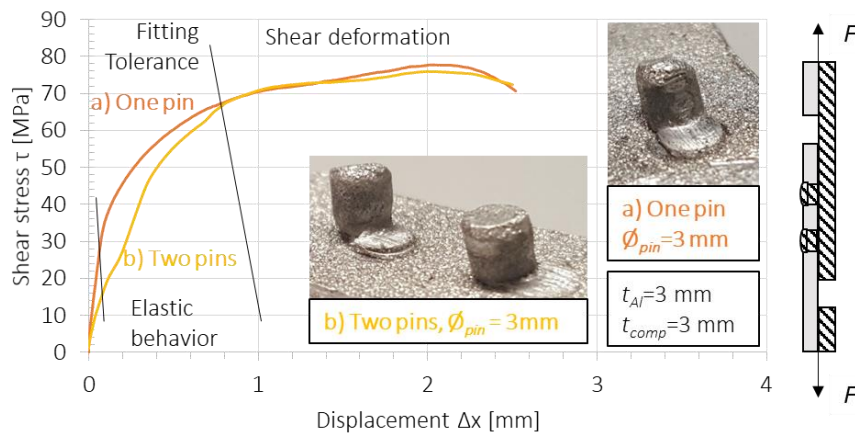

FIGURE 4.25 SHEAR STRESS-DISPLACEMENT CURVE

For the configuration with two pins, two points of inflection can be located. The plastic shear deformation of the aluminium pin started at about 35 N/mm² for one pin. For two pins, the yield stress decreases nearly to the half. This leads to the conclusion that, at first, only one pin transmits the shear force. Over a stress of about 70 N/mm², both stress-displacement curves are similar. The main cause is the positioning accuracy of the pins.

To investigate thoroughly the shear behaviour of the joint, a third configuration made of one pin taken from the second line was defined. The choice of defining two one-pin joining configurations was related to the need of understanding the process temperature influence on the outcome, being the lines performed at different thermal conditions. A significant difference in terms of strength behaviour was measured between the one-pin configurations. The average τ_{max} obtained from joints belonging to the last defined configuration (one pin from the second line) is ~20% lower than that measured on the similar configuration (one pin from the first line). This result is notable since the standard error is less than 2%.

TABLE 4.7 TENSILE TEST DATA

	One pin (first line)	One pin (second line)	Two pins
τ_{max} [MPa]	93,23	73,43	99,13
Standard Error	1,66	0,47	9,67

As proof of concept, the outcomes of two tensile tests performed on samples from the two configurations are displayed in Figure 4.26. More in detail, the test belonging to the configuration with one pin from the first line was defined as Sample 1, while that one belonging to the configuration with one pin from the second line was defined Sample 2. The illustrated distributions confirmed a quite different behaviour between the two samples that can be justified by a dissimilar softening condition of the material during the FSF process that affects the pin performance.

A)

B)
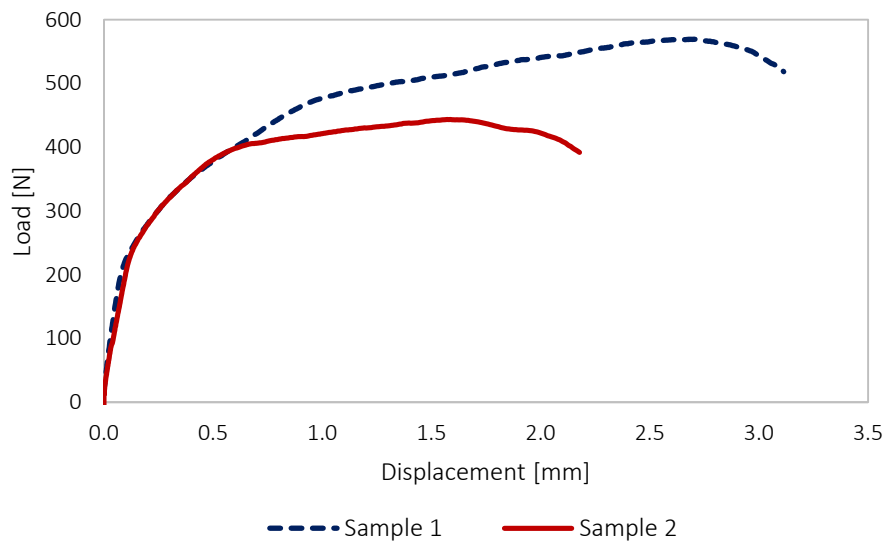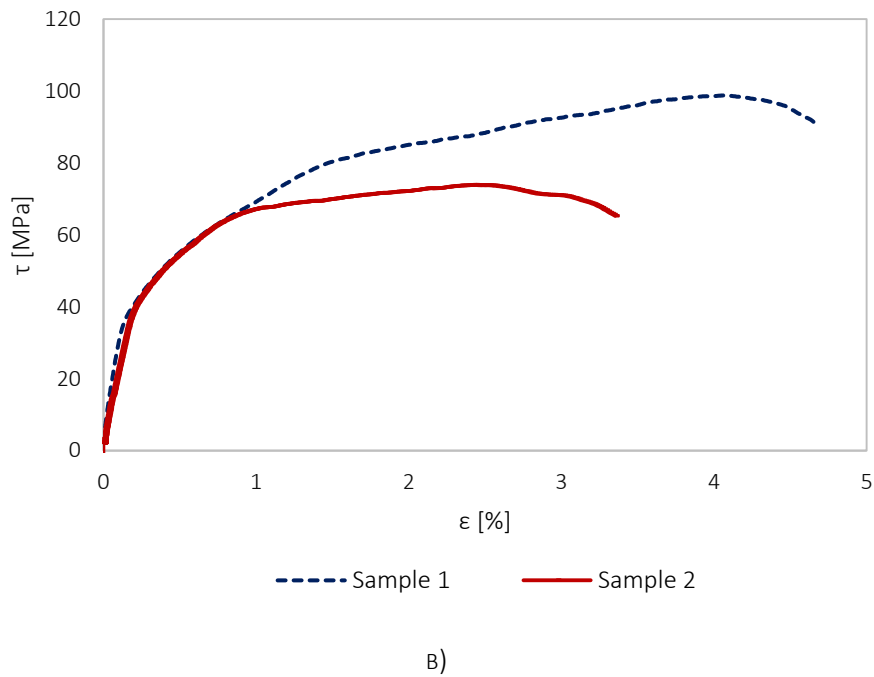
FIGURE 4.26 A) LOAD – DISPLACEMENT DISTRIBUTION, B) τ − ε DISTRIBUTION

4.2.3. IMPROVEMENT OF THE PIN EXTRUSION AND TOMOGRAPHIC OBSERVATIONS OF THE RESULTS

The approach discussed below aims at proposing a knowledge improvement of the Friction Stir Forming technique for producing pins to use for joining purposes. The attention was focused on the main process parameters, which can affect the quality of the extruded pins that have a key role in the performance of the connection.

EXPERIMENTAL EQUIPMENT

To perform and improve the FSF method, a new equipment was designed and manufactured. It was installed on a Mazak Nexsus 410 A vertical CNC machine. The following Figure 4.27 shows the parts the equipment is made up of.

A)

B)
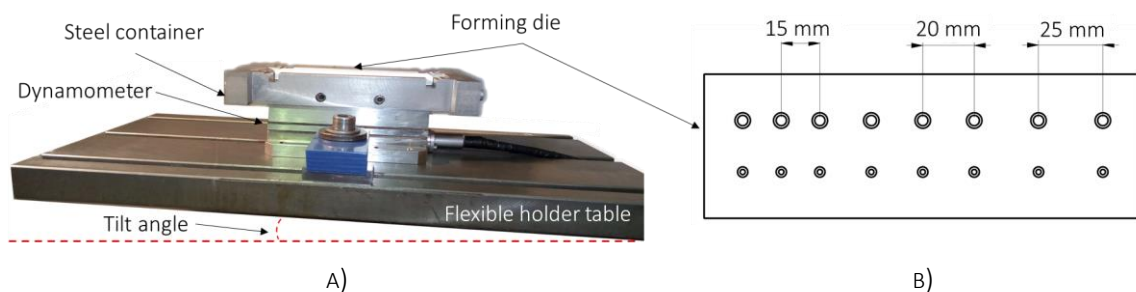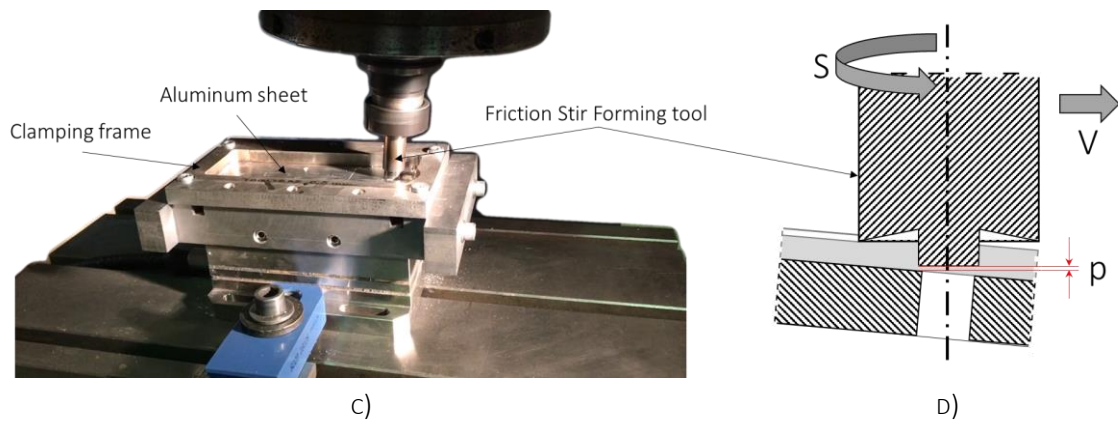
Specifically, it consists of:
- a steel container, where the forming die is positioned inside (Figure 4.27 A));
- a forming die, made of two lines of holes with a diameter $\varnothing$ of 4 mm and 6 mm, respectively. This element was also designed to evaluate if the distance between the holes d might have an influence on the process outputs. Therefore, three measures, i.e. 15 mm, 20 mm and 25 mm, reported in Figure 4.27 B), were analysed. The forming die was lubricated to avoid the aluminium sticking, which can affect the material flow during the process and the pins separation at the end of the forming phase;
- a steel clamping frame, used to lock the sheet during the forming process (Figure 4.27 C));
- a rigid tool, named FSF tool (Figure 4.27 C) and D)), characterized of a shoulder of 15 mm and a probe of 5 mm. A cavity on the tool face in contact with the sheet was performed according to Ohashi et al. (2017). At the beginning of the process the FSF tool was plugged into the sheet up to a controlled residual depth p, measured as reported in Figure 4.27 D). The rotational movement of this tool inside the aluminium sheet allowed the pins extrusion through the holes of the forming die;
- a dynamometer for monitoring the forces along the tool axis and the tool movement. The whole equipment was laid on it and mounted on a flexible holder table (Figure 4.27 A)), which allows to change the defined tilt angle α. This last investigated variable, indeed, affects both the overrun of the processed material and the material flow into the holes of the forming die.

MATERIAL AND METHOD

To the aim of this research and according to the previous described experimental investigation, the Aluminum EN AW-1050A-H111 was processed (material properties listed in Table 4.6). Samples of 180x80x3 mm were cut from a sheet.

To pursue the aim of this research and for a full comprehension of the process mechanics an experimental investigation was designed including geometrical and process variables, preliminary

screened and chosen aiming at improving quality and properties of the extruded pins. In Table 4.8, the set process parameters and their ranges are listed.

TABLE 4.8 EXPERIMENTAL PLAN PARAMETERS

Parameter	Low	Medium	High
Spindle speed S [RPM]	1500	-	3000
Forming velocity V [mm/min]	25	165	300
Residual depth p [mm]	0.1	0.2	0.3
Tilt angle α [°]	2	5	7.5
Distance between holes d [mm]	15	20	25
Hole diameter $\varnothing$ [mm]	4	-	6

Furthermore, a monitoring of the forces on the rigid forming tool along its movement was performed to understand the different phases of the process and how the distance between the pins affects the obtained trends. Finally, the mechanical behaviour of the manufactured pins was evaluated by a shear stress measurements performed by an Instron tensile testing machine with a load cell of 5kN (Figure 4.28 A)). A travel speed of 1 mm/min was used to avoid the interference of any dynamic effects. This experimental investigation was performed on specimens cut from the manufactured sheets isolating one pin for each test. These specimens were blocked on a holed plate, which was designed to avoid any out-of-plane stress during the analysis (Figure 4.28 B)).

A)   B)
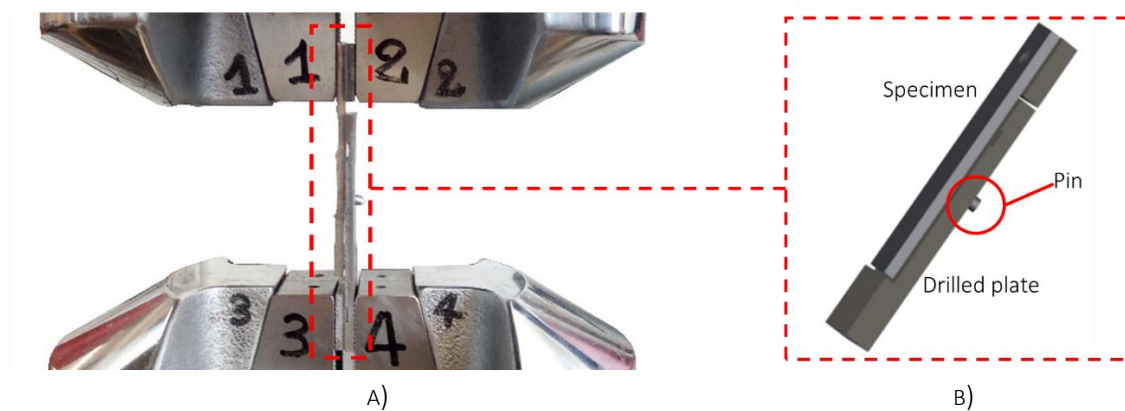
FIGURE 4.28 SHEAR STRESS EQUIPMENT USED TO MEASURE THE MECHANICAL BEHAVIOUR OF THE MANUFACTURED PINS

RESULTS

Considering the performed tests, it has to be highlighted that, taking advantage of the designed equipment, d and α are variables whose effects can be assessed in each performed test and, therefore, their analysis does not require specific experimental run. Consequently, the experimental plan had to be set up considering the other four parameters. Furthermore, a preliminary set of tests were performed keeping fixed the residual depth (p=0.1 mm) and the tilt angle (α=5 °) according the investigation described in the previous paragraph. A total amount of 6 different configurations were performed first, each one repeated three times for evaluating the process repeatability.

The first obtained outcomes are schematically presented in Figure 4.29. Specifically, a coloured working window was drawn classifying the results in three distinct zones for different spindle speed *S* and forming velocity *V*. A first class was named *wave zone* (yellow area) and corresponds to the lowest forming velocity (V=25 mm/min). Here, the sheets were characterized by rough material edges left on their top surface by the forming movement of rigid tool. Even if the pins resulted formed, they presented macroscopic porosities, sign of a low quality of the process. The burr was observed along both the processed pin lines, but its size incremented when *α* was reduced and *d* increased.

A second class was named *cold zone* (light blue area), so defined because the lowest spindle speed (S=1500) combined with high forming velocities (V=[165÷300] mm/min) led to low temperatures during the process. In this case, the material resulted torn up rather than stirred, so this was considered as an area of un-formability.

A last class was defined as *formability zone* (green area) and matched with the highest quality of the samples. Specifically, the highest value of spindle speed (S=3000 RPM) and forming velocity (V=[165÷300] mm/min) led to sound specimens with pins properly formed. These results assessed the strong correlation between *S* and *F*, as far as allowed to exclude the low value of both the velocities for the second part of the analysis.
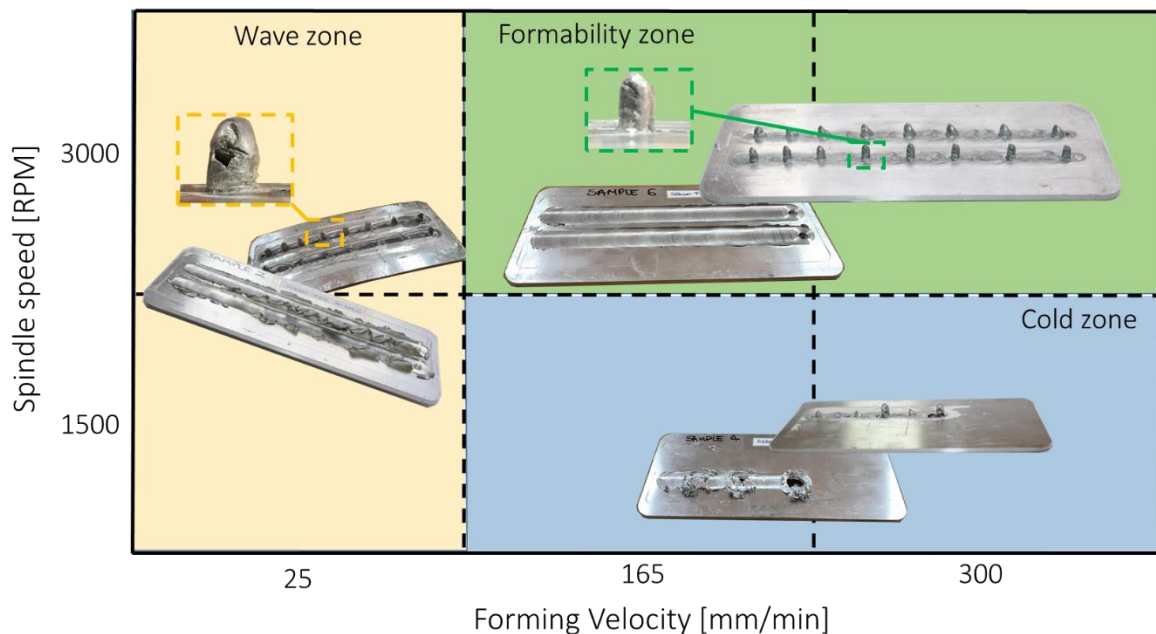
FIGURE 4.29 EXPERIMENTS CLUSTERING OBTAINED CHANGING SPINDLE SPEED AND FORMING VELOCITY (AT p=0.1 mm AND α=5 °)

FORCES MEASUREMENT AND ASSESSMENT

As already mentioned, for a full comprehension of the process mechanism, the force distributions due to the punch movement were monitored during the experimental tests. The forming die was fixed on a Kistler piezoelectric dynamometer, linked to a data acquisition system by a proper charge amplifier. Any undesired vibrational movement was negligible taking into account the high global

stiffness of the whole equipment. The vertical (Fz) and horizontal (Fx) components of the total forces were monitored (Figure 4.30). The holes and the dynamometer were coaxial, therefore the registered components were analysed without considering the effect of the tilt angle α. The two components were detected for various process configurations connecting their trend to the different phases of the forming sequence.
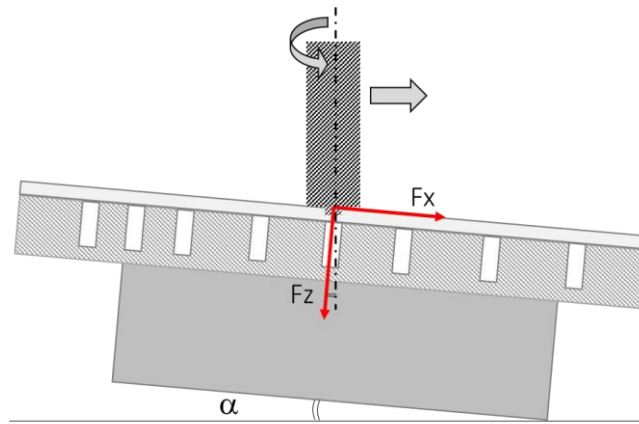
FIGURE 4.30 SKETCH OF THE FORCES MEASUREMENT SYSTEM

Considering the force values at various forming times, three main zones can be highlighted. They are displayed in the following Figure 4.31.
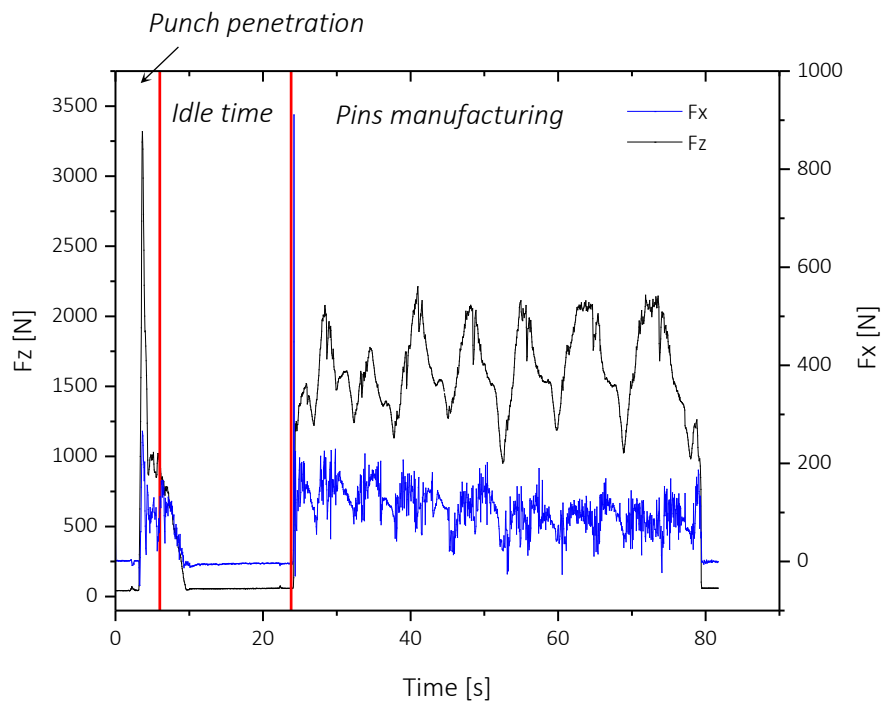
FIGURE 4.31 FORCE MEASURED DURING THE TEST CARRIED OUT AT S=3000 RPM, V=165 mm/min, α=5°, p=0.1 mm, Ø=4 mm

More in detail, the first zone was characterized by the punch penetration: both Fz and Fx presented a steep increment when the punch became in contact with the sheet. Specifically, the trend of Fz was characterized by a momentary peak that suddenly decreased when the punch moved to its penetrating depth, increasing the material temperature, as well. The second zone, fixed at about 10 seconds, was named *idle phase*: both Fz and Fx reduced their value because the punch continued rotating on the spot. This phase, in the first tests, was overrated to quantify a suitable idle time that could be assessed in few seconds. This was evaluated looking at the decrement of the forces and considering, before starting the punch translation, as ultimate time that one when a plateau of the forces was recorded. The third was attributed to the manufacturing step: due to the punch movement, both the Fx and Fz increased suddenly up to a maximum value and then approached to a relative cyclic evolution. The irregular trends were justified by the presence of the holes on the forming die below the worked sheet. Briefly, during the punch movement, the forces increased due to the material stack under its back face. The holes on the die forming allowed an escape to the gathered material with the formation of the pins and the force fell down.

Peaks and valleys of Fx and Fz curves followed a similar timeline. Being the Fz the most relevant and being that one without a persistent scattering, the attention was focused just on its trend to analyse the forming phase of FSF process. Furthermore, the forces measured during this last step were displayed with respect of the punch displacement to allow the comparison between tests performed at different velocities.

Figure 4.32 reports the Fz distribution as a function of the punch movement and the relative holes position for specific setting of the process parameters. The distance between holes *d* leads to different shapes of the recorded curves. The influence of this variable was discussed overlapping the force trends for the three investigated *d* values and justifying their evolution taking into account the relative position between punch and hole. The analysis was performed comparing the curves avoiding the transient conditions due to the process starting and the transition between two different *d*. Therefore, the third, fifth and seventh force variations reported in Figure 4.32 were overlapped in Figure 4.33.
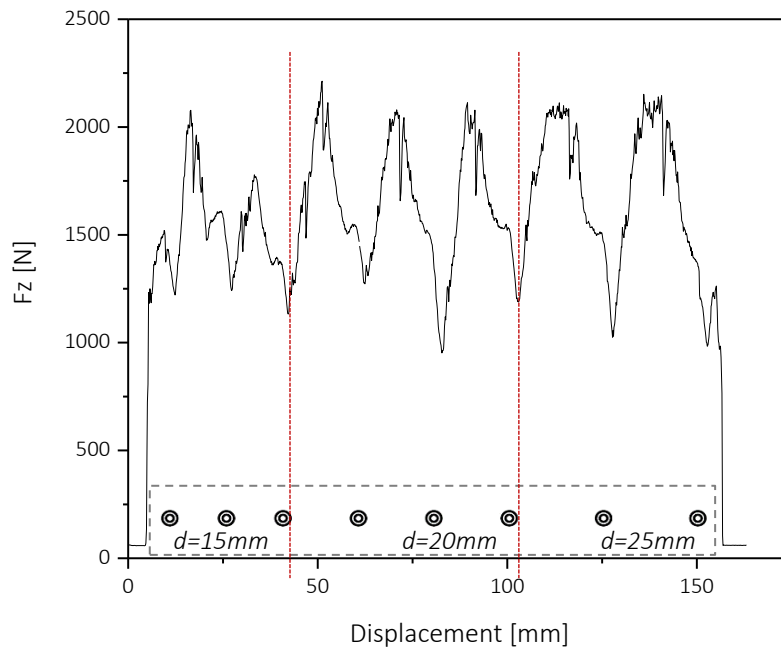
FIGURE 4.32 FORCE DISTRIBUTION ACCORDING TO THE HOLES POSITION (S=3000 RPM, V=165 mm/min, α=5.0°, p=0.1 mm, Ø=4 mm)

Specifically, Fz started increasing once the probe of the rigid tool left the previous hole (step 1 in Figure 4.33 A)). The curve gradually increased up to the shoulder of the tool reaching the next hole or a maximum value. Looking at Figure 4.33 B), Fz reached the lowest peak for d=15 mm. Indeed, for this configuration, the holes were excessively close to each other and the force stopped growing before reaching the biggest capacity. This happened because the successive hole did not allow to fulfil the volume with the stacked material under the rotating tool. The other two distances led to a similar peak value. However, for d=25 mm, the peak occurred when the tool was still far from the next hole (Figure 4.33 B)). Therefore, a more emphasized stationary condition can be observed for d=25 mm respect to d=20 mm (Figure 4.33 B)). However, the influence of the following hole caused an initial instability zone and a consistent curve scattering was recorded with a gradual decrement of the force values (step 3 Figure 4.33 C)). This instability ended once the probe reached the beginning of the hole (step 4 in Figure 4.33 C)). At that point, indeed, the trend of the Fz curve decreased progressively up to a minimum point (step 1 in Figure 4.33 A) and D)). Furthermore, in this decreasing phase, an inflection point can be detected, where the force trend changed its concavity. This point corresponds to the maximum interaction between probe and hole (step 4 in Figure 4.33 D)), where their axes coincide.

The remarks just described have confirmed that the pins distance is a variable that needs to be optimised to improve the process performance. Summarizing, a short distance between the holes leads to empty pins due to a not enough material gathering before the manufacturing phase starts. Vice versa, using a larger *d* too much material is collected under the tool and this might lead to

undesired material leakage on the top of the sheet. The described effects are dependent on the holes position as well as on its interaction with all the highlighted process parameters.
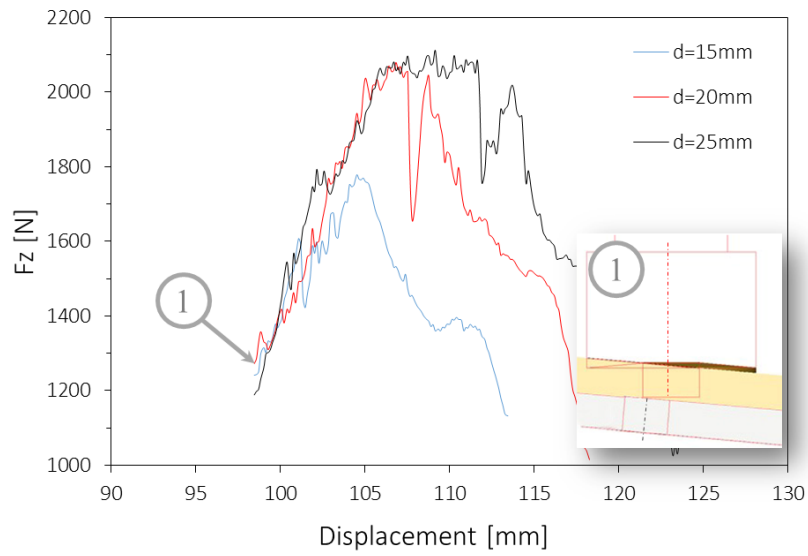
A)
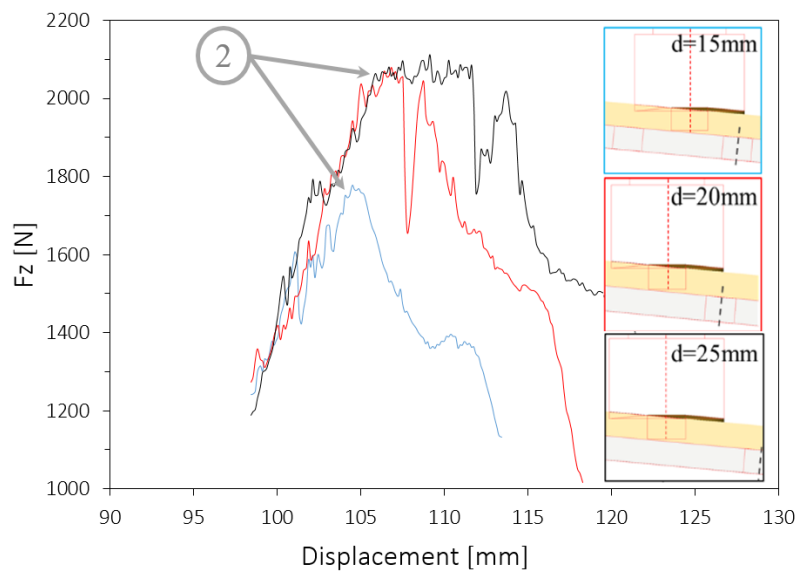
B)
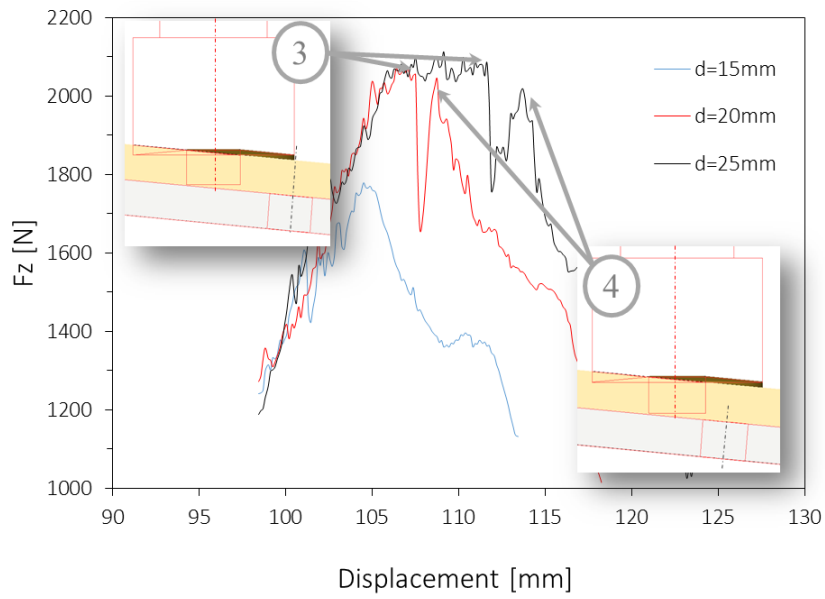
c)
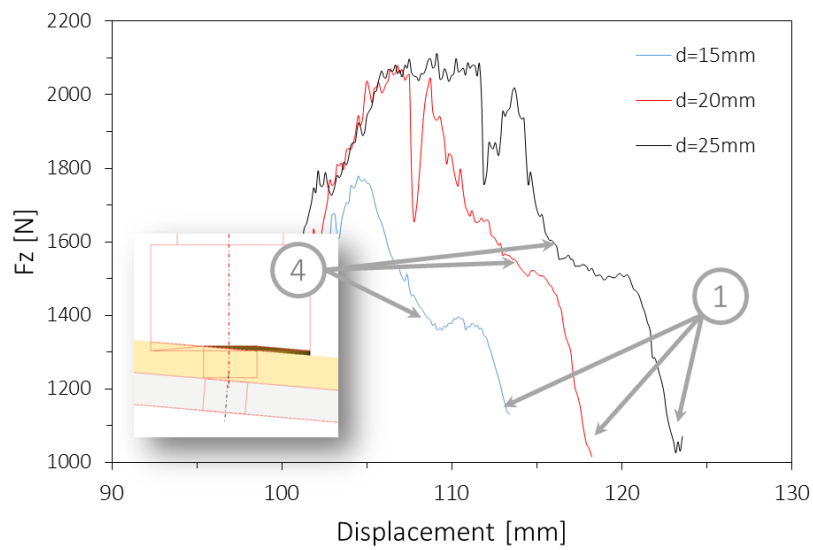
d)

FIGURE 4.33 OVERLAPPING OF THE FORCE VARIATION ACCORDING TO THE HOLES POSITION (S=3000 RPM, V=165 MM/MIN, A=5.0 °, P=0.1 MM, Ø=4 MM)

A further interesting observation can be deduced comparing the force distributions during the manufacturing step changing the investigated process parameters. The trends are displayed in Figure 4.34.
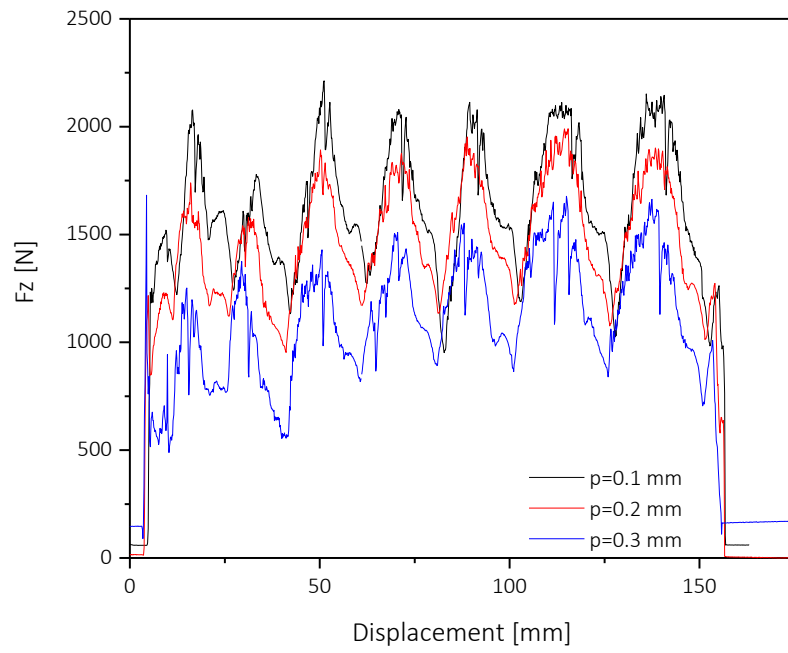
A)
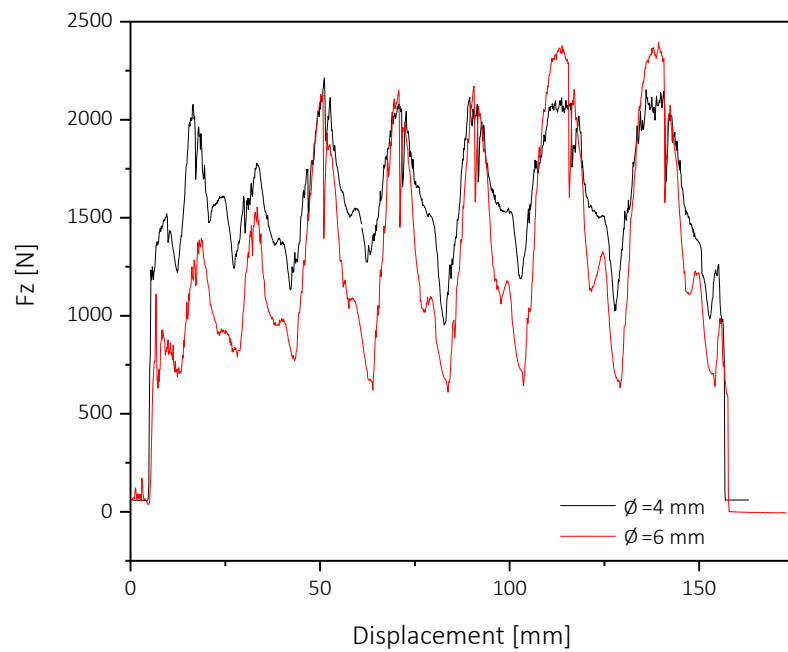
B)
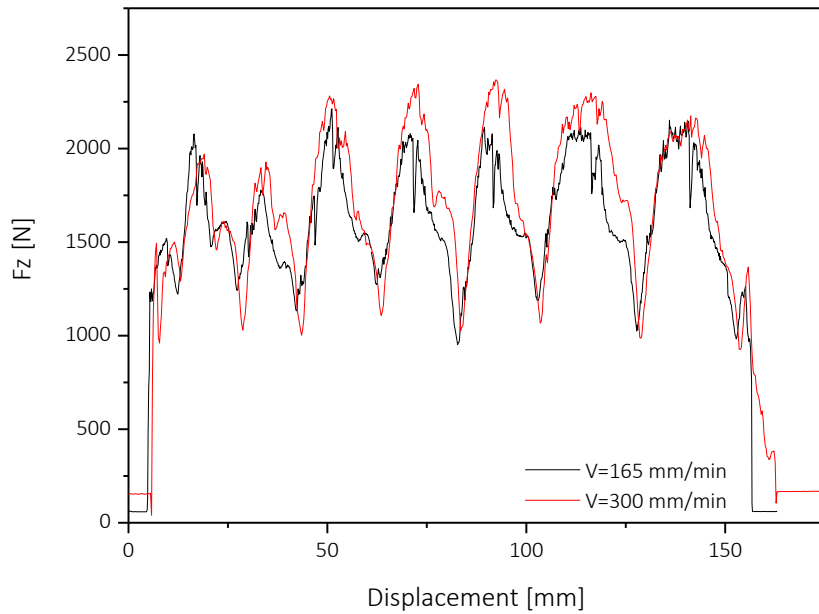
C)
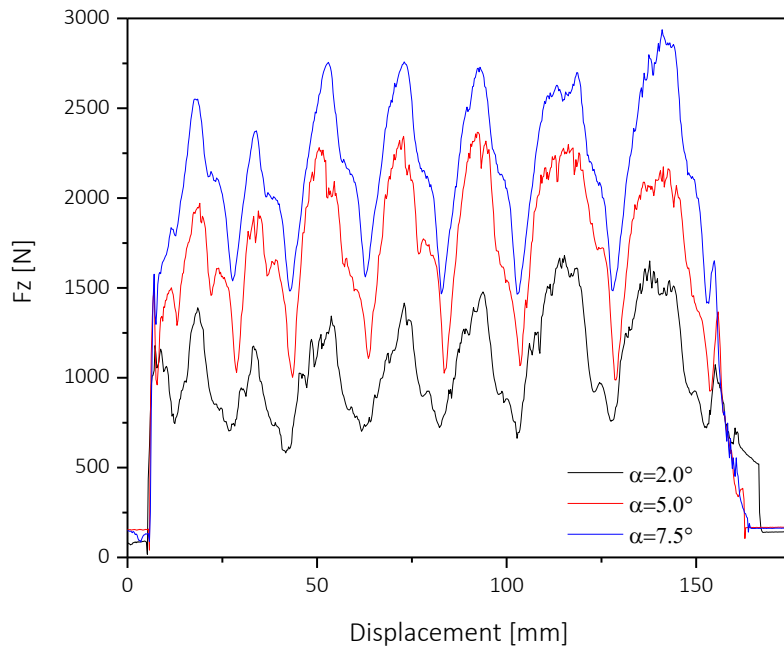
D)

FIGURE 4.34 COMPARISON OF F_z FOR EACH INVESTIGATED PROCESS PARAMETER

The first comparison was carried out keeping all the variables constant and changing only the tool residual depth p: an increase of p caused a lower penetration of the punch into the sheet and therefore a lower quantity of material moved during the forming phase. As a consequence also the force values resulted lower when a higher value of p was considered (Figure 4.34 A).

The same comparison was performed isolating the effect of the hole diameter Ø. In this case, if the hole is wider, the tool displacement without the influence of the hole is restricted. This led to a narrowing of the curve amplitude between two successive valleys, as confirmed in Figure 4.34 B). Furthermore, deeper valleys can be observed for the biggest pins because more material left the stirring zone and was extruded through the forming die. At the same time, the F_z increased faster once the tool moved to the next hole at the end of the forming phase. When the stationary conditions were reached (d=25 mm), the force was higher for the configuration with pins of a diameter of 6 mm. This trend should be due to higher friction forces at the bearing zone of the forming die caused by a wider shearing surface.

The effects of the forming velocity V on the F_z variation are displayed in Figure 4.34 C). The curves for V=165 mm/min and 300 mm/min are characterized by the same trend. A slight decreasing of the forces was observed for the slowest velocity. This was ascribed to material edges left on the top surface of the sheet. The burr could appear reducing the forming velocity and increasing the distance between holes. The effect was relevant for the lowest analysed forming velocity V=25 mm/mm, but the defect appeared also setting V=165 mm/min and d longer than 20 mm. The decrease of the gathered material volume in the forming zone led to the F_z reduction.

Finally, the tilt angle influence on the F_z variation is reported in Figure 4.34 D). The rigid tool penetrated deeply the sheet when the α value increased. A bigger volume of material was affected when the interaction between the tool and the workpiece was higher. Therefore, it can be observed that the force trends are similar and the curves appear just shifted to higher values according to the tilt angle increment.

X-RAY MICRO-TOMOGRAPHIC ANALYSIS

A deep investigation has been carried out on the internal structure of the extruded aluminium pins. An x-ray micro-tomographic analysis has been performed to quantify the distribution of the material within the manufactured pins. More in detail, the aim was to measure the percentage of voids and understand if it was affected by the process parameters setting.

The x-ray micro-tomography uses x-rays to create cross-sections of a physical object and aims at recreating a 3D model without destroying the original one. The resolution of the acquired images depends on the pixels size and, in this case, they are in the micrometre range, as the prefix of the name suggests. The technique finds application in several scientific fields, such as radiology, archaeology, biology, geophysics, materials science. Two types of scanner setup may be identified. In the first one, the x-ray source and the detector are typically stationary during the scan while the sample rotates. In the second case, the specimen is stationary while the x-ray tube and detector rotate around. To the aim of this research, the first scanning typology was used and a specific software program allowed to build the volume of every pin by *stacking* each individual slice one on top of the other.

Before scanning and testing the samples by means of the tensile machine, the height of the manufactured pins was measured (each sample is made of two lines of eight pins each one, as shown in Figure 4.27 B)). The report is displayed in Figure 4.35. Higher pins have been obtained if compared to the preliminary investigation (Figure 4.21).
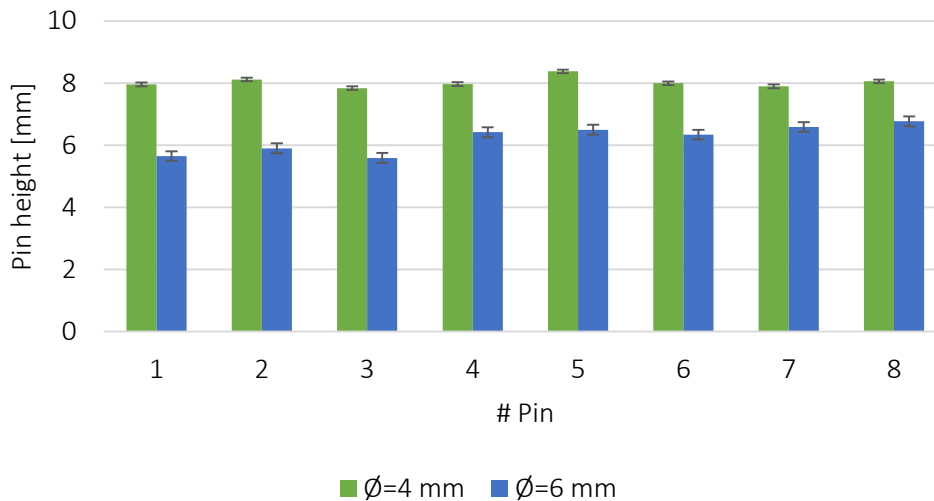
FIGURE 4.35 PIN HEIGHT DISTRIBUTION

A pre-screening phase allowed a qualitative selection of the pins to scan and to analyse by means of the x-ray micro-tomography.

A deep observation and quantification of the pins reconstruction allowed to affirm that the voids contained within the pins can be considered derisory. In fact, an average of 2.61% was calculated.

More in detail, the following tables contain the measured values, both in terms of pin height and of void percentage. Pins were compared changing just one process parameter. Each table, except Table 4.11, contains the values of the pin at the fifth position on the original sample.

All process parameters, except the distance between holes, seem affecting the presence of voids within the pins. Furthermore, the lowest percentage of voids is caused by the highest value of the slope angle. This was expected, since a higher slope should drive better the material into the holes during the FSF process.

TABLE 4.9 S=3000 RPM, p=0.1 mm, α=5°

Scanned pin	Variable parameter F [mm/min]	Ø=4 mm		Ø=6 mm	
		Height [mm]	Void [%]	Height [mm]	Void [%]
T1	25	7.02	4.40%	7.85	12.70%
T2	165	7.98	1.10%	5.90	1.58%
T3	300	7.17	3.34%	6.02	6.46%

TABLE 4.10 S=3000 RPM, F=300 mm/min, p=0.1 mm

Scanned sample	Variable parameter α [°]	Ø=4 mm		Ø=6 mm	
		Height [mm]	Void [%]	Height [mm]	Void [%]
T3	5.0	7.17	3.34%	6.02	6.46%
T4	7.5	8.38	0.63%	6.50	1.44%

TABLE 4.11 S=3000 RPM, F=300 mm/min, p=0.1 mm, α=7.5°

Scanned sample	Variable parameter Holes distance [mm]	Ø=4 mm		Ø=6 mm	
		Height [mm]	Void [%]	Height [mm]	Void [%]

T5	15	7.84	0.43%	5.59	1.86%
T4	20	8.38	0.63%	6.50	1.44%
T6	25	7.90	0.23%	6.59	1.86%

TABLE 4.12 S=3000 RPM, F=165 mm/min, α=7.5°

Scanned sample	Variable parameter p [mm]	Ø=4 mm		Ø=6 mm	
		Height [mm]	Void [%]	Height [mm]	Void [%]
T2	0.1	7.98	3.34%	5.9	6.46%
T7	0.2	5.08	2.62%	3.88	2.67%

In Figure 4.36 and Figure 4.37 the scanned samples characterized, respectively, by the maximum and minimum percentage of voids are displayed. Figure 4.36 A) and Figure 4.37 A) show the real manufactured pins, Figure 4.36 B) and Figure 4.37 B) are the snapshots of the pin reconstruction after the x-ray micro-tomography, while in Figure 4.36 C) and Figure 4.37 C) the voids contained within the pins are visible.

A)   B)   C)

FIGURE 4.36 SAMPLE T1_ F=25 mm/min, S=3000 RPM, p=0.1 mm, α=5°, Ø=6 mm. A) Manufactured pin, B) pin reconstruction, C) voids content

A)   B)   C)

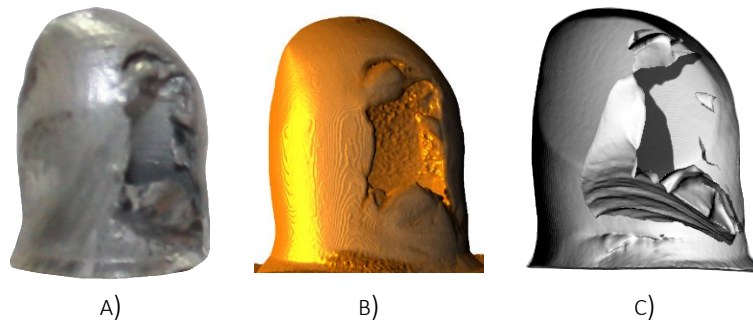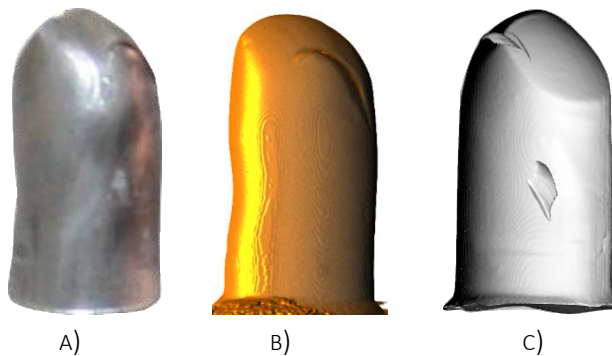FIGURE 4.37 SAMPLE T6_F=300 mm/min, S=3000 RPM, p=0.1 mm, α=7.5°, Ø=4 mm. A) Manufactured pin, B) pin reconstruction, C) voids content

AP SHEAR TESTS

As mentioned above, to analyse the mechanical behaviour of the manufactured pins lap shear tests were performed. For each test, a strip was cut from the original sample along the short dimension and the selected pin was isolated (Figure 4.38)

FIGURE 4.38 EXAMPLE OF TESTED PIN

More in detail, the tests were necessary to understand how the mechanical properties of the manufactured pins change at different working conditions. It has to be considered also that the plastic deformation the material is subjected to and the related temperatures reached during the forming phase could affect the mechanical properties of the pins. Theoretically, these variables cause diametrically opposed effects. Indeed, the plastic deformation hardens the material due to the increment of dislocation density, while the increment of the temperature tends to soften the material due to a grain recrystallization, reducing therefore its strength. These considerations were taken into account to quantify the effect of each investigated process parameter reported in the following graphs.

More in detail, considering the influence of the forming velocity (Figure 4.39 A)), a lower V increases the manufacturing process. This caused an overheating of the formed materials and the pins showed a reduced strength due to the grain growth related to the quantity of the released energy. Concerning the effects of the tilt angle α (Figure 4.39 B)) and residual depth (Figure 4.39 C)), the pin obtained with the configurations of α=7.5° as well as p=0.1 mm showed higher shear stresses, respectively, than α=5.0° e p=0.2 mm. A higher α and a lower p led to a bigger interaction between rigid tool and sheet and a more relevant plastic deformation. The lowest tilt angle, α=2.5°, as well as a reduced residual depth p=0.3 mm were not taken into account because this configuration did not allow the pin manufacturing.

The distance between the pins has proved to have low impact on the variation of this mechanical property (Figure 4.39 D)). A slight strength decrement can be observed for longer d and this can be due to the staying of the material in that region (plateau zone of the force diagrams) where the heating contribution exceeds the hardening effects. Finally, a more consistent extrusion phase and related forming level, due to a reduced hole diameter, make the pins obtained with d=4 mm more stress resistant than the ones manufactured with d=6 mm (Figure 4.39 E)).
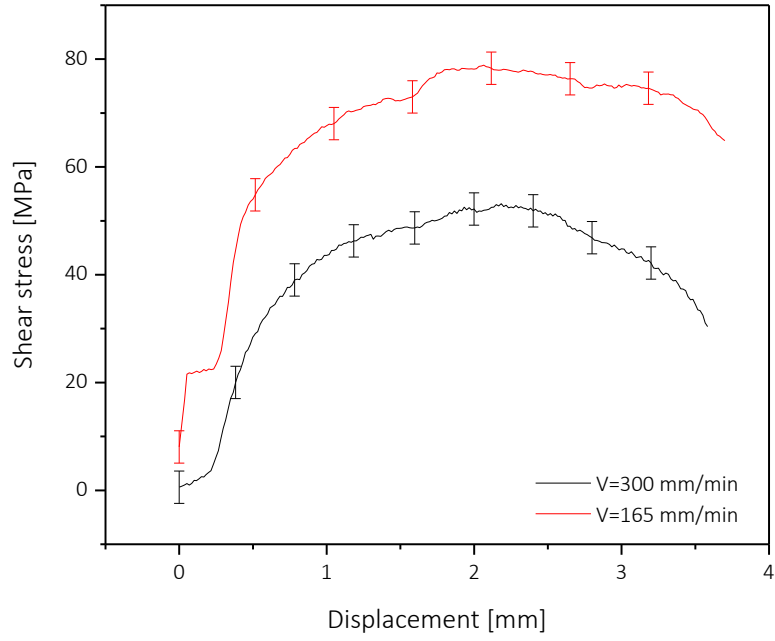
A)
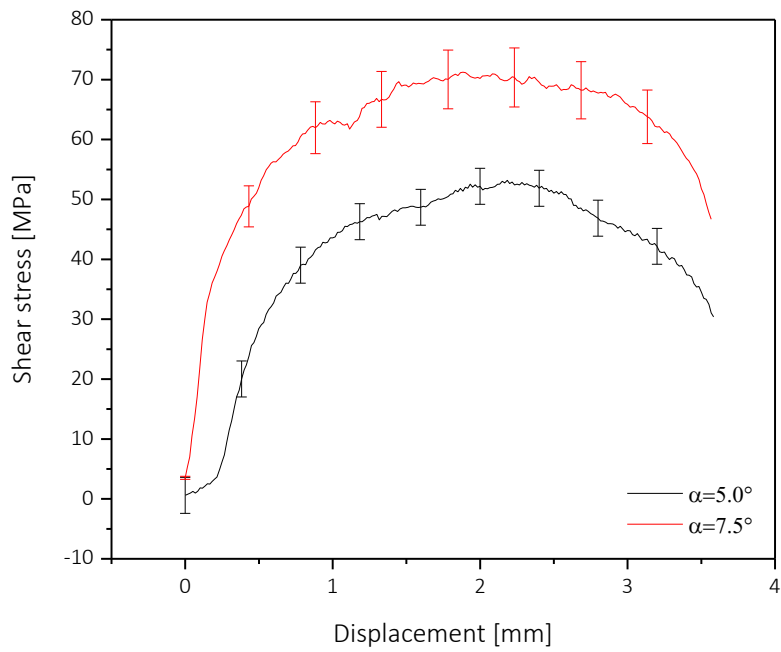
B)
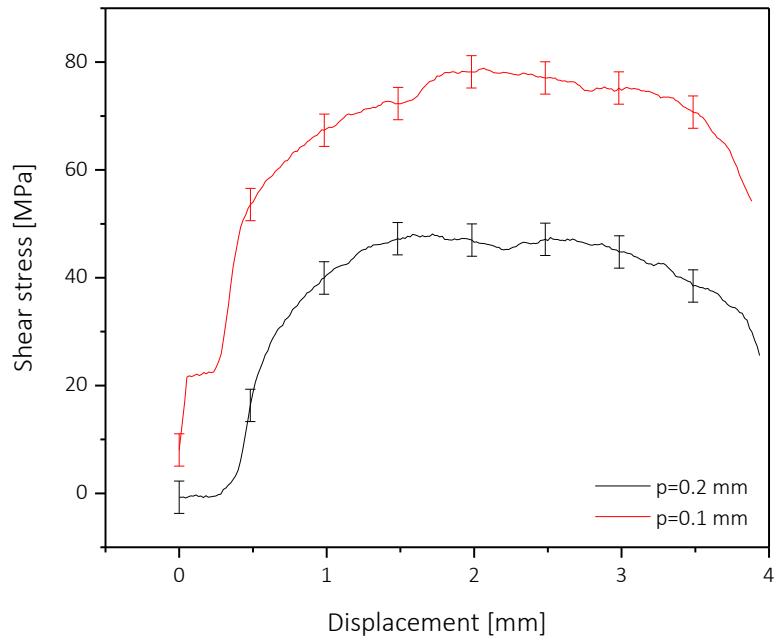
c)
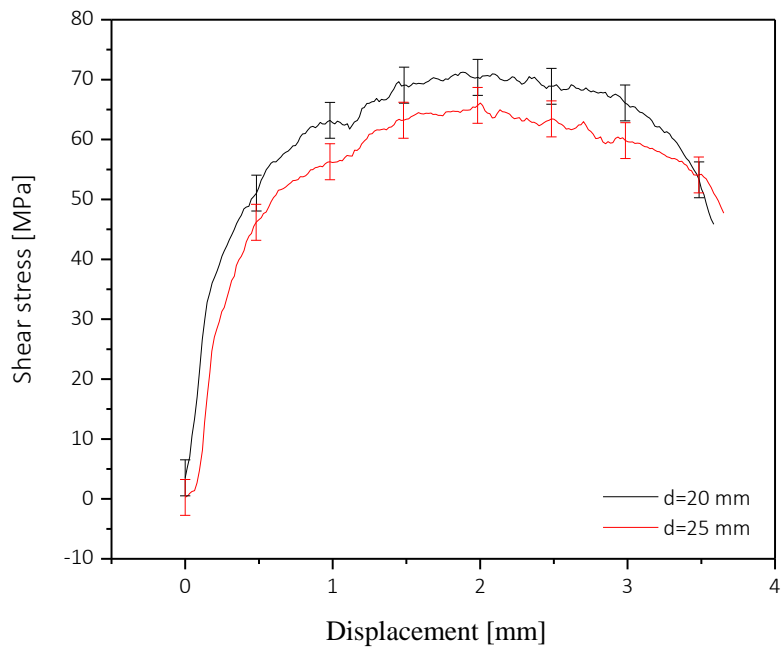
D)
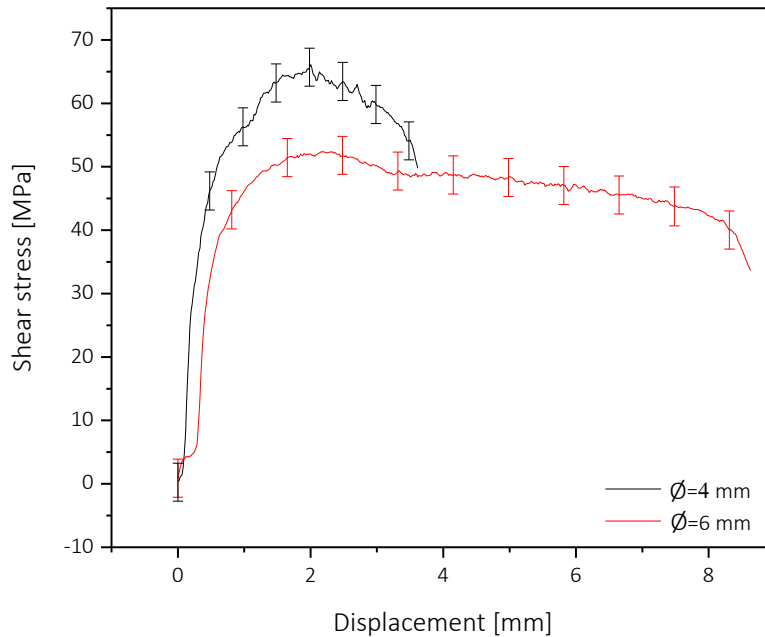
E)

FIGURE 4.39 SHEAR STRESS COMPARISONS FOR EACH INVESTIGATED PROCESS PARAMETER

Summing up, the friction stir forming process was performed for manufacturing pins to join with composite sheets. A preliminary study was carried out for forming pins using the process parameters reported in the literature. The joint was successfully performed, demonstrating therefore its feasibility, and the composite and pin strength was analysed.

A second investigation was designed aiming at improving the quality and the structure of the aluminium pins. The attention was focused on the main variables that have to be set for optimizing the process. A preliminary screening of the variables, using also data available in literature, was carried out pointing out how high forming velocity and low spindle speed cannot be combined because lead to cold forming conditions. Furthermore, the lowest investigated forming velocity was also discarded to prevent the burr formation on the top of the processed sheet surface. Therefore, a working window was defined and suitable process parameter ranges were determined. They were used in new tests carried out to the aim of monitoring the forces arisen during the forming phase, highlighting how their trend depend on the relative position between the rotating tool and the position of the holes on the forming die.

The influence of each investigated variable on the force variation was pointed out since it may be linked to the flow material during the pin manufacturing phase. Indeed, an increment of the forces along the symmetric axes of the holes forming die leads to extrude more material, increasing therefore the pin size. Finally, the internal structure of the pins was analysed by means of the x-ray micro-tomography technique and the mechanical behaviour of the obtained pins assessed by shear stress tests, discussing the influence of the investigated process parameters as well.

137

CONCLUSIONS

*"Every science consists in the coordination of facts;
if the different observations were entirely isolated, there would be no science."*

Auguste Comte

The main goal of this thesis was the experimental validation of thermoplastic polymers and composites workability by two typologies of innovative downstream manufacturing processes.

To this aim, after a wide study of the state of the art, this research work was divided into two main sections.

The first one (Chapter 3) reported investigations on the Single Point Incremental Forming process, considered as a relevant alternative technology to manufacture high quality, customized components in low volume and at reasonable costs.

Sheet blanks of polypropylene (PP), characterized a T_g of about 8 °C, were first tested. The process parameters were set according to the state-of-the-art. An exception was represented by the process temperature, not investigated in previous studies. To the aim of this first preliminary tests, both *cold* and *hot* SPIF were performed in order to analyse the temperature influence on the material formability. The manufactured truncated cones were classified according to the occurrence of cracks or wrinkles. It was observed that tests carried out setting a temperature higher than the room one, presented just wrinkles that followed the rotational tool movement and not cracks. The impact of the spindle speed, considered by previous studies as the main influent process parameter, was evaluated in terms of springback measuring the final height of each sample. An excessive springback was not recorded because the material remained in the rubbery state. On the other hand, the impact of the temperature was analysed in terms of surface roughness, but a substantial difference on the results was not highlighted.

The second polymeric material analysed was the poly(methyl methacrylate) (PMMA) characterized by a T_g of 114 °C, therefore higher than the room temperature. The hot SPIF was here necessary and the outcomes were classified in three typologies: broken, sound and springback. As regards the sound samples, the accuracy error was estimated by comparing the real profile, obtained by a Minolta Laser scanning system, with the ideal profile. It was observed that the height of the

sample was more reduced when the sheet had a bigger thickness. To understand the reason of this behaviour, the temperature on the bottom surface of the processed sheet was numerically estimated and the results showed that the thermal gradient was very high in case of sheets 6 mm thick. Therefore, the used equipment is not suitable to form sheets with thicknesses greater than a certain threshold. The statistical analysis of the results highlighted that the spindle speed and the initial temperature are the parameters that mainly affected the outcomes. Their influence was also examined scanning the sample surface by the SEM technique. The observations allowed to identify four conditions and to conclude that the effect of the external heating source on the part quality is more pronounced than the heating generated by the spindle speed.

The first two experimental investigations allowed to extend the tests on a third material. It was a composite characterised by a thermoplastic matrix (PA6) and reinforced with short glass fibers. The material forming limits and the temperature influence were first analysed. The preliminary tests highlighted that the SPIF cannot be performed with the punch in direct contact with the sheet. Therefore the successive tests were carried out superimposing an aluminium sheet on the composite one, proving the feasibility of the process and particular attention was paid to the thickness distribution and the part accuracy. This latter represented the main drawback: a distortion out of the forming area was observed and this can be probably attributed to high residual stresses in the sheet and could be reduced using a backing plate that fits with the sample geometry. To investigate deeply and optimize the part accuracy a hexagonal pyramid was selected as the geometry to shape and a new power setting and cooling modes were defined. The best accuracy was obtained using a fast heating and air cooling mode. Furthermore, the measure of the final heights confirmed the good accuracy. The PA6 samples were also scanned by SEM for studying if and how the process parameters may affect the glass fibers or may degrade the thermoplastic matrix. The observations did not highlight any material alteration or fibers distortion.

In conclusion, this first part of the research aimed at extending the potentiality of the Single Point Incremental Forming process, already defined by the scientific community for shaping metal sheet, to polymeric and composite materials, which are characterized by a transition temperature higher than the room one. This was proved supplying heat from an external heating source during the forming phase which improved the formability and reduced the forming forces. Nevertheless, the additional cost in equipment and energy consumption remain the main drawbacks.

The second section (Chapter 4) discussed two innovative variants for joining dissimilar materials and more in detail to connect metals with polymers and composites. The connection of multi-materials is considered a real challenge, because of the materials incompatibility and differences, but due to the advantages related to their use, this secondary manufacturing process is gaining the interest of researchers and industries.

The first tested technique was the Friction Riveting performed by using sheets of pure and reinforced polyamide 6 (PA6) and bars of titanium Grade 2 and of aluminium AA 6060. A DoE was carried out and the quality of the connection and the link between the process parameters and the process outputs (temperature, forging load and pulling strength) were analysed. The main results are here summarised:

- the strength of the connection increases if the total linear stroke increases

- the rotational speed affects the friction phase, increasing the process temperature and the anchoring force of the rivet inside the connected parts.
- the percentage of glass fibers has a considerable impact on the quality of the joints and on the temperature variation
- the material of the rivet (titanium or aluminium) does not affect the values of the joint strength.

Furthermore, the strain distribution and the surface quality of the joined sheets were analysed using Electronic Speckle Pattern Interferometry (ESPI) highlighting that spindle speed has an important influence on the material strain around the rivet.

The last part of this thesis focused on a new process variant for joining dissimilar material without using additional external parts. It was based on the Friction Stir Forming operational principle. The aim was to use this latter mentioned technology for manufacturing pins from an aluminium sheet. The first tests were carried out using the same process parameters of a study reported in the scientific literature (Ohashi et al., 2017), but unfortunately the obtained results were not the same of the cited study, therefore it was necessary to carry out some preliminary tests in order to understand the suitable combinations of process parameters. The manufactured pins where then joined with a composite sheet preliminary drilled. The mechanical strength of the joints was assessed by tensile shear tests. To analyse the static tensile performance, the cross-section of the composite was considered and the cross section ratio was estimated and the failure behaviours defined. To test the mechanical behaviour of pins, three configurations were tested, one of them aimed at understanding the influence of the process temperature on the results.

Finally, an improvement of the Friction Stir Forming technique for producing pins to use for joining purposes was studied. New geometrical and process variables were included in the experimental investigation and the force distributions were monitored. Longer pins were obtained. Furthermore, the internal structure of the extruded aluminium pins was analysed by the x-ray micro-tomography, aiming at quantifying the distribution of the material within pins. The results revealed an average of 2.61% of voids. The mechanical behaviour of the new manufactured pins was also assessed and the effect of each process parameter quantified.

REFERENCES

Abdel-Wahab, A.A., Ataya, S., Silberschmidt, V. V., 2017. Temperature-dependent mechanical behaviour of PMMA: Experimental analysis and modelling. Polym. Test. 58, 86–95. https://doi.org/10.1016/j.polymertesting.2016.12.016

Abounaim, M., Hoffmann, G., Diestel, O., Cherif, C., 2010. Thermoplastic composite from innovative flat knitted 3D multi-layer spacer fabric using hybrid yarn and the study of 2D mechanical properties. Compos. Sci. Technol. 70, 363–370. https://doi.org/10.1016/j.compscitech.2009.11.008

Abrate, S., Walton, D.A., 1992. Machining of composite materials. Part I: Traditional methods. Compos. Manuf. 3, 75–83. https://doi.org/10.1016/0956-7143(92)90119-F

Ahmad, J., 2009. Machining of Polymer Composites. Springer US, Boston, MA. https://doi.org/10.1007/978-0-387-68619-6

Alhashmy, H., 2012. Fabrication of Aluminium Matrix Composites (AMCs) by Squeeze Casting Technique Using Carbon Fiber as Reinforcement. University of Ottawa (Canada).

Altin Karataş, M., Gökkaya, H., 2018. A review on machinability of carbon fiber reinforced polymer (CFRP) and glass fiber reinforced polymer (GFRP) composite materials. Def. Technol. 14, 318–326. https://doi.org/10.1016/j.dt.2018.02.001

Altmeyer, J., dos Santos, J.F., Amancio-Filho, S.T., 2014. Effect of the friction riveting process parameters on the joint formation and performance of Ti alloy/short-fibre reinforced polyether ether ketone joints. Mater. Des. 60, 164–176. https://doi.org/10.1016/j.matdes.2014.03.042

Amancio-Filho, S.T., 2011. Friction Riveting: development and analysis of a new joining technique for polymer-metal multi-materials structures. Weld. World 55, 13–24.

Amancio-Filho, S.T., Blaga, L.-A., 2018. Joining of Polymer–Metal Hybrid Structures. Principles and Applications.

Amancio-Filho, S.T., dos Santos, J.F., 2009. Joining of polymers and polymer-metal hybrid structures: Recent developments and trends. Polym. Eng. Sci. 49, 1461–1476. https://doi.org/10.1002/pen.21424

Amancio-Filho, S.T., Roeder, J., Nunes, S.P., dos Santos, J.F., Beckmann, F., 2008. Thermal degradation of polyetherimide joined by friction riveting (FricRiveting). Part I: Influence of rotation speed. Polym. Degrad. Stab. 93, 1529–1538. https://doi.org/10.1016/j.polymdegradstab.2008.05.019

Amancio Filho, S.T., dos Santos, J.F., Ventzke, V., 2008. Determination of fracture mechanisms under tensile loading in a commercial available engineering thermoplastic material joined by

FricRiveting, in: Book of Abstracts: 5th Intern. Conference on Fracture of Polymers, Composites and Adhesives. Elsevier.

Ambrogio, G., Filice, L., Gagliardi, F., 2012. The application of a damage model based on the absorbed plastic energy for sheetbreaking prediction in incremental forming. Steel Res. Int. SPL. ISSUE, 435–438.

Ambrogio, G., Filice, L., Guerriero, F., Guido, R., Umbrello, D., 2011. Prediction of incremental sheet forming process performance by using a neural network approach. Int. J. Adv. Manuf. Technol. 54, 921–930. https://doi.org/10.1007/s00170-010-3011-x

Antończak, A.J., Nowak, M., Szustakiewicz, K., Pigłowski, J., Abramski, K.M., 2013. The influence of organobentonite clay on CO2 laser grooving of nylon 6 composites. Int. J. Adv. Manuf. Technol. 69, 1389–1401. https://doi.org/10.1007/s00170-013-5098-3

Ashter, S.A., 2013. Thermoforming of Single and Multilayer Laminates: Plastic Films Technologies, Testing, and Applications. William Andrew.

Bagudanch, I., Garcia-Romeu, M.L., Centeno, G., Elías-Zúñiga, A., Ciurana, J., 2015. Forming force and temperature effects on single point incremental forming of polyvinylchloride. J. Mater. Process. Technol. 219, 221–229. https://doi.org/10.1016/j.jmatprotec.2014.12.004

Bagudanch, I., Garcia-Romeu, M.L., Sabater, M., 2016. Incremental forming of polymers: process parameters selection from the perspective of electric energy consumption and cost. J. Clean. Prod. 112, 1013–1024. https://doi.org/10.1016/j.jclepro.2015.08.087

Bagudanch, I., Martínez-Romero, O., Elías-Zúñiga, A., Garcia-Romeu, M.L., 2014. Identifying Polymeric Constitutive Equations for Incremental Sheet Forming Modelling. Procedia Eng. 81, 2292–2297. https://doi.org/10.1016/j.proeng.2014.10.323

Bhatnagar, N., Naik, N.K., Ramakrishnan, N., 1993. EXPERIMENTAL INVESTIGATIONS OF DRILLING ON CFRP COMPOSITES. Mater. Manuf. Process. 8, 683–701. https://doi.org/10.1080/10426919308934873

Birat, K., Pervaiz, M., Faruk, O., Tjong, J., Sain, M., 2015. Green Composite Manufacturing via Compression Molding and Thermoforming, in: Manufacturing of Natural Fibre Reinforced Polymer Composites. Springer International Publishing, Cham, pp. 45–63. https://doi.org/10.1007/978-3-319-07944-8_3

Blaga, L., Bancilă, R., dos Santos, J.F., Amancio-Filho, S.T., 2013. Friction Riveting of glass–fibre-reinforced polyetherimide composite and titanium grade 2 hybrid joints. Mater. Des. 50, 825–829. https://doi.org/10.1016/j.matdes.2013.03.061

Blaga, L., dos Santos, J.F., Bancila, R., Amancio-Filho, S.T., 2015. Friction Riveting (FricRiveting) as a new joining technique in GFRP lightweight bridge construction. Constr. Build. Mater. 80, 167–179. https://doi.org/10.1016/j.conbuildmat.2015.01.001

Borba, N.Z., Blaga, L., dos Santos, J.F., Amancio-Filho, S.T., 2018. Direct-Friction Riveting of polymer composite laminates for aircraft applications. Mater. Lett. 215, 31–34. https://doi.org/10.1016/j.matlet.2017.12.033

Borges, M.F., Amancio-Filho, S.T., dos Santos, J.F., Strohaecker, T.R., Mazzaferro, J.A.E., 2012. Development of computational models to predict the mechanical behavior of Friction Riveting joints. Comput. Mater. Sci. 54, 7–15. https://doi.org/10.1016/j.commatsci.2011.10.031

Boria, S., Scattina, A., Belingardi, G., 2017. Impact behavior of a fully thermoplastic composite.

Compos. Struct. 167, 63–75. https://doi.org/10.1016/j.compstruct.2017.01.083

Bouffioux, C., Lequesne, C., Vanhove, H., Duflou, J.R., Pouteau, P., Duchêne, L., Habraken, A.M., 2011. Experimental and numerical study of an AlMgSc sheet formed by an incremental process. J. Mater. Process. Technol. 211, 1684–1693. https://doi.org/10.1016/j.jmatprotec.2011.05.010

Brent Strong, A., Hauwiller, P.B., 1989. Incremental Forming of Large Thermoplastic Composites. J. Thermoplast. Compos. Mater. 2, 122–132. https://doi.org/10.1177/089270578900200204

British Plastics Federation, 2018. British Plastics Federation 2018 - Popypropylene [WWW Document]. URL http://www.bpf.co.uk/plastipedia/polymers/PP.aspx

Brydson, J.A., 1999. Plastics materials.

Chaves, C.E., Inforzato, D.J., Fernandez, F.F., 2018. Principles of Mechanical Fastening in Structural Applications, in: Joining of Polymer-Metal Hybrid Structures: Principles and Applications. pp. 147–185.

Darwish, S.M.H., 2010. Science of Weld: Adhesive Joints. pp. 1–36. https://doi.org/10.1007/8611_2010_35

Davarpanah, M.A., Mirkouei, A., Yu, X., Malhotra, R., Pilla, S., 2015. Effects of incremental depth and tool rotation on failure modes and microstructural properties in Single Point Incremental Forming of polymers. J. Mater. Process. Technol. 222, 287–300. https://doi.org/10.1016/j.jmatprotec.2015.03.014

Davarpanah, M.A., Zhang, Z., Bansal, S., Cao, J., Malhotra, R., 2016. Preliminary investigations on Double Sided Incremental Forming of thermoplastics. Manuf. Lett. 8, 21–26. https://doi.org/10.1016/j.mfglet.2016.05.003

Davim, J.P., 2015. Machinability of Fibre-Reinforced Plastics. De Gruyter.

Davim, J.P., Mata, F., 2005. Optimisation of surface roughness on turning fibre-reinforced plastics (FRPs) with diamond cutting tools. Int. J. Adv. Manuf. Technol. 26, 319–323. https://doi.org/10.1007/s00170-003-2006-2

deLorenzi, H.G., Nied, H.F., 1987. Blow molding and thermoforming of plastics: Finite element modeling. Comput. Struct. 26, 197–206. https://doi.org/10.1016/0045-7949(87)90250-1

Deng, S., Djukic, L., Paton, R., Ye, L., 2015. Thermoplastic–epoxy interactions and their potential applications in joining composite structures – A review. Compos. Part A Appl. Sci. Manuf. 68, 121–132. https://doi.org/10.1016/j.compositesa.2014.09.027

Dhanawade, A., Kumar, S., 2017. Experimental study of delamination and kerf geometry of carbon epoxy composite machined by abrasive water jet. J. Compos. Mater. 51, 3373–3390. https://doi.org/10.1177/0021998316688950

Di Franco, G., Fratini, L., Pasta, A., 2013. Analysis of the mechanical performance of hybrid (SPR/bonded) single-lap joints between CFRP panels and aluminum blanks. Int. J. Adhes. Adhes. 41, 24–32. https://doi.org/10.1016/j.ijadhadh.2012.10.008

Di Franco, G., Fratini, L., Pasta, A., 2012. Influence of the distance between rivets in self-piercing riveting bonded joints made of carbon fiber panels and AA2024 blanks. Mater. Des. 35, 342–349. https://doi.org/10.1016/j.matdes.2011.09.036

DuPont, n.d. DuPont [WWW Document]. URL http://www.dupont.com

Ebewele, R.O., 2000. Polymer science and technology. CRC press.

Edwards, W.L., Grimm, T.J., Ragai, I., Roth, J.T., 2017. Optimum Process Parameters for Springback Reduction of Single Point Incrementally Formed Polycarbonate. Procedia Manuf. 10, 329–338. https://doi.org/10.1016/j.promfg.2017.07.002

El-Taweel, T.A., Abdel-Maaboud, A.M., Azzam, B.S., Mohammad, A.E., 2009. Parametric studies on the CO_2 laser cutting of Kevlar-49 composite. Int. J. Adv. Manuf. Technol. 40, 907–917. https://doi.org/10.1007/s00170-008-1412-x

El Bouami, S., Habak, M., Franz, G., Velasco, R., Vantomme, P., 2016. Effect of tool geometry and cutting parameters on delamination and thrust forces in drilling CFRP/Al-Li. p. 080012. https://doi.org/10.1063/1.4963487

Eriksson, L., Johansson, E., Kettaneh-Wold, N., Wikström, C., Wold, S., 2000. Design of Experiments Principles and Applications.

Esteves, J.V., Goushegir, S.M., dos Santos, J.F., Canto, L.B., Hage, E., Amancio-Filho, S.T., 2015. Friction spot joining of aluminum AA6181-T4 and carbon fiber-reinforced poly(phenylene sulfide): Effects of process parameters on the microstructure and mechanical strength. Mater. Des. 66, 437–445. https://doi.org/10.1016/j.matdes.2014.06.070

Fakirov, S., 2008. Oriented polymer materials. John Wiley & Sons.

Feistauer, E.E., Guimarães, R.P.., Ebel, T., dos Santos, J.F., Amancio-Filho, S.T., 2016. Ultrasonic joining: A novel direct-assembly technique for metal-composite hybrid structures. Mater. Lett. 170, 1–4. https://doi.org/10.1016/j.matlet.2016.01.137

Filice, L., Fratini, L., Micari, F., 2002. Analysis of Material Formability in Incremental Forming. CIRP Ann. 51, 199–202. https://doi.org/10.1016/S0007-8506(07)61499-1

Fiorotto, M., Sorgente, M., Lucchetta, G., 2010. Preliminary studies on single point incremental forming for composite materials. Int. J. Mater. Form. 3, 951–954. https://doi.org/10.1007/s12289-010-0926-6

Franzen, V., Kwiatkowski, L., Martins, P.A.F., Tekkaya, A.E., 2009. Single point incremental forming of PVC. J. Mater. Process. Technol. 209, 462–469. https://doi.org/10.1016/j.jmatprotec.2008.02.013

Franzen, V., Kwiatkowski, L., Martins, P.A.F., Tekkaya, A.E., 2008. On the capability of single point incremental forming for manufacturing polymer sheet parts, in: ICTP2008, 9th International Conference on Theory of Plasticity.

Fratini, L., Ambrogio, G., Di Lorenzo, R., Filice, L., Micari, F., 2004. Influence of mechanical properties of the sheet material on formability in single point incremental forming. CIRP Ann. 53, 207–210. https://doi.org/10.1016/S0007-8506(07)60680-5

Fratini, L., Ruisi, V.F., 2009. Self-piercing riveting for aluminium alloys-composites hybrid joints. Int. J. Adv. Manuf. Technol. 43, 61–66. https://doi.org/10.1007/s00170-008-1690-3

Gaugel, S., Sripathy, P., Haeger, A., Meinhard, D., Bernthaler, T., Lissek, F., Kaufeld, M., Knoblauch, V., Schneider, G., 2016. A comparative study on tool wear and laminate damage in drilling of carbon-fiber reinforced polymers (CFRP). Compos. Struct. 155, 173–183. https://doi.org/10.1016/j.compstruct.2016.08.004

Geis, T., Klingelhöller, C., Hintze, W., 2014. Constant Depth Scoring of Fibre Reinforced Plastic Structures to Prevent Delamination. Procedia CIRP 14, 205–210.

https://doi.org/10.1016/j.procir.2014.03.103

Gessler, A., 2011. Braided reinforcements for composites, in: Composite Reinforcements for Optimum Performance. Elsevier, pp. 116–156. https://doi.org/10.1533/9780857093714.2.116

Gonçalves, J., Dos Santos, J.F., Canto, L.B., Amancio-Filho, S.T., 2015. Friction spot welding of carbon fiber-reinforced polyamide 66 laminate. Mater. Lett. 159. https://doi.org/10.1016/j.matlet.2015.08.036

Goushegir, S.M., 2016. Friction spot joining (FSpJ) of aluminum-CFRP hybrid structures. Weld. World 60, 1073–1093. https://doi.org/10.1007/s40194-016-0368-y

Goushegir, S.M., dos Santos, J.F., Amancio-Filho, S.T., 2015. Influence of process parameters on mechanical performance and bonding area of AA2024/carbon-fiber-reinforced poly(phenylene sulfide) friction spot single lap joints. Mater. Des. 83, 431–442. https://doi.org/10.1016/j.matdes.2015.06.044

Gutowski, T., Hoult, D., Dillon, G., Gonzalez-Zugasti, J., 1991. Differential geometry and the forming of aligned fibre composites. Compos. Manuf. 2, 147–152. https://doi.org/10.1016/0956-7143(91)90133-2

Guu, Y.H., Hocheng, H., Tai, N.H., Liu, S.Y., 2001. Effect of electrical discharge machining on the characteristics of carbon fiber reinforced carbon composites. J. Mater. Sci. 36: 2037. https://doi.org/10.1023/A:1017539100832

Guzman-Maldonado, E., Hamila, N., Naouar, N., Moulin, G., Boisse, P., 2016. Simulation of thermoplastic prepreg thermoforming based on a visco-hyperelastic model and a thermal homogenization. Mater. Des. 93, 431–442. https://doi.org/10.1016/j.matdes.2015.12.166

Hayashi, H., Nakagawa, T., 1994. Recent trends in sheet metals and their formability in manufacturing automotive panels. J. Mater. Process. Technol. 46, 455–487. https://doi.org/10.1016/0924-0136(94)90128-7

Hendel, N., 2003. Vacuum formable nylon sheets. IAPD Mag. 44–45.

Hintze, W., Brügmann, F., 2017. Influence of Curved Workpiece Contours on Delamination During end Milling of FRP. Procedia CIRP 62, 62–67. https://doi.org/10.1016/j.procir.2016.06.115

Hintze, W., Cordes, M., Koerkel, G., 2015. Influence of weave structure on delamination when milling CFRP. J. Mater. Process. Technol. 216, 199–205. https://doi.org/10.1016/j.jmatprotec.2014.09.004

Hocheng, H., Puw, H.Y., Huang, Y., 1993. Preliminary study on milling of unidirectional carbon fibre-reinforced plastics. Compos. Manuf. 4, 103–108. https://doi.org/10.1016/0956-7143(93)90077-L

Horvat, G.L., Surface, S.C., 1989. Assembled camshafts for automotive engines. J. Mater. Shap. Technol. 7, 133–136. https://doi.org/10.1007/BF02834742

http://altairuniversity.com/, n.d. http://altairuniversity.com/wp-content/uploads/2014/02/3DMeshing.pdf [WWW Document]. URL http://altairuniversity.com/wp-content/uploads/2014/02/3DMeshing.pdf

Hussain, S.A., Pandurangadu, V., Kumar, K.P., Bharathi, V.V.A., 2011. Predictive Model for Surface Roughness in Turning Glass Fiber Reinforced Plastics by Carbide Tool (K-20) Using Soft Computing. Jordan J. Mech. Ind. Eng. 5(5).

REFERENCES

Jahanmir, S., Ramulu, M., Koshy, P., 1999. Machining of ceramics and composites.

Jeswiet, J., Micari, F., Hirt, G., Bramley, A., Duflou, J., Allwood, J., 2005. Asymmetric Single Point Incremental Forming of Sheet Metal. CIRP Ann. 54, 88–114. https://doi.org/10.1016/S0007-8506(07)60021-3

Jeswiet, J., Young, D., 2005. Forming limit diagrams for single-point incremental forming of aluminium sheet. Proc. Inst. Mech. Eng. Part B J. Eng. Manuf. 219, 359–364. https://doi.org/10.1243/095440505X32210

Jiao, J., Wang, Q., Wang, F., Zan, S., Zhang, W., 2017. Numerical and experimental investigation on joining CFRTP and stainless steel using fiber lasers. J. Mater. Process. Technol. 240, 362–369. https://doi.org/10.1016/j.jmatprotec.2016.10.013

Jobey, C., Allanic, N., Mousseau, P., Deterre, R., 2016. Prediction of thickness distribution of thermoformed multilayer ABS/PMMA sheets. p. 170033. https://doi.org/10.1063/1.4963589

Jung, K.-W., Kawahito, Y., Takahashi, M., Katayama, S., 2013. Laser direct joining of carbon fiber reinforced plastic to aluminum alloy. J. Laser Appl. 25, 032003. https://doi.org/10.2351/1.4794297

Kalpakjian, S., Schmid, S., 2014. Manufacturing engineering and technology. Pearson, NJ, USA.

Kapidžić, Z., Nilsson, L., Ansell, H., 2014. Conceptual studies of a composite–aluminum hybrid wing box demonstrator. Aerosp. Sci. Technol. 32, 42–50. https://doi.org/10.1016/j.ast.2013.11.002

Katayama, S., Kawahito, Y., 2008. Laser direct joining of metal and plastic. Scr. Mater. 59, 1247–1250. https://doi.org/10.1016/j.scriptamat.2008.08.026

Kaufman, S.G., Spletzer, B.L., Guess, T.L., 1997. Freeform fabrication of polymer-matrix composite structures, in: Proceedings of International Conference on Robotics and Automation. IEEE, pp. 317–322. https://doi.org/10.1109/ROBOT.1997.620057

Kim, Y.., Park, J.., 2002. Effect of process parameters on formability in incremental forming of sheet metal. J. Mater. Process. Technol. 130–131, 42–46. https://doi.org/10.1016/S0924-0136(02)00788-4

Klein, P., 2009. Fundamentals of Plastics Thermoforming. Synth. Lect. Mater. Eng. 1, 1–97. https://doi.org/10.2200/S00184ED1V01Y200904MRE001

Kopeliovich, D., 2004. Thermoforming [WWW Document]. URL http://www.substech.com

Kumar, D., Singh, K.K., Zitoune, R., 2016. Experimental investigation of delamination and surface roughness in the drilling of GFRP composite material with different drills. Adv. Manuf. Polym. Compos. Sci. 2, 47–56. https://doi.org/10.1080/20550340.2016.1187434

Lambiase, F., Ko, D.-C., 2017. Two-steps clinching of aluminum and Carbon Fiber Reinforced Polymer sheets. Compos. Struct. 164, 180–188. https://doi.org/10.1016/j.compstruct.2016.12.072

Lau, H.C., Bhattacharya, S.N., Field, G.J., 1998. Melt strength of polypropylene: Its relevance to thermoforming. Polym. Eng. Sci. 38, 1915–1923. https://doi.org/10.1002/pen.10362

Lau, W.S., Lee, W.B., 1991. A COMPARISON BETWEEN EDIVI WIRE-CUT AND LASER CUTTING OF CARBON FIBRE COMPOSITE MATERIALS. Mater. Manuf. Process. 6, 331–342. https://doi.org/10.1080/10426919108934760

Lauwers, B., Kruth, J.P., Liu, W., Eeraerts, W., Schacht, B., Bleys, P., 2004. Investigation of material

removal mechanisms in EDM of composite ceramic materials. J. Mater. Process. Technol. 149, 347–352. https://doi.org/10.1016/j.jmatprotec.2004.02.013

Le, V.S., Ghiotti, A., Lucchetta, G., 2008. Preliminary Studies on Single Point Incremental Forming for Thermoplastic Materials. Int. J. Mater. Form. 1, 1179–1182. https://doi.org/10.1007/s12289-008-0191-0

Lee, C.-J., Lee, J.-M., Ryu, H.-Y., Lee, K.-H., Kim, B.-M., Ko, D.-C., 2014. Design of hole-clinching process for joining of dissimilar materials – Al6061-T4 alloy with DP780 steel, hot-pressed 22MnB5 steel, and carbon fiber reinforced plastic. J. Mater. Process. Technol. 214, 2169–2178. https://doi.org/10.1016/j.jmatprotec.2014.03.032

Lee, Y.S., Wetzel, E.D., Wagner, N.J., 2003. No Title. J. Mater. Sci. 38, 2825–2833. https://doi.org/10.1023/A:1024424200221

Leite, W., Campos Rubio, J., Mata Cabrera, F., Carrasco, A., Hanafi, I., 2018. Vacuum Thermoforming Process: An Approach to Modeling and Optimization Using Artificial Neural Networks. Polymers (Basel). 10, 143. https://doi.org/10.3390/polym10020143

Lessard, H., Lebrun, G., Benkaddour, A., Pham, X.-T., 2015. Influence of process parameters on the thermostamping of a [0/90] 12 carbon/polyether ether ketone laminate. Compos. Part A Appl. Sci. Manuf. 70, 59–68. https://doi.org/10.1016/j.compositesa.2014.12.009

Lim, L.-T., Auras, R., Rubino, M., 2008. Processing technologies for poly(lactic acid). Prog. Polym. Sci. 33, 820–852. https://doi.org/10.1016/j.progpolymsci.2008.05.004

Lionetto, F., Balle, F., Maffezzoli, A., 2017. Hybrid ultrasonic spot welding of aluminum to carbon fiber reinforced epoxy composites. J. Mater. Process. Technol. 247, 289–295. https://doi.org/10.1016/j.jmatprotec.2017.05.002

Lionetto, F., Dell'Anna, R., Montagna, F., Maffezzoli, A., 2016. Modeling of continuous ultrasonic impregnation and consolidation of thermoplastic matrix composites. Compos. Part A Appl. Sci. Manuf. 82, 119–129. https://doi.org/10.1016/j.compositesa.2015.12.004

Liu, S., Chen, T., Wu, C., 2017. Rotary ultrasonic face grinding of carbon fiber reinforced plastic (CFRP): a study on cutting force model. Int. J. Adv. Manuf. Technol. 89, 847–856. https://doi.org/10.1007/s00170-016-9151-x

Lopez-Cruz, P., Laliberté, J., Lessard, L., 2017. Investigation of bolted/bonded composite joint behaviour using design of experiments. Compos. Struct. 170, 192–201. https://doi.org/10.1016/j.compstruct.2017.02.084

Lozano-Sánchez, L.M., Sustaita, A.O., Soto, M., Biradar, S., Ge, L., Segura-Cárdenas, E., Diabb, J., Elizalde, L.E., Barrera, E.V., Elías-Zúñiga, A., 2017. Mechanical and structural studies on single point incremental forming of polypropylene-MWCNTs composite sheets. J. Mater. Process. Technol. 242, 218–227. https://doi.org/10.1016/j.jmatprotec.2016.11.032

Magin, J., Balle, F., 2014. Solid state joining of aluminum, titanium and their hybrids by ultrasonic torsion welding. Materwiss. Werksttech. 45, 1072–1083. https://doi.org/10.1002/mawe.201400355

Mariam, M., Afendi, M., Abdul Majid, M.S., Ridzuan, M.J.M., Gibson, A.G., 2018. Tensile and fatigue properties of single lap joints of aluminium alloy/glass fibre reinforced composites fabricated with different joining methods. Compos. Struct. 200, 647–658. https://doi.org/10.1016/j.compstruct.2018.06.003

Marques, T.A., Silva, M.B., Martins, P.A.F., 2012. On the potential of single point incremental forming of sheet polymer parts. Int. J. Adv. Manuf. Technol. 60, 75–86. https://doi.org/10.1007/s00170-011-3585-y

Martin, P.J., 2009. Thermoforming of polymers, in: Advances in Polymer Processing. Elsevier, pp. 352–383. https://doi.org/10.1533/9781845696429.3.352

Martins, P.A.F., Kwiatkowski, L., Franzen, V., Tekkaya, A.E., Kleiner, M., 2009. Single point incremental forming of polymers. CIRP Ann. 58, 229–232. https://doi.org/10.1016/j.cirp.2009.03.095

Martinsen, K., Hu, S.J., Carlson, B.E., 2015. Joining of dissimilar materials. CIRP Ann. 64, 679–699. https://doi.org/10.1016/j.cirp.2015.05.006

Matsumura, T., Tamura, S., 2016. Temperature analysis in CFRP drilling, in: AIP Conference Proceedings. p. Vol. 1769, No. 1, 080005.

MatWeb [WWW Document], n.d. URL http://www.matweb.com/

Mazumdar, S., 2001. Composites manufacturing: materials, product, and process engineering. CrC press.

Meyer, A., 2003. Friction Hydro Pillar Processing Bonding Mechanism and Properties. GKSS FORSCHUNGSZENTRUM GEESTHACHT 1(4).

Micari, F., Ambrogio, G., Filice, L., 2007. Shape and dimensional accuracy in Single Point Incremental Forming: State of the art and future trends. J. Mater. Process. Technol. 191, 390–395. https://doi.org/10.1016/j.jmatprotec.2007.03.066

Mikell P. Groover, 2010. Fundamentals of Modern Manufacturing: Materials, Processes, and Systems, 4th ed.

Mitschang, P., Velthuis, R., Didi, M., 2013. Induction Spot Welding of Metal/CFRPC Hybrid Joints. Adv. Eng. Mater. 15, 804–813. https://doi.org/10.1002/adem.201200273

Moreno, D.D.P., Saron, C., 2017. Low-density polyethylene waste/recycled wood composites. Compos. Struct. 176, 1152–1157. https://doi.org/10.1016/j.compstruct.2017.05.076

Murray, B.R., Doyle, A., Feerick, P.J., Semprimoschnig, C.O.A., Leen, S.B., Ó Brádaigh, C.M., 2017. Rotational moulding of PEEK polymer liners with carbon fibre/PEEK over tape-placement for space cryogenic fuel tanks. Mater. Des. 132, 567–581. https://doi.org/10.1016/j.matdes.2017.07.026

Nagatsuka, K., Yoshida, S., Tsuchiya, A., Nakata, K., 2015. Direct joining of carbon-fiber–reinforced plastic to an aluminum alloy using friction lap joining. Compos. Part B Eng. 73, 82–88. https://doi.org/10.1016/j.compositesb.2014.12.029

Nied, H.F., Taylor, C.A., Delorenzi, H.G., 1990. Three-dimensional finite element simulation of thermoforming. Polym. Eng. Sci. 30, 1314–1322. https://doi.org/10.1002/pen.760302009

Ning, F., Cong, W., Wei, J., Wang, S., Zhang, M., 2015. Additive Manufacturing of CFRP Composites Using Fused Deposition Modeling: Effects of Carbon Fiber Content and Length, in: Volume 1: Processing. ASME, p. V001T02A067. https://doi.org/10.1115/MSEC2015-9436

Nishihara, T., 2003. Development of Friction Stir Forming. Mater. Sci. Forum 426–432, 2971–2978. https://doi.org/10.4028/www.scientific.net/MSF.426-432.2971

Nurul Fazita, M.R., Jayaraman, K., Bhattacharyya, D., Mohamad Haafiz, M.K., Saurabh, C., Hussin, M.,

H.P.S., A., 2016. Green Composites Made of Bamboo Fabric and Poly (Lactic) Acid for Packaging Applications—A Review. Materials (Basel). 9, 435. https://doi.org/10.3390/ma9060435

Ohashi, T., Tabatabei, H.M., Nishihara, T., 2017. Cylindrical extrusions on A5083 aluminum alloy plate fabricated by friction stir forming. p. 080002. https://doi.org/10.1063/1.5008082

Osswald, T., Hernández-Ortiz, J.P., 2006. Polymer processing. Hanser, Munich.

Pagliarulo, V., Rocco, A., Langella, A., Riccio, A., Ferraro, P., Antonucci, V., Ricciardi, M.R., Toscano, C., Lopresto, V., 2015. Impact damage investigation on composite laminates: comparison among different NDT methods and numerical simulation. Meas. Sci. Technol. 26, 085603. https://doi.org/10.1088/0957-0233/26/8/085603

Periyasamy, P., Mohan, B., Balasubramanian, V., Rajakumar, S., Venugopal, S., 2013. Multi-objective optimization of friction stir welding parameters using desirability approach to join Al/SiCp metal matrix composites. Trans. Nonferrous Met. Soc. China 23, 942–955. https://doi.org/10.1016/S1003-6326(13)62551-0

Pielichowski, K., Njuguna, J., 2005. Thermal degradation of polymeric materials. iSmithers Rapra Publishing.

Piquet, R., Ferret, B., Lachaud, F., Swider, P., 2000. Experimental analysis of drilling damage in thin carbon/epoxy plate using special drills. Compos. Part A Appl. Sci. Manuf. 31, 1107–1115. https://doi.org/10.1016/S1359-835X(00)00069-5

Pramanik, A., Basak, A.K., Dong, Y., Sarker, P.K., Uddin, M.S., Littlefair, G., Dixit, A.R., Chattopadhyaya, S., 2017. Joining of carbon fibre reinforced polymer (CFRP) composites and aluminium alloys – A review. Compos. Part A Appl. Sci. Manuf. 101, 1–29. https://doi.org/10.1016/j.compositesa.2017.06.007

Prashantha, I.S.N.V.R., Ravi Shankarb, D.V. Manzoor Hussainc, M. Chandra Moulid, B., 2018. Critical Analysis in Milling of GFRP Composites by Various End Mill Tools. Mater. Today 14607–14617.

Puw, H.Y., Hocheng, H., 1993. MACHINABILITY TEST OF CARBON FIBER-REINFORCED PLASTICS IN MILLING. Mater. Manuf. Process. 8, 717–729. https://doi.org/10.1080/10426919308934875

Qiu, K., Ming, W., Shen, L., An, Q., Chen, M., 2017. Study on the cutting force in machining of aluminum honeycomb core material. Compos. Struct. 164, 58–67. https://doi.org/10.1016/j.compstruct.2016.12.060

Rajasekaran, T., Palanikumar, K., Vinayagam, B.K., 2011. Application of fuzzy logic for modeling surface roughness in turning CFRP composites using CBN tool. Prod. Eng. 5, 191–199. https://doi.org/10.1007/s11740-011-0297-y

Rajenthirakumar, D., Sridhar, R., 2014. Single Point Incremental Sheet Forming of Polymer on Computer Numerically Controlled (CNC) Milling Machine Tool. Key Eng. Mater. 622–623, 420–426. https://doi.org/10.4028/www.scientific.net/KEM.622-623.420

Rimašauskas, M., Juzėnas, K., Rimašauskienė, R., Pupelis, E., 2014. The research of single point incremental forming process for composite mould production. Mechanics 20. https://doi.org/10.5755/j01.mech.20.4.7045

Robnik-Šikonja, lgor, M., Kononenko, I., 2003. Theoretical and Empirical Analysis of ReliefF and RReliefF. Mach. Learn. 53, 23–69. https://doi.org/10.1023/A:1025667309714

Sakin, R., Ay, İ., Yaman, R., 2008. An investigation of bending fatigue behavior for glass-fiber reinforced polyester composite materials. Mater. Des. 29, 212–217.

REFERENCES

https://doi.org/10.1016/j.matdes.2006.11.006

Sakundarini, N., Taha, Z., Abdul-Rashid, S.H., Ghazila, R.A.R., 2013. Optimal multi-material selection for lightweight design of automotive body assembly incorporating recyclability. Mater. Des. 50, 846–857. https://doi.org/10.1016/j.matdes.2013.03.085

Salamone, J.C., 1996. Polymeric Materials Encyclopedia. CRC Press.

Sato, Y.S., Park, S.H.C., Michiuchi, M., Kokawa, H., 2004. Constitutional liquation during dissimilar friction stir welding of Al and Mg alloys. Scr. Mater. 50, 1233–1236. https://doi.org/10.1016/j.scriptamat.2004.02.002

Schell, J.S.U., Amory, L., Guillon, D., 2016. Movement of patches during thermoforming: Experiment and simulation. p. 170032. https://doi.org/10.1063/1.4963588

Seidlitz, H., Fritzsche, S., Bambach, M., Gerstenberger, C., 2016. High load-bearing multi-material-joints of metal sheets and composites by incremental in-situ forming processes. p. 070011. https://doi.org/10.1063/1.4963464

Shaw, D., Tseng, C.N., 1992. Analysis of delamination in a laminate drilled by waterjet. Mach. Compos. Mater. 89–96.

Shen, N., Samanta, A., Wang, Q., Ding, H., 2017. Selective laser melting of fiber-reinforced glass composites. Manuf. Lett. 14, 6–9. https://doi.org/10.1016/j.mfglet.2017.09.001

Shetty, N., Shahabaz, S.M., Sharma, S.S., Divakara Shetty, S., 2017. A review on finite element method for machining of composite materials. Compos. Struct. 176, 790–802. https://doi.org/10.1016/j.compstruct.2017.06.012

Singh, I., Bhatnagar, N., Viswanath, P., 2008. Drilling of uni-directional glass fiber reinforced plastics: Experimental and finite element study. Mater. Des. 29, 546–553. https://doi.org/10.1016/j.matdes.2007.01.029

Sorrentino, L., Simeoli, G., Iannace, S., Russo, P., 2015. Mechanical performance optimization through interface strength gradation in PP/glass fibre reinforced composites. Compos. Part B Eng. 76, 201–208. https://doi.org/10.1016/j.compositesb.2015.02.026

Spur, G., Wunsch, U.E., 1988. Turning of fiber-reinforced plastics. Manuf. Rev. 1(2), 124–129.

Su, P., Gerlich, A., North, T.H., Bendzsak, G.J., 2006. Energy Generation and Stir Zone Dimensions in Friction Stir Spot Welds. https://doi.org/10.4271/2006-01-0971

Tekinalp, H.L., Kunc, V., Velez-Garcia, G.M., Duty, C.E., Love, L.J., Naskar, A.K., Blue, C.A., Ozcan, S., 2014. Highly oriented carbon fiber–polymer composites via additive manufacturing. Compos. Sci. Technol. 105, 144–150. https://doi.org/10.1016/j.compscitech.2014.10.009

Thompson, R., 2007. Manufacturing processes for design professionals. Thames & Hudson, London.

Throne, J.L., 2008. Understanding thermoforming. OH: Hanser Gardner Publications.

Tuttle, M.E., 2012. Structural analysis of polymeric composite materials. CRC Press.

U.S. Department of Defense, 2002a. Composite Materials Handbook Volume 1. Polymer Matrix Composites: Guidelines for Characterization of Structural Materials, in: Composite Materials Handbook. Department of Defense Handbook, USA.

U.S. Department of Defense, 2002b. Composite Materials Handbook Volume 2. Polymer Matrix Composites Materials Properties, in: Composite Materials Handbook. Department of Defense,

USA.

Ueda, M., Miyake, S., Hasegawa, H., Hirano, Y., 2012. Instantaneous mechanical fastening of quasi-isotropic CFRP laminates by a self-piercing rivet. Compos. Struct. 94, 3388–3393. https://doi.org/10.1016/j.compstruct.2012.04.027

Uhlmann, E., Sammler, F., Richarz, S., Heitmüller, F., Bilz, M., 2014. Machining of Carbon Fibre Reinforced Plastics. Procedia CIRP 24, 19–24. https://doi.org/10.1016/j.procir.2014.07.135

Upadhyay, P., Hovanski, Y., Carlson, B., Boettcher, E., Ruokolainen, R., Busuttil, P., 2017. Joining Dissimilar Material Using Friction Stir Scribe Technique. pp. 147–155. https://doi.org/10.1007/978-3-319-52383-5_16

Uzun, H., Dalle Donne, C., Argagnotto, A., Ghidini, T., Gambaro, C., 2005. Friction stir welding of dissimilar Al 6013-T4 To X5CrNi18-10 stainless steel. Mater. Des. 26, 41–46. https://doi.org/10.1016/j.matdes.2004.04.002

Vantal, M.H., Monasse, B., Bellet, M., 1995. Numerical simulation of the thermoforming of multi-layer polymer sheets, in: NUMIFORM'95, 5th Int. Conf. on Numerical Methods in Industrial Forming Processes. p. 1089.

Walczyk, D.F., Hosford, J.F., Papazian, J.M., 2003. Using Reconfigurable Tooling and Surface Heating for Incremental Forming of Composite Aircraft Parts. J. Manuf. Sci. Eng. 125, 333. https://doi.org/10.1115/1.1561456

Walter, J., Hustedt, M., Staehr, R., Kaierle, S., Jaeschke, P., Suttmann, O., Overmeyer, L., 2014. Laser Cutting of Carbon Fiber Reinforced Plastics – Investigation of Hazardous Process Emissions. Phys. Procedia 56, 1153–1164. https://doi.org/10.1016/j.phpro.2014.08.030

Warby, M.K., Whiteman, J.R., Jiang, W.-G., Warwick, P., Wright, T., 2003. Finite element simulation of thermoforming processes for polymer sheets. Math. Comput. Simul. 61, 209–218. https://doi.org/10.1016/S0378-4754(02)00077-0

Xavior, M.A., Kumar, J.P.A., 2017. Machinability of Hybrid Metal Matrix Composite - A Review. Procedia Eng. 174, 1110–1118. https://doi.org/10.1016/j.proeng.2017.01.264

Xu, J., Mkaddem, A., El Mansori, M., 2016. Recent advances in drilling hybrid FRP/Ti composite: A state-of-the-art review. Compos. Struct. 135, 316–338. https://doi.org/10.1016/j.compstruct.2015.09.028

Yang, Y., Vervust, T., Dunphy, S., Van Put, S., Vandecasteele, B., Dhaenens, K., Degrendele, L., Mader, L., De Vriese, L., Martens, T., Kaufmann, M., Sekitani, T., Vanfleteren, J., 2018. 3D Multifunctional Composites Based on Large-Area Stretchable Circuit with Thermoforming Technology. Adv. Electron. Mater. 4, 1800071. https://doi.org/10.1002/aelm.201800071

Zhang, J.Z., Chen, J.C., Kirby, E.D., 2007. Surface roughness optimization in an end-milling operation using the Taguchi design method. J. Mater. Process. Technol. 184, 233–239. https://doi.org/10.1016/j.jmatprotec.2006.11.029